University of South Carolina

Scholar Commons

Tectonics of the South Georgia Rift

David Michael Heffner
University of South Carolina

Recommended Citation

TECTONICS OF THE SOUTH GEORGIA RIFT

by

David M. Heffner

Bachelor of Science
Furman University, 2001

Master of Science
University of South Carolina, 2008

_____

Submitted in Partial Fulfillment of the Requirements

For the Degree of Doctor of Philosophy in

Geological Sciences

College of Arts and Sciences

University of South Carolina

2013

Accepted by:

James H. Knapp, Major Professor

David L. Barbeau, Committee Member

C. W. Clendenin, Jr., Committee Member

Camelia C. Knapp, Committee Member

Lacy Ford, Vice Provost and Dean of Graduate Studies

DEDICATION

This dissertation is dedicated to my wife Beth for her love, support, and perseverance through this graduate school adventure. I would also like to dedicate this dissertation to my son James, who over the last two years has shown me what is truly important in life.

ACKNOWLEDGEMENTS

ABSTRACT

Triassic rifting of the supercontinent Pangea left behind numerous basins on what is now the eastern North American margin. The South Georgia Rift (SGR) was thought to be the best preserved of these basins having been capped by thick basalt flows of the Central Atlantic Magmatic Province (CAMP) and later buried beneath the Cretaceous and younger Coastal Plain. Because it is buried beneath the Coastal Plain, the SGR is only known through sparse drilling and geophysical methods. Despite this limited dataset, the SGR is the only one of the eastern North American Triassic basins known to overlie the ancient Alleghanian suture between Laurentia and Gondwana, although it isn't clear what influence this lithospheric weakness played in formation of the rift.

The SGR has been variably interpreted as a singular large basin or as isolated sub-basins separated by transfer zones. Transfer zones are rift-transverse structural features that link major faults of rift sub-basins and accommodate differences in extensional strain. Transfer zones have been previously hypothesized to be present in the SGR based on onshore projections of Central Atlantic fracture zones, but observations confirming their existence, such as reversal in sub-basin polarity, have been lacking.

Three separate hypotheses are tested related to the SGR: 1) the J-Horizon corresponds everywhere with basalt; 2) transfer zones are an important structural component of the SGR; 3) structural features of the Central Atlantic Ocean are related to transfer zones of the SGR. Reanalysis of existing well and seismic data shows that the extent of the flood basalt in the SGR is restricted and that the J-Horizon coincides with

the base of the Coastal Plain. Subsurface mapping reveals reversals in sub-basin polarity,

confirming the existence of previously hypothesized transfer zones. Small circle

projections of the transfer zones correlate with oceanic features, and Central Atlantic

fracture zones project onshore into inferred transfer zones of the SGR. The results of

these studies suggest that tectonic inheritance of the Alleghanian suture played an

important role in the rifting of Pangea and that tectonic inheritance may be an important

process for the formation of an ocean basin.

TABLE OF CONTENTS

LIST OF TABLES

LIST OF FIGURES

LIST OF ABBREVIATIONS

BMA .... Brunswick Magnetic Anomaly

BSMA .... Blake Spur Magnetic Anomaly

CAMP .... Central Atlantic Magmatic Province

CP .... Coastal Plain

COCORP .... Consortium for Continental Reflection Profiling

DOE .... United States Department of Energy

ECMA .... East Coast Magnetic Anomaly

ENA .... Eastern North American

ENARS .... Eastern North American Rift System

FZ .... Fracture Zones

MAR .... Mid Atlantic Ridge

NA .... North America

SDR .... Seaward Dipping Reflectors

SGR .... South Georgia Rift

SRNL .... Savannah River National Lab

TZ .... Transfer Zone

USGS .... United States Geological Survey

CHAPTER 1

INTRODUCTION

How does a continent break apart? This is one of the fundamental questions in the geosciences, first asked in the days of Suess (1891) and Gregory (1896), and later identified as one of the major processes of plate tectonics (Wilson, 1966). Yet this question is still largely unanswered more than a century later (GeoPRISMS Draft Science Plan, 2010). This dissertation aims to address aspects of this question through studies of the South Georgia Rift (SGR), a large rift basin buried beneath the Coastal Plain of South Carolina, Georgia, Alabama, and Florida.

1.1 THE SOUTH GEORGIA RIFT

The Eastern North American Rift System (ENARS) comprises a northeast trending series of Triassic aged rift basins that record the tectonic events just prior to the breakup of Pangea and opening of the Atlantic Ocean (Figure 1.1; Olsen, 1997; Schlische, 2003). These basins are filled by continent-derived fluvial and lacustrine redbeds, referred to as the Newark Supergroup, and Jurassic aged diabase and basalt of the Central Atlantic Magmatic Province (Olsen, 1997). While the exposed basins of the ENARS have contributed much to our understanding of rifting processes and the development of passive margins, relatively little is known about the buried SGR, encountered by sparse well penetrations and inferred through geophysical methods (Daniels and Zietz, 1978; Chowns and Williams, 1983; McBride, 1991).

Figure 1.1. Location of the Eastern North American Rift System.
Exposed basins shown in red and buried basins shown in gray.

The South Georgia Rift (SGR) is thought by many workers to be the southernmost and largest of the eastern North American Triassic rift basins (Daniels and Zietz, 1983; Klitgord et al., 1984; Olsen, 1997; Withjack et al., 1998; Schlische, 2003). Redbeds brought to the surface as cuttings from a deep water well drilled near Florence, South Carolina were the first reported observation that "Newark Supergroup like rocks" were present beneath portions of the Coastal Plain (Darton, 1896). Sporadic petroleum test wells drilled throughout Georgia and scientific wells drilled in South Carolina further provided evidence that Triassic basins were present under much of the Coastal Plain (Applin and Applin, 1964; Marine and Siple, 1974; Gohn et al., 1978).

Daniels et al. (1983) first proposed on the basis of aero-magnetic data that the seemingly separate pockets of Triassic rock under the Coastal Plain of Georgia and South Carolina are encompassed within a singular giant rift basin, which they called the South Georgia Basin (Figure 1.2A). Chowns and Williams (1983) completed a comprehensive study of deep wells in Georgia, Florida, and Alabama to assess the extent of the SGR and relied on interpretations of potential field data for determining the boundaries where little to no well control was available (Figure 1.2B). As part of a larger study investigating the entire eastern North American margin, Klitgord et al. (1986) produced a very different picture of the extent of the SGR based solely on interpretation of aero-magnetic data (Figure 1.2C). Sartain and See (1997) studied the southwestern portion of the SGR, integrating interpretations of potential fields data with Landsat and seismic reflection data to produce an isopach map of the southwestern part of the basin (Figure 1.2D).
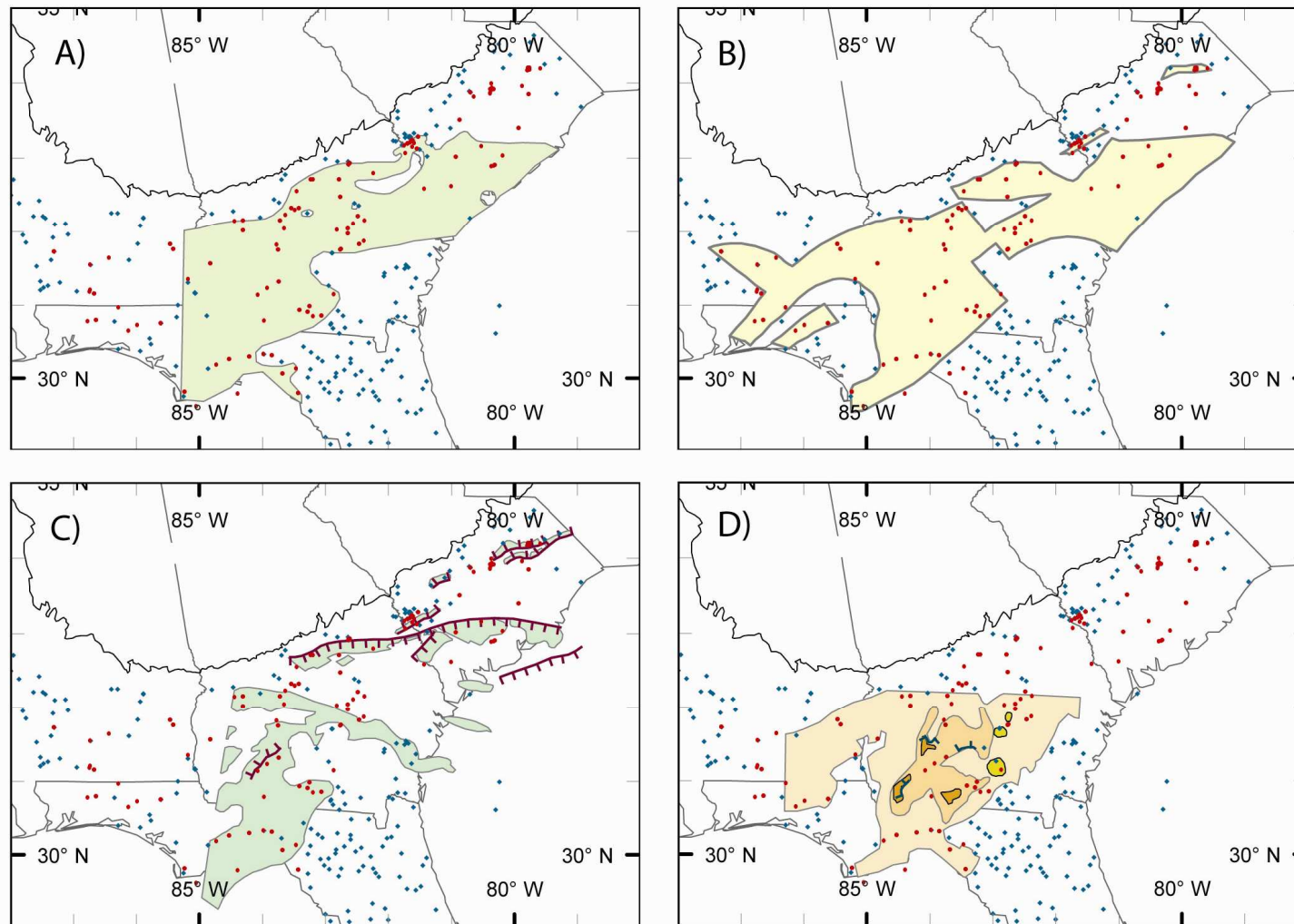
Figure 1.2. Previous interpretations of the extent of the South Georgia Rift. A) Daniels et al. (1983). B) Chowns and Williams (1983). C) Klitgord et al. (1986). D) Sartain and See (1997).

A few attempts have been made to map structures of the SGR (Figure 1.3). The bounding faults have largely been interpreted from active source seismic data although several faults have been interpreted from borehole data and other geophysical methods (Behrendt et al., 1981; Petersen et al., 1984; Behrendt, 1985; Tauvers and Muehlberger, 1987; Ball et al., 1988; Klitgord et al., 1988; McBride, 1991; Domoracki, 1995). Interpretations of geophysical data have generally suggested the southwestern SGR has a complex horst and graben architecture (McBride, 1991; Sartain and See, 1997).

The generalized stratigraphy of the SGR is a Triassic redbed syn-rift section that is intruded by Jurassic diabase sills and dikes, and locally topped by basalt flows (Gohn et al., 1978; Chowns and Williams, 1983; Heffner et al., 2012). A prominent unconformity separates the Triassic / Jurassic section from the Cretaceous and younger Coastal Plain and is easily identifiable on seismic reflection profiles. Sediments generally appear to originate from a fluvial environment; however, alluvial conglomeratic deposits are encountered near the border faults of the Riddleville and Dunbarton Basins (Figure 1.3; Chowns and Williams, 1983).

1.2 RIFTING AND MAGMATISM

Magmatism has long been an associated component of continental rifting (Bailey, 1977). Although asthenospheric upwelling and the associated magmatism has been invoked as a causal mechanism for continental rifting, at the present it seems that rift-related volcanism is merely a consequence of lithospheric thinning (Ziegler and Cloetingh, 2004). This is illustrated by the fact that many of the identified plumes with associated hot spot tracks are in the middle of tectonic plates, and some so called passive rifts lack volcanic rocks (White and McKenzie, 1989; Ziegler and Cloetingh, 2004).
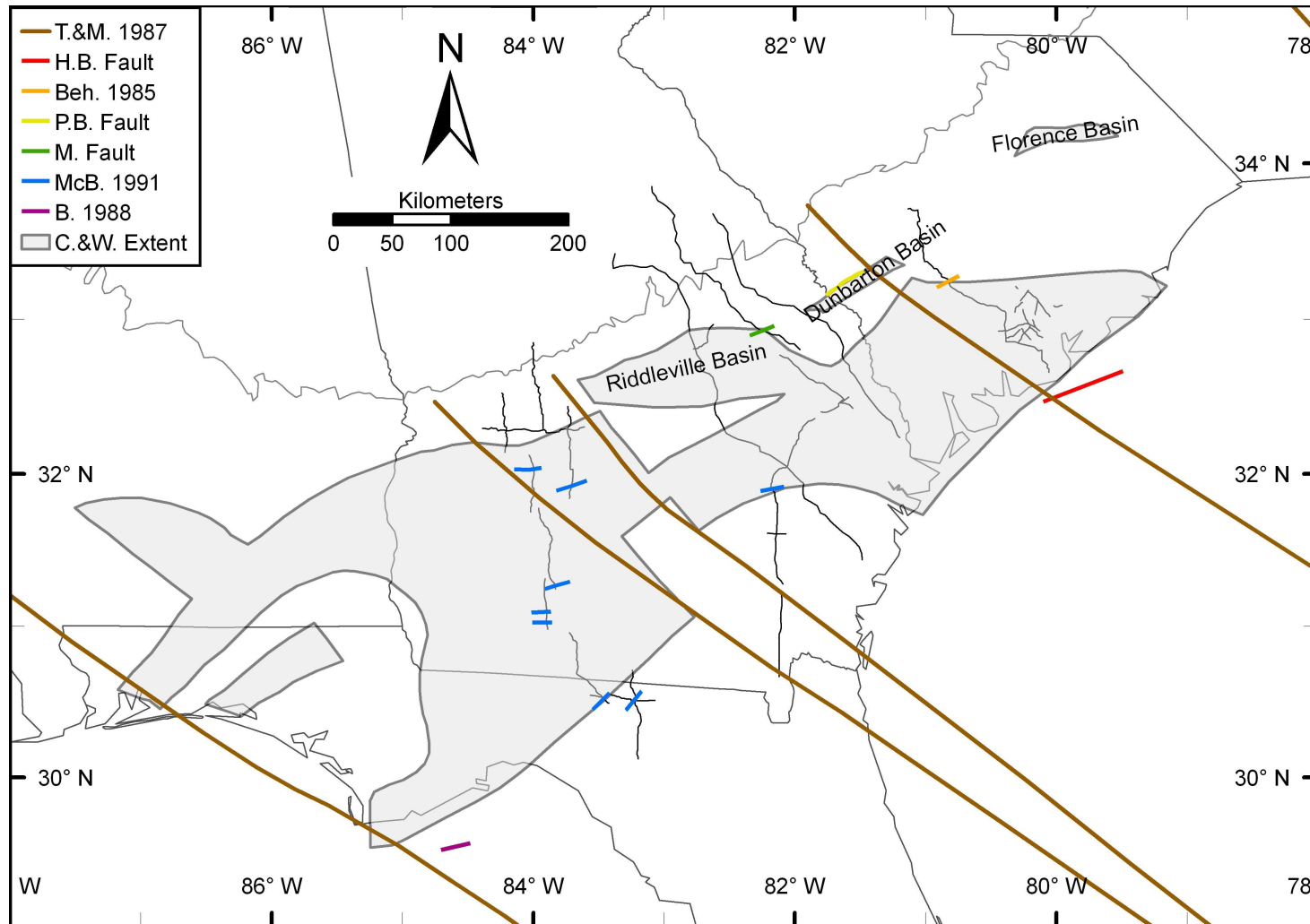
Figure 1.3. Previous interpretations of structure within the South Georgia Rift (SGR). T&M - Tauvers and Muehlberger (1987), H.B. - Helena Banks, Beh. 1985 - Behrendt (1985), P.B. - Pen Branch, M. - Magruder, McB. 1991 - McBride (1991), B. 1988 - Ball et al. (1988), C&W Extent - Chowns and Williams (1983) mapped extent of the SGR.

However, when continental rifting occurs over an anomalously hot mantle, massive volcanism does occur, and a large igneous province is emplaced (White and McKenzie, 1989). The Central Atlantic Magmatic Province (CAMP) is one such large igneous province associated with the breakup of Pangea (Marzoli et al., 1999).

CAMP is arguably one of the largest igneous provinces in the world, spanning four continents and covering an estimated areal extent of seven to ten million square kilometers prior to erosion (Marzoli et al., 1999; McHone, 2000). The mafic rocks that make up the province were emplaced within a relatively short span of 0.6–2 million years and are well dated near the Triassic / Jurassic boundary, ca. 200 Ma (Olsen, 1997; Marzoli et al., 1999; Hames et al., 2000; McHone, 2000; Olsen et al., 2003; Nomade et al., 2007). CAMP rocks are present in buried basins, such as the South Georgia Rift (SGR), where they are encountered in sparse well penetrations and inferred through geophysical investigations (Chowns and Williams, 1983; Daniels et al., 1983; Gohn 1983; McBride et al., 1989).

A prominent, low frequency, high-amplitude, two-cycle seismic reflection, referred to as the J-Horizon, has been observed in many of the onshore and offshore seismic lines in the South Carolina – Georgia region (Dillon et al., 1979; Hamilton et al., 1983; Schilt et al., 1983; McBride et al., 1989; Austin et al., 1990; Oh et al., 1995). This reflection is characteristically sub-horizontal and occurs between 0.8 – 1.2 s two-way travel time (twtt) in the Charleston, South Carolina area. It has been correlated with the Clubhouse Crossroads basalt in South Carolina (Hamilton et al., 1983; Schilt et al, 1983) and diabase in the Horace Parker #1 well in Georgia (McBride et al., 1989) leading to the conclusion that flood basalt covers the SGR. The interpretation that the J-Horizon

originates from flood basalt is the strongest line of evidence used to link CAMP to the opening of the Atlantic (Austin et al., 1990; Oh et al., 1995) and to suggest the rift-drift transition of eastern North America was diachronous (Withjack et al., 1998; Schlische et al., 2003). Reanalysis of well data, however, shows that most sub-Coastal Plain wells in the SGR do not encounter basalt, and in many wells diabase also is not present.

1.3 RIFT STRUCTURE

Early models of continental rifting suggested that rifts are symmetrical in nature (McKenzie, 1978); however, seismic images and later models of rifts suggested that they are typically asymmetrical in nature, where a single normal fault bounds a rotated block on one end, and the rift basin stratigraphy pinches out towards the opposite hinge side (Bally, 1982; Gibbs, 1984; Wernicke, 1985). Additionally it was observed that along the axis of a rift this asymmetric geometry would reverse polarity, such that the bounding faults of adjacent basins could be found on opposite sides of the rift (Gibbs, 1984; Lister et al., 1986; Rosendahl, 1987). These reversals in basin polarity occur across rift-transverse structural features referred to as transfer zones (Morley et al., 1991).

Transfer zones are rift-transverse structures that can range from discrete faults to more complex zones of deformation consisting of ramps, overlapping normal faults, en echelon strike-slip faults, and folds (Gibbs, 1984; Rosendahl, 1987; Morley et al., 1990; Faulds and Varga, 1998; Morley, 1999). Gibbs (1984) recognized that a cross-fault system should be expected in an extensional setting. These cross-faults, termed transfer faults by Gibbs (1984), connect different loci of extension, transferring strain between major normal fault systems of a rift (Figure 1.4; Faulds and Varga, 1998). Similar cross-

rift features are observed in the East African Rift; however, these features are generally

thought to be structurally more complex (Rosendahl, 1987; Morley et al., 1990).
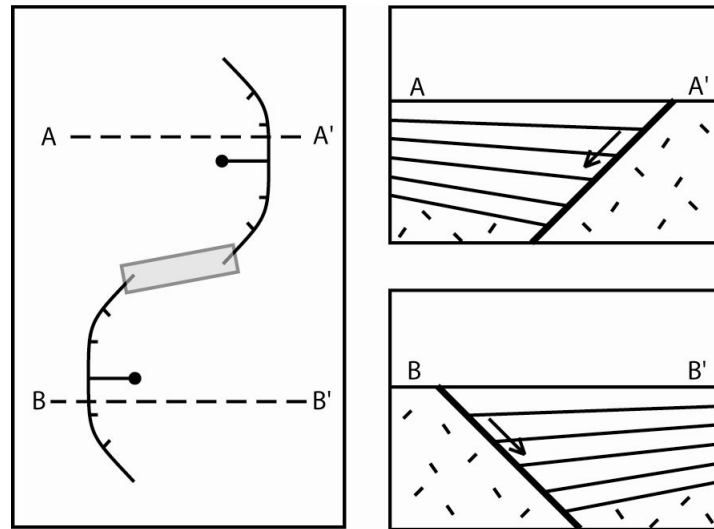
Figure 1.4. Schematic of rift system illustrating half
graben structure, and a reversal in sub-basin polarity
across a transfer zone.

There are a number of different proposed classification schemes and

terminologies for describing transfer zones (Rosendahl, 1987; Morley et al., 1990; Faulds

and Varga, 1998; Schlische and Withjack, 2009). For this paper, the more generic term

"transfer zone" is generally used (Morley, 1999), since the spatial resolution of the data is

too sparse to truly constrain the nature of these structures. In some cases, the term

"transfer fault" (Gibbs, 1984) is used to define a discrete transfer zone where border

faults are "hard-linked", or the term "accommodation zone" (Rosendahl, 1987) is used to

refer to a more complex zone of deformation where normal faults are "soft-linked"

through ramps and folds.

While transfer zones should not be confused with lithospheric scale

intracontinental transform faults, which are active plate boundaries, they function very

similarly to oceanic transform faults that separate mid-ocean ridge spreading center

9

segments (Faulds and Varga, 1998). Extensional strain is transmitted through transfer

zones between two adjacent rift basins or basin segments, and differences in extensional

strain are accommodated by movement on faults within the transfer zone (Gibbs, 1984;

Rosendahl, 1987; Faulds and Varga, 1998; Morley, 1999). This has important

implications for balancing strain in a rift, as much of the extension may be taken up by

strike-slip motion on faults within a transfer zone (Gibbs, 1984).

Early studies of the SGR generally interpreted its sub-basins to be symmetrical

graben (e.g., Marine and Siple, 1974). Later studies, which incorporated active source

seismic reflection data, indicated that the sub-basins of the SGR had a half-graben

structure (Petersen et al., 1984; Ball et al., 1988; McBride, 1991; Domoracki, 1995).

Several studies have projected oceanic fracture zones onshore (Tauvers and

Muehlberger, 1987; Etheridge et al., 1989), and an along-strike disparity in basin

architecture has been observed (McBride, 1991). The purported presence of transfer

zones within the SGR, however, has been a contentious issue (McBride and Nelson,

1988; Tauvers and Muehlberger, 1988; McBride, 1991). There are no hard-linked

transfer faults in the exposed basins to the north (Schlische, 2003), and evidence for these

transfer zone projections has been historically lacking (Behrendt et al., 1981; McBride

and Nelson, 1988). As stated by McBride:

> "No dominant reversal in fault polarity is observed between the three transects
>
> across the basin and no direct evidence of intervening northwest trending transfer
>
> or strike-slip faults exists as proposed by Salvador (1987) or Tauvers and
>
> Muehlberger (1987). Clearly, more reflection profiling is needed to complete,
>
> and test the interpretation of along-strike variation in the rift" (1991, p. 1079).

1.4 RIFT TO DRIFT

Successful continental rifts ultimately result in the formation of ocean basins, and thus it has long been thought that the structures of an ocean basin, and in particular oceanic transform faults, are inherited from the initial continental break (Wilson, 1965). Oceanic transform faults are only active plate boundaries between ridge segments, where the plates slide past each other. Beyond the region of active spreading and transform displacement, the relict transform faults are preserved as fracture zones. These fracture zones are striking bathymetric features near the mid-ocean ridges, and can be mapped from discontinuities in the magnetic lineation patterns of the oceanic crust (Klitgord and Schouten, 1986). The fracture zones preserve the flow line of the plate, and trend approximately along the small circles of a stage pole for their given time (Klitgord and Schouten, 1986).

A prime candidate for the precursors of transform faults are transfer zones, which have been identified in many of Earth's active and ancient rifts (Gibbs, 1984; Rosendahl, 1987; Faulds and Varga, 1998; Morley, 1999). Thomas (2005) has even argued that transform faults are tectonically inherited through multiple Wilson cycles, taken up both as compressive and then subsequently extensional structures. Previous studies of the western Central Atlantic have projected oceanic fracture zones onto the southeastern North American margin largely based on the assumption that the pole of rotation has remained constant from the rift stage through about 154 Ma (Etheridge et al., 1989; Klitgord et al., 1986; Sykes, 1978; Tauvers and Muehlberger, 1987). Recent reconstructions of Pangea, however, have suggested that there was a change in the pole of

11

rotation during the early drift stage of the Central Atlantic (Schettino and Turco, 2009; Labails et al., 2010).

1.5 ORGANIZATION

This dissertation is organized into three content chapters, each one written as a manuscript intended for publication, and a concluding chapter. Chapter 2 revisits the hypothesis that a large flood basalt province covers the SGR. Chapter 3 provides a comprehensive interpretation of the major structures of the SGR. Chapter 4 addresses the hypothesis that rift structures are inherited by an ocean basin. Finally, Chapter 5 discusses the conclusions of this study and suggests avenues for future research.

CHAPTER 2

PRESERVED EXTENT OF JURASSIC FLOOD BASALT IN THE SOUTH GEORGIA RIFT: A NEW INTERPRETATION OF THE J-HORIZON

Approximately 200 million years ago at the end of the Triassic, the Central Atlantic Magmatic Province (CAMP), one of the largest igneous provinces in the world was emplaced within a very short period of time. The flows, sills, and dikes that mark the event are predominantly preserved in Triassic rift basins along the Atlantic margins. Conventional wisdom implies that the areally largest of the CAMP flows is preserved in the South Georgia Rift (SGR), a Triassic rift basin buried beneath the Atlantic Coastal Plain. The extent of this flow has been mapped on the basis of a prominent seismic reflection referred to as the J-Horizon. This seismic horizon has been used as a time marker for estimating the end of rifting in the southern United States and the beginning of sea floor spreading. Reanalysis of existing well and seismic data, however, shows that the extent of the flood basalt is only limited to a few areas and that the J-Horizon coincides with the base of the Coastal Plain. This reopens the question of how CAMP relates to the rift-drift transition of eastern North America.

Heffner , D.M., Knapp, J.H., Akintunde, O.M., and Knapp, C.C., 2012, Preserved extent of Jurassic flood basalt in the South Georgia Rift: A new interpretation of the J horizon: Geology, v. 40, p. 167–170.

2.1. INTRODUCTION

At the end of the Triassic period, as Pangea was in the midst of rifting, a massive igneous province was emplaced in what would become the Central Atlantic region. The remnants of this mafic igneous province, often referred to as the Central Atlantic Magmatic Province (CAMP), can still be found in basalt flows, diabase dikes, and diabase sills scattered along the East Coast of North and South America, and in western Africa and Europe (Marzoli et al., 1999). The mafic igneous rocks associated with CAMP are predominantly preserved in Triassic rift basins, and include well-known flood basalts and the Palisade sill of the Newark basin. CAMP is arguably one of the largest igneous provinces in the world, spanning four continents and covering an estimated areal extent of seven to ten million square kilometers prior to erosion (Marzoli et al., 1999; McHone, 2000). The mafic rocks that make up the province were emplaced within a relatively short span of 0.6–2 Million years and are well dated near the Triassic / Jurassic boundary, ~200 Ma (Olsen, 1997; Marzoli et al., 1999; Hames et al., 2000; McHone, 2000; Olsen et al., 2003; Nomade et al., 2007). CAMP rocks are present in buried basins, such as the South Georgia Rift (SGR), where they are encountered in sparse well penetrations and inferred through geophysical investigations (Chowns and Williams, 1983; Daniels et al., 1983; Gohn 1983; McBride et al., 1989). There have been some recent suggestions that the basalt encountered in the Clubhouse Crossroads wells in South Carolina may represent a different igneous event (Hames et al., 2010), however for reasons explained by Olsen et al. (2003) this basalt is considered here to be a part of CAMP.

A prominent, low frequency, high-amplitude, two-cycle reflection, referred to as the J-Horizon, has been observed in many of the onshore and offshore seismic lines in the

South Carolina – Georgia region (Dillon et al., 1979; Hamilton et al., 1983; Schilt et al., 1983; McBride et al., 1989; Austin et al., 1990; Oh et al., 1995). This reflection is characteristically sub-horizontal and occurs between 0.8 – 1.2 s two-way travel time (twtt) in the Charleston, South Carolina area. It has been correlated with the Clubhouse Crossroads basalt in South Carolina (Hamilton et al., 1983; Schilt et al, 1983) and diabase in the Horace Parker #1 well in Georgia (McBride et al., 1989); leading to the conclusion that flood basalt covers the SGR (Figure 2.1). The interpretation that the J-Horizon originates from flood basalt is the strongest line of evidence used to link CAMP to the opening of the Atlantic (Austin et al., 1990; Oh et al., 1995), and to suggest the rift-drift transition of eastern North America was diachronous (Withjack et al., 1998; Schlische et al., 2003).

Reanalysis and integration of well and seismic data shows that most sub-Coastal Plain wells in the SGR do not encounter basalt; and in many wells, diabase also is not present. Absence suggests that the areal extent of basalt flows in the SGR is not as regional as previously proposed and that the ubiquitous J-Horizon may have a different origin. The J-Horizon is hypothesized here to correspond with the base of the Coastal Plain irrespective of basalt.

2.2. WELL DATA

A database of 321 wells (Appendix A), that penetrated the Coastal Plain in South Carolina, Georgia, Eastern Alabama, and Northern Florida, was compiled from scientific literature, and federal and state government sources, as part of an ongoing project to investigate the SGR (Figure 2.1). Although the majority of cataloged wells in South
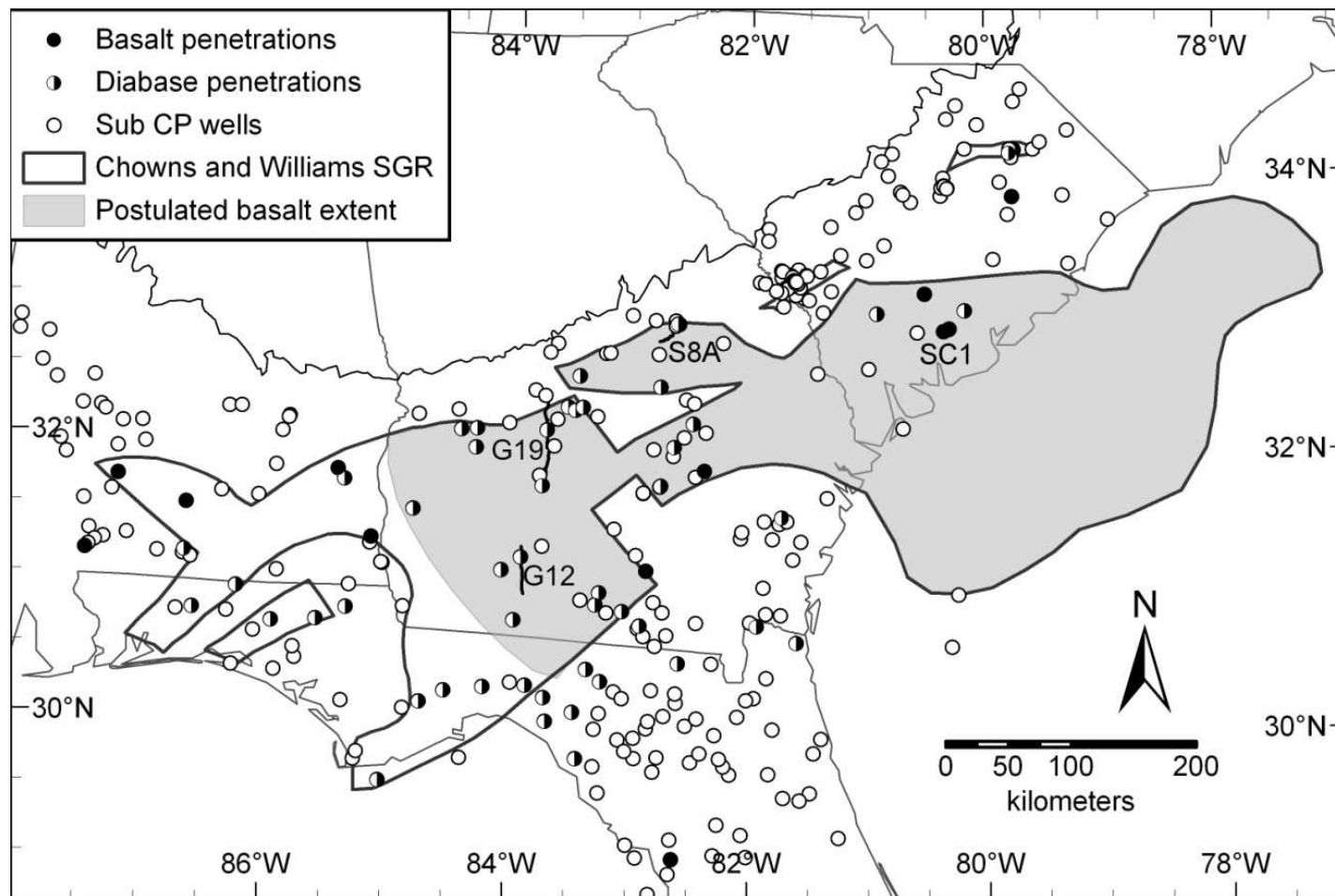
Figure 2.1. Map (modified from McBride et al., 1989; Chowns and Williams, 1983) of the South Georgia Rift (SGR) with postulated flood basalt / diabase extent from McBride et al. (1989) shown in gray. The location of wells that are reported to encounter basalt are shown as filled circles, wells that penetrate diabase are shown as half filled circles, and wells which penetrated the base of the Coastal Plain (CP) but did not encounter mafic igneous rock are shown as open circles. The position of four seismic lines is also shown: SC1 – USGS SC-1; S8A – SeisData 8A; G12 – COCORP GA-12; G19 – COCORP GA-19.

Carolina were drilled for ground water resources and research, wells in other states were drilled for oil tests. Only a few of the compiled wells encountered basalt, although many of the wells within the SGR did penetrate diabase (Figure 2.1). Diabase, an intrusive rock, is distinguished from basalt on the basis of a coarser texture, and the presence of overlying metamorphic aureoles. A simplified geology of seven of these wells is presented in Figure 2.2 and discussed below.

The Clubhouse Crossroads #3 (CC#3) and the St. George #1 (DOR-211) are two of the wells in South Carolina that penetrated basalt directly beneath the Coastal Plain (Figures 2.1 and 2.2). CC#3 was the third in a series of three wells drilled near Summerville, South Carolina by the U.S. Geological Survey to develop a better understanding of the geology underlying the Charleston area. The first two Clubhouse Crossroads wells bottomed in basalt, while CC#3 penetrated through the 256 m basalt layer and bottomed in red beds (Gohn, 1983). DOR-211 was drilled 34 km to the northwest of CC#3. This well penetrated the base of the Coastal Plain at 599 m and was drilled through 30 m of basalt.

The Norris-Lightsey #1 well (COL-241) in South Carolina was a deep oil test drilled ~70 km west of Summerville, South Carolina. The hole penetrated the base of the Coastal Plain at a depth of ~610 m and reached a total depth of ~4115 m, but never encountered basalt. Two thin diabase layers, each ~3 m thick, were penetrated at depths of 1200 and 1227 m, and several thicker layers of diabase were encountered at 1410 m and below (Figure 2.2). Pollen collected from cuttings between 1373 m and 2184 m was dated by Traverse (1987) to be Late Triassic in age.

17
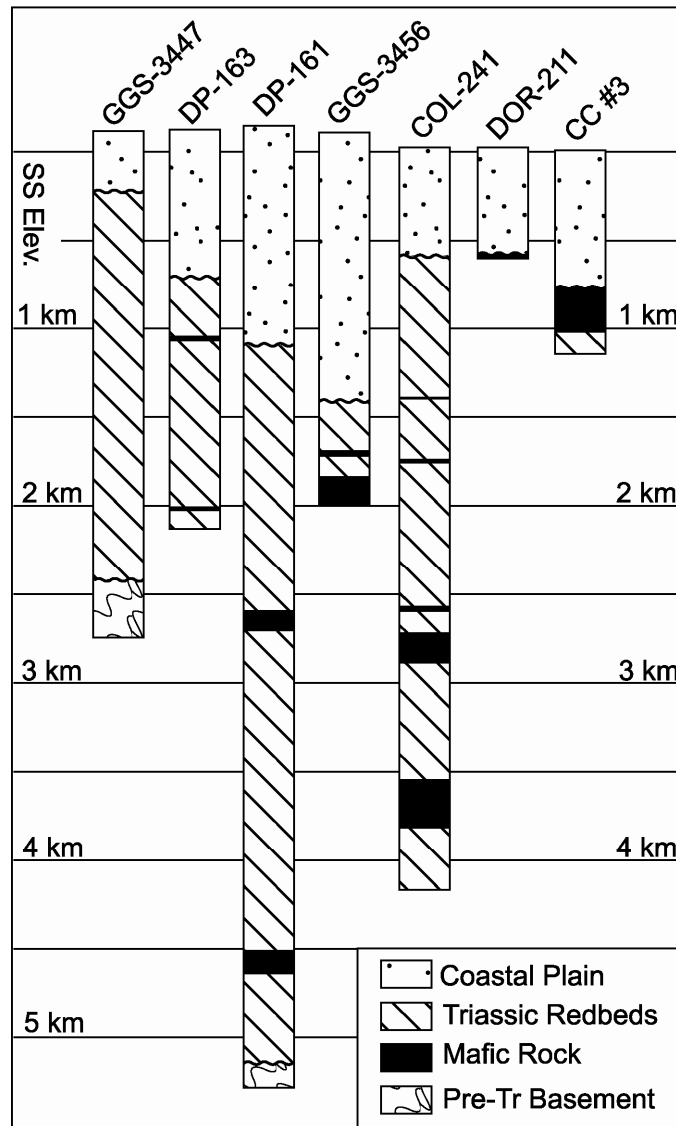
Figure 2.2. Select wells which penetrate the Coastal Plain and encounter Triassic red beds and/or Jurassic basalt/diabase.

The Ronnie Leadford #1 (DP-163) and Horace Parker #1 (GGS-3456) are two wells in Georgia that encounter mafic igneous rock more than 250 m below the bottom of the Coastal Plain. DP-163 was drilled to a depth of 2254 m and penetrated the base of the Coastal Plain at a depth of 835 m. Two mafic igneous layers are interpreted from the gamma log to be at 1167 – 1198 m and 2140 –2153 m. GGS-3456 was drilled to a depth of 2104 m and bottomed in mafic igneous rock. McFadden et al. (1986) reported a Cretaceous / Triassic(?) contact at a depth of 1515 m. The top of the first basaltic unit, which is 37 m thick, is at a depth of 1795 m, and the top of the next mafic igneous layer is at 1942 m. Although the geology log refers to the igneous rocks in this well as basalt, it reports metamorphic aureoles above both layers suggesting they are intrusive.

The McNair #1 (DP-161) and McCoy #1 (GGS-3447) are two wells in Georgia that penetrated the entire SGR stratigraphic section without encountering basalt. DP-161 is ~9 km South of COCORP GA-19. This well penetrated the base of the Coastal Plain at a depth of 1237 m and encountered diabase at a depth 2740 m (Figure 2.2). GGS-3447 is near the northern border of the SGR in the Riddleville basin. This well encountered the base of the Coastal Plain at 338 m and bottomed in schist (Figure 2.2).

2.3. SEISMIC DATA

As part of the characterization of the SGR, ~3000 km of 2D reflection seismic sections were acquired. These include COCORP lines in South Carolina, Georgia, and Florida, three regional SeisData profiles, and seismic profiles in the Charleston, South Carolina area reprocessed by Chapman and Beale (2010). A small subset of this data, which can be correlated to nearby wells, is shown in Figures 2.3 and 2.4. All well correlations are on the basis of simple depth to time conversion using an interval velocity
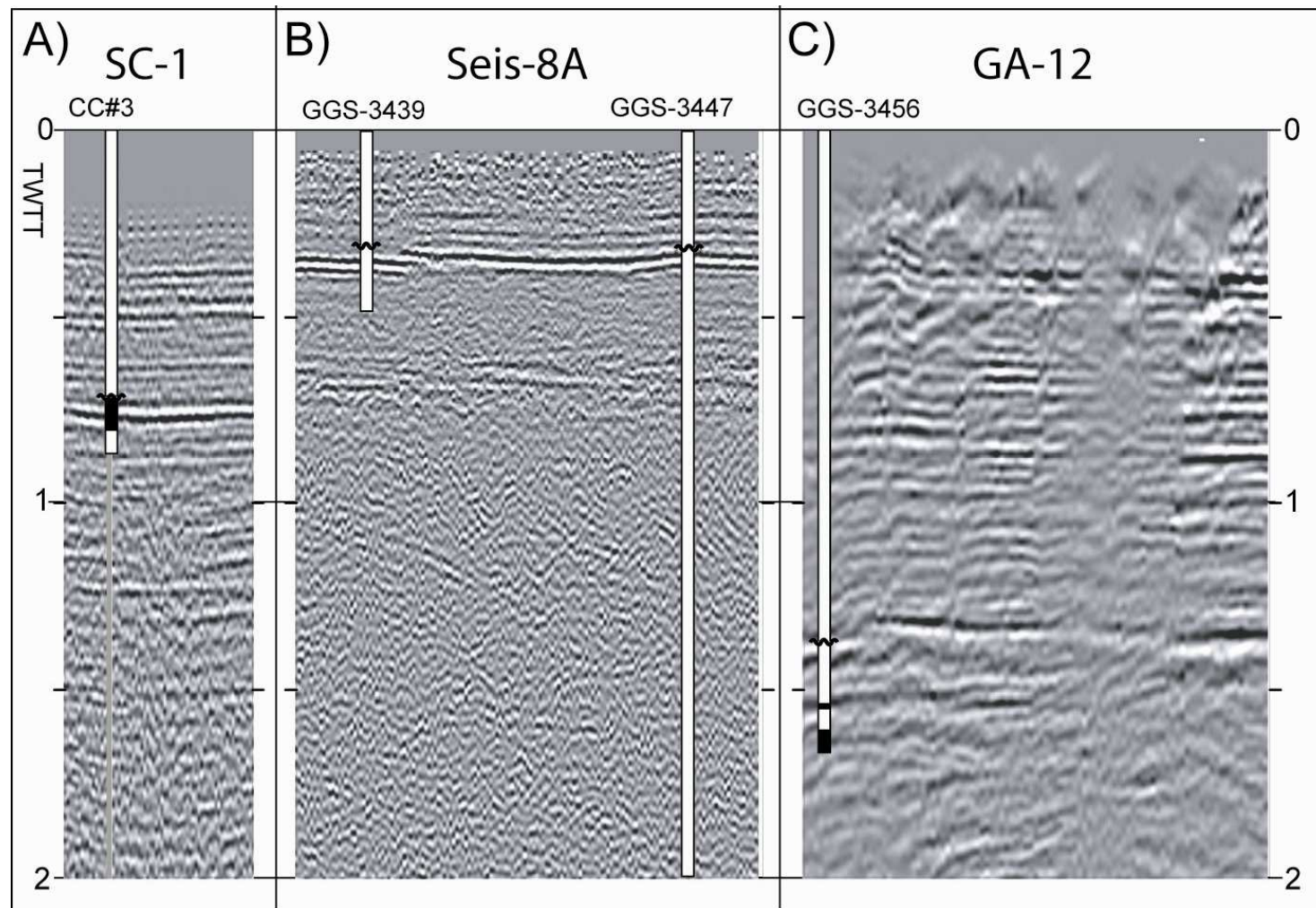
Figure 2.3. A portion of the stacked seismic data in two-way travel time (twtt) for A) USGS SC-1, modified from Chapman and Beale (2010), B) SeisData 8A, licensed and provided courtesy of Geophysical Pursuit, Inc., and C) COCORP GA-12, modified from McBride et al. (1989). All wells are converted to time as described in the text. The fall line unconformity is marked on the wells as a short undulating line, and mafic igneous layers are marked in black. Sections are vertically exaggerated 2x at a velocity of 2.2 km/s.
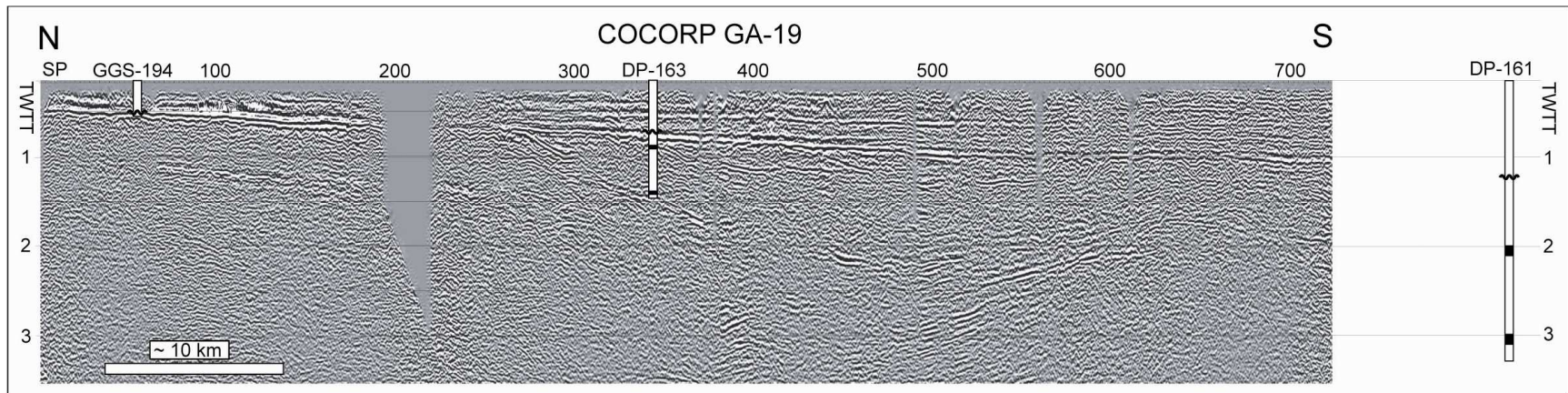
Figure 2.4. Stacked seismic section in two-way travel time (twtt) of COCORP GA-19, after McBride (1991). The three wells shown are GGS-194, DP-161, and DP-163. All wells are converted to time based on interval velocities of 2.2 km/s for the Coastal Plain sediments, 3.5 km/s for the Triassic red beds, 5.5 km/s for the basaltic rock, and 5.0 km/s for metamorphic basement. The fall line unconformity is marked on the wells as a short undulating line, and mafic igneous layers are marked in black. Section is vertically exaggerated 2x at a velocity of 2.2 km/s.

of 2.2 km/s for the Coastal Plain, 3.5 km/s for Triassic red beds, 5.5 km/s for basaltic layers, and 5.0 km/s for metamorphic basement.

A 2 km portion of USGS SC-1 is shown in Figure 2.3A and is tied to CC#3. The J-Horizon, as described by Hamilton et al. (1983), can be seen as the strong reflection at 0.75s. Other sub-horizontal reflections are present above the J-Horizon and are interpreted to result from changes in lithology in the Coastal Plain. As can be seen in Figure 2.3A, the basalt layer in CC#3 correlates very well with the J-Horizon.

A 5 km portion of SeisData 8A is shown in Figure 2.3B. A prominent reflection is observed at 0.4 s and is interpreted to be the J-Horizon with weaker sub-horizontal Coastal Plain reflections above. Neither of the two wells correlated with this seismic section encounter mafic igneous rocks. GGS-3439 lies outside the basin, bottoming in schist immediately beneath the base of the Coastal Plain. GGS-3447 penetrates entirely through the SGR and bottoms in schist. In both wells, the base of the Coastal Plain correlates with the J-Horizon.

A 5 km portion of COCORP GA-12 is shown in Figure 2.3C. The pronounced reflection at 1.4 s is interpreted to be the J-Horizon. Above this reflection are weaker sub-horizontal reflections interpreted to be from the Coastal Plain. Our depth-to-time conversion of GGS-3456 also shows a correlation between the base of the Coastal Plain and the J-Horizon. As shown in Figure 2.2, GGS-3456 does encounter mafic igneous rock; but in Figure 2.3C, the upper mafic igneous layer correlates with a reflection below the J-Horizon at 1.5 s.

The upper 3.5s for the full length of the COCORP GA-19 section is shown in Figure 2.4. A distinct reflection dips south starting at ~0.4 s and ending at 1s and is

22

interpreted to be the J-Horizon. Above this reflection are weaker Coastal Plain

reflections which also dip very slightly to the south. Two wells are tied directly to the

line, GGS-194 and DP-163. GGS-194 lies outside the basin, bottoming into Piedmont

metamorphic rocks directly beneath the Coastal Plain. DP-163 penetrated SGR red beds

and encountered two layers of mafic igneous rock. In both wells, the base of the Coastal

Plain correlates with the J-Horizon. The two mafic igneous layers in DP-163 appear in

Figure 2.4 to correlate with two steeply dipping reflections. DP-161 also is plotted with a

converted time for the Coastal Plain / Triassic basin contact at ~1.1 s.

2.4. DISCUSSION

As seen in Figure 2.1, only 13 of the catalogued wells actually encounter basalt,

while the other 49 that intersect mafic igneous rocks encounter diabase. The widespread

presence of diabase sills and dikes throughout the SGR suggests that an extensive flood

basalt may have once existed above the SGR; however, the limited distribution of wells

which actually encountered basalt shows that the present day extent of basalt in the SGR

is areally confined.

The idea that an extensive Jurassic volcanic layer exists directly beneath the

Coastal Plain was first proposed by Dillon et al. (1979) on the basis of a strong reflection

observed in offshore seismic data. This reflection, later named the "J" by Schilt et al.

(1983), correlated with a high velocity refractor (5.8 – 6.2 km/s) and projected onshore

towards the Clubhouse Crossroads basalt in South Carolina. There are weaknesses to this

interpretation as pointed out by Dillon et al. (1979): refraction velocities are more in line

with basement velocities (Ackermann, 1983), and this reflection also projects towards

rhyolite in Georgia. Stronger evidence for the true nature of the J-Horizon is found in

seismic to well correlations. While the J-Horizon does correlate with basalt in Figure 2.3A, it does not in Figure 2.3B where this reflection is tied to two wells, neither of which intersected mafic igneous rocks. However in both of these panels the J-Horizon does correlate with the base of the Coastal Plain. This is also the case with Figure 2.3C, in which the base of the Coastal Plain in GGS-3456 correlates with the J-Horizon, an interpretation in contrast with McBride et al. (1989).

McBride et al. (1989) correlated GGS-3456 with COCORP GA-12, and interpreted a prominent reflection at 0.9 s as the base of the Coastal Plain; they interpreted the diabase layers in GGS-3456 as being one layer of mafic igneous rocks intercalated with sedimentary rocks, and correlated this package with the J-Horizon at 1.4 s. McBride et al. (1989) suggested that the sedimentary section between the base of the Cretaceous Coastal Plain (at 1515 m) and the mafic igneous package (at 1804 m) was Jurassic in age, and corresponded with relatively sub-horizontal reflections. This interpretation, however, requires an unreasonably fast velocity for the Tertiary-Cretaceous Coastal Plain sediments (3.3 km/s) and an unreasonably slow velocity for the Jurassic sedimentary section (1.156 km/s); thus the correlation of the J-Horizon with the base of the Coastal Plain is preferred.

The hypothesis that the J-Horizon corresponds with the base of the Coastal Plain is further tested by COCORP GA-19 which is tied to two wells (Figure 2.4). On this seismic line the interpreted J-Horizon is at 0.4 s on the north end, and 1.0 s on the south end. From shotpoint 1 – 500 this reflection dips at a rate of ~0.01 s/km, and then it appears to level out until shotpoint 675 where it resumes dipping toward the south. The J-Horizon intersects both GGS-194 and DP-163, at the base of the Coastal Plain in each

well. Extrapolating the J-Horizon 40 km to the north and 9 km to the South of GA-19, with a dip of 0.01 s/km, puts it intersecting the Fall Line at a time of 0 s and intersecting well DP-161 at a time of 1.09 s. On the basis of these simple calculations, the projection of the J-Horizon to known contacts demonstrates that the J-Horizon originates from the unconformity at the base of the Coastal Plain. The characteristics of this reflection are suggested to result from the strong acoustic impedance contrast between the poorly consolidated, low velocity Coastal Plain sediments and all underlying higher velocity formations.

This reinterpretation of the J-Horizon has larger implications as to the timing of the opening of the Atlantic Ocean. Austin et al. (1990) and Oh et al. (1995) observed that the J-Horizon overlay seaward dipping reflectors (SDRs), suggesting that CAMP was related to the start of sea floor spreading. This observation, along with the sub-horizontal nature of the J-Horizon, led Withjack et al. (1998) and Schlische et al. (2003) to conclude that the breakup of Pangea was a diachronous event with rifting ceasing in the southern basins prior to 200 Ma. The new interpretation that the J-Horizon is simply the base of the Coastal Plain eliminates the strongest line of evidence that the SDRs are unequivocally related to CAMP. This lack of a physical connection however does not prove that the SDRs are unrelated to CAMP. The only way to truly know the age of the SDRs is through sampling and dating.

2.5. REFERENCES CITED

Ackermann, H.D., 1983, Seismic-refraction study in the area of the Charleston, South Carolina, 1886 earthquake, in Gohn, G.S., ed., Studies Related to the Charleston, South Carolina, Earthquake of 1886—Tectonics and Seismicity: U.S. Geological Survey Professional Paper 1313, p. F1–F20.

Austin, J.A., Stoffa, P.L., Phillips, J.D., Oh, J., Sawyer, D.S., Purdy, G.M., Reitet, E., and Makris, J., 1990, Crustal structure of the southeast Georgia Embayment-Carolina Trough: preliminary results of a composite seismic image of a continental suture(?) and a volcanic passive margin: Geology, v. 18, p. 1023–1027, doi:10.1130/0091-7613(1990)018<1023:CSOTSG>2.3.CO;2.

Chapman, M.C., and Beale, J.N., 2010, On the Geologic Structure at the Epicenter of the 1886 Charleston, South Carolina, Earthquake: Bulletin of the Seismological Society of America, v. 100, p. 1010–1030, doi:10.1785/0120090231.

Chowns, T.M., and Williams, C.T., 1983, Pre-Cretaceous rocks beneath the Georgia Coastal Plain—Regional Implications, in Gohn, G.S., ed., Studies Related to the Charleston, South Carolina, Earthquake of 1886—Tectonics and Seismicity: U.S. Geological Survey Professional Paper 1313, p. L1–L42.

Daniels, D.L., Zietz, I., and Popenoe, P., 1983, Distribution of subsurface lower Mesozoic rocks in the southeastern United States as interpreted from regional aeromagnetic and gravity maps, in Gohn, G.S., ed., Studies Related to the Charleston, South Carolina, Earthquake of 1886—Tectonics and Seismicity: U.S. Geological Survey Professional Paper 1313, p. K1–K24.

Dillon, W.P., Paull, C.K., Buffler, R.T., and Fail, J.P., 1979, Structure and development of the Southeast Georgia Embayment and northern Blake Plateau – Preliminary analysis, in Watkins, J.S., Montadert, L., and Dickerson, P.W., eds., Geological and geophysical investigations of continental margins: American Association of Petroleum Geologists Memoir 29, p. 27-41.

Gohn, G.S., 1983, Geology of the basement rocks near Charleston, South Carolina—Data from detrital rock fragments in lower Mesozoic(?) rocks in Clubhouse Crossroads test hole #3, in Gohn, G.S., ed., Studies Related to the Charleston, South Carolina, Earthquake of 1886—Tectonics and Seismicity: U.S. Geological Survey Professional Paper 1313, p. E1–E22.

Hames, W.E., Renne, P.R., and Ruppel, C., 2000, New evidence for geologically instantaneous emplacement of earliest Jurassic Central Atlantic magmatic province basalts on the North American margin: Geology, v. 28, p. 859–862, doi:10.1130/0091-7613(2000)28<859:NEFGIE>2.0.CO;2.

Hames, W.E., Salters, V.J., Morris, D., and Billor, M.Z., 2010, The Middle Jurassic flood basalts of southeastern North America: Geological Society of America Abstracts with Programs, v. 42, p. 196.

Hamilton, R.M., Behrendt, J.C., and Ackermann, H.D., 1983, Land multichannel seismic-reflection evidence for tectonic features near Charleston, South Carolina, in Gohn, G.S., ed., Studies Related to the Charleston, South Carolina, Earthquake of 1886—Tectonics and seismicity: U.S. Geological Survey Professional Paper 1313, p. I1–I18.

Marzoli, A., Renne, P.R., Piccirillo, E.M., Ernesto, M., Bellieni, G., and De-Min, A., 1999, Extensive 200-million-year-old continental flood basalts of the Central Atlantic Magmatic Province: Science, v. 284, p. 616–618, doi:10.1126/science.284.5414.616.

McBride, J.H., 1991, Constraints on the structure and tectonic development of the early Mesozoic South Georgia Rift, southeastern United States; seismic reflection data processing and interpretation: Tectonics, v. 10, p. 1065–1083, doi:10.1029/90TC02682.

McBride, J.H., Nelson, K.D., and Brown, L.D., 1989, Evidence and implications of an extensive Mesozoic rift basin and basalt/diabase sequence beneath the southeast Coastal Plain: Geological Society of America Bulletin, v. 101, p. 512–520, doi:10.1130/0016-7606(1989)101<0512:EAIOAE>2.3.CO;2.

McFadden, S.S., Hetrick, J.H., Kellam, M.F., Rodenbeck, S.A., and Huddlestun, P.F., 1986, Geologic data of the Gulf Trough area, Georgia: Georgia Geological Survey Information Circular, v. 56, p. 211–214.

McHone, J.G., 2000, Non-plume magmatism and rifting during the opening of the central Atlantic Ocean: Tectonophysics, v. 316, p. 287–296, doi:10.1016/S0040-1951(99)00260-7.

Nomade, S., Knight, K.B., Beutel, E., Renne, P.R., Verati, C., Feraud, G., Marzoli, A., Youbi, N., and Bertrand, H., 2007, Chronology of the Central Atlantic Magmatic Province: implications for the Central Atlantic rifting processes and the Triassic-Jurassic biotic crisis: Palaeogeography, Palaeoclimatology, Palaeoecology, v. 244, p. 326–344, doi:10.1016/j.palaeo.2006.06.034.

Oh, J., Austin, A., Phillips, J.D., Coffin, M.F., and Stoffa, P.L., 1995, Seaward-dipping reflectors offshore the southeastern United States: seismic evidence for extensive volcanism accompanying sequential formation of the Carolina Trough and Blake Plateau basin: Geology, v. 23, p. 9–12, doi:10.1130/0091-7613(1995)023<0009:SDROTS>2.3.CO;2.

Olsen, P.E., 1997, Stratigraphic record of the early Mesozoic breakup of Pangea in the Laurasia-Gondwana rift system: Annual Review of Earth and Planetary Sciences, v. 25, p. 337–401, doi:10.1146/annurev.earth.25.1.337.

Olsen, P.E., Kent, D.V., Et-Touhami, M., and Puffer, J., 2003, Cyclo-, magneto-, and bio-stratigraphic constraints on the duration of the CAMP event and its relationship to the Triassic-Jurassic boundary, in Hames, W.E., McHone, J.G., Renne, P.R., and Ruppel, C., eds., The Central Atlantic Magmatic Province Insights from fragments of Pangea: Washington, D.C., American Geophysical Union, p. 7–32.

Schilt, F.S., Brown, L.D., Oliver, J.E., and Kaufman, S., 1983, Subsurface structure near Charleston, South Carolina – Results of COCORP reflection profiling in the Atlantic Coastal Plain, in Gohn, G.S., ed., Studies Related to the Charleston, South Carolina, Earthquake of 1886—Tectonics and seismicity: U.S. Geological Survey Professional Paper 1313, p. H1–H19.

Schlische, R.W., Withjack, M.O., and Olsen, P.E., 2003, Relative timing of CAMP, rifting continental breakup, and basin inversion: tectonic significance, in Hames, W.E., McHone, J.G., Renne, P.R., and Ruppel, C., eds., The Central Atlantic Magmatic Province Insights from fragments of Pangea: Washington, D.C., American Geophysical Union, p. 33–59.

Traverse, A., 1987, Pollen and spores date origin of rift basins from Texas to Nova Scotia as early late Triassic: Science, v. 236, p. 1469–1472, doi:10.1126/science.236.4807.1469.

Withjack, M.O., Schlische, R.W., and Olsen, P.E., 1998, Diachronous Rifting, Drifting, and Inversion on the Passive Margin of Central Eastern North America: An Analog for Other Passive Margins: The American Association of Petroleum Geologists Bulletin, v. 82, p. 817–835.

11 April 2013

David M. Heffner
PhD Candidate
Department of Earth and Ocean Science
University of South Carolina

Dear David,
Permission is granted for your use of the following material in your dissertation at the
University of South Carolina.

Heffner, D.M., Knapp, J.H., Akintunde, O.M., and Knapp, C.C., Preserved extent of
Jurassic flood basalt in the South Georgia Rift: A new interpretation of the J horizon,
Geology, February 2012, v. 40, p. 167-170, doi: 10.1130/G32638.1.

Best regards,

Jeanette Hammann

Jeanette Hammann
Associate Director, GSA Publications
(303) 357-1048
jhammann@geosociety.org

CHAPTER 3

TRANSFER ZONES OF THE SOUTH GEORGIA RIFT, USA: OBLIQUE RIFTING AND TECTONIC INHERITANCE OF THE ALLEGHANIAN SUTURE

The South Georgia Rift (SGR) is a buried Triassic rift system, which extends from the Atlantic margin to the Gulf of Mexico, and straddles the Late Paleozoic Alleghanian suture. Previous interpretations of the SGR have focused on mapping the spatial extent of the basin and not its regional structure-style. In this study, the SGR is mapped based on integration of existing observations and interpretations with additional well and seismic data.

Regional subsurface mapping suggests that the SGR comprises a series of asymmetric sub-basins that reverse polarity along the rift axis. From these reversals in polarity, two transfer zones are mapped that trend approximately orthogonal to the rift axis. Additional transfer zones are inferred from changes in basin geometry and stratigraphic thickness of the basin fill. The mapped structures correspond locally with Jurassic basalt flows and felsic volcanic rocks, suggesting there may be a relationship between magmatism and structural setting. A regional isopach map suggests upper crustal extension was more pronounced along the Alleghanian suture, although deformation was accommodated over a 400 km zone. Oblique rifting over the pre-existing continental weakness appears to have influenced the geometry of the SGR.

3.1. INTRODUCTION

Transfer zones are rift-transverse structures that transmit extensional strain between rift sub-basins, and accommodate differences in extensional strain and strain rate through movement on faults within the transfer zone (Gibbs, 1984; Rosendahl, 1987; Faulds and Varga, 1998; Morley, 1999b). These structures can range from discrete faults to more complex zones of deformation (Gibbs, 1984; Rosendahl, 1987; Morley et al., 1990; Faulds and Varga, 1998; Morley, 1999b).

Rift system asymmetry has been observed in many rifts, where the bounding normal faults of adjacent sub-basins may be found on opposite flanks of the rift (Rosendahl, 1987; Faulds and Varga, 1998). These reversals in basin polarity require a transfer zone to accommodate differences in extension along the rift. Transfer zones have been observed in rifts globally with one exception being the exposed Triassic rift basins of eastern North America (Schlische, 2003).

The exposed Triassic basins of eastern North America are characterized as elongate asymmetric troughs 20 - 80 km wide that trend sub-parallel to the regional Paleozoic tectonic fabric and appear to have formed through reactivation of older compressional faults (Schlische, 2003). The entire Triassic extensional system is roughly 400 km wide and underlain by a gently undulating Moho (Withjack et. al., 1998; Withjack et al., 2012).

The South Georgia Rift (SGR) is also a Triassic basin system preserved along the eastern North American margin, with a flat Moho, and a similar width scale to the more northerly Triassic basin system (Figure 3.1; Cook et al., 1980; McBride, 1991). The SGR, however, does differ from the other Triassic basins along the eastern North

American margin in that well data show it straddles the Late Paleozoic Alleghanian suture between Gondwana and Laurentia and extends southwest to the Gulf of Mexico (Chowns and Williams, 1983; Daniels et al., 1983).
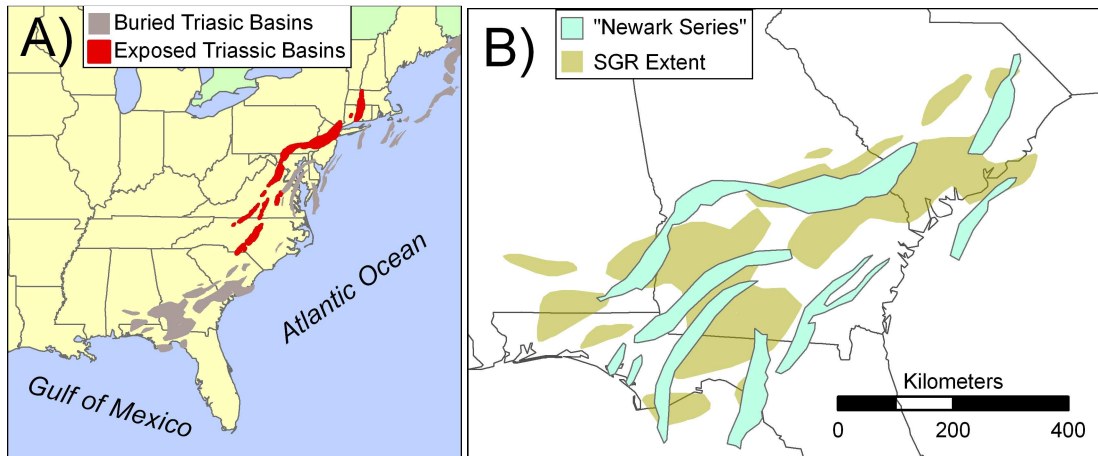
Figure 3.1. Triassic rift basins of eastern North America. A) Exposed Triassic basins are shown in red and buried basins are shown in grey (after Olsen, 1997; after Withjack et al., 1998; this study). B) Comparison of width extent of South Georgia Rift with Triassic rift system in the central US onshore and offshore (after Olsen, 1997 and Withjack et al., 1998).

The SGR is oblique to the proposed Alleghanian suture and has been suggested to exhibit a change in structural style along the axis of the rift (Chowns and Williams, 1983; Tauvers and Muehlberger, 1987; McBride, 1991; Sartain and See, 1997). Modeling studies indicate that transfer zones will develop in oblique rifts and in particular to accommodate changes in the structural style of a rift (Corti et al., 2003; van Wijk, 2005; van Wijk and Blackman, 2005). Several studies have projected oceanic fracture zones onshore as transfer zones (Tauvers and Muehlberger, 1987; Etheridge et al., 1989); however, the purported presence of transfer zones within the SGR has not been substantiated through observations of reversals in sub-basin polarity (McBride and Nelson, 1988; Tauvers and Muehlberger, 1988, McBride, 1991). The purpose of this study is to better define the geometry and major structures of the SGR through regional

mapping based on compilation of available well data and seismic reflection and refraction data. Observations are presented here that suggest the SGR is divided into three structural domains separated by transfer zones (Figure 3.2), and for the first time, a regional isopach map of the preserved basin thickness is presented.

3.2. BACKGROUND

3.2.1 SOUTH GEORGIA RIFT

Redbeds brought to the surface as cuttings from a deep-water well drilled near Florence, South Carolina were the first reported observation that "Newark Supergroup-like rocks" were present beneath portions of the Coastal Plain (Darton, 1896). Sporadic exploration and scientific drilling provided further evidence that Triassic basins were present beneath the Coastal Plain of South Carolina, Georgia, Alabama, and Florida (Applin and Applin, 1964; Marine and Siple, 1974; Gohn et al., 1978). Daniels et al. (1983) proposed, on the basis of aeromagnetic data, that these seemingly separate pockets of Triassic rock were encompassed within a singular giant rift basin, which they called the South Georgia Rift (Figure 3.3A). Chowns and Williams (1983) completed a comprehensive study of deep wells in Georgia, Florida, and Alabama to assess the extent of the South Georgia Rift and relied on interpretations of potential field data for determining the boundaries where well control was not available (Figure 3.3B). As part of a larger study investigating the entire eastern North American margin, Klitgord et al. (1988) produced a different picture of the extent of the SGR based solely on interpretation of aero-magnetic data (Figure 3.3C). Sartain and See (1997) studied the southwestern portion of the SGR by integrating interpretations of potential field data with Landsat and seismic reflection data to produce an isopach of the basin (Figure 3.3D).
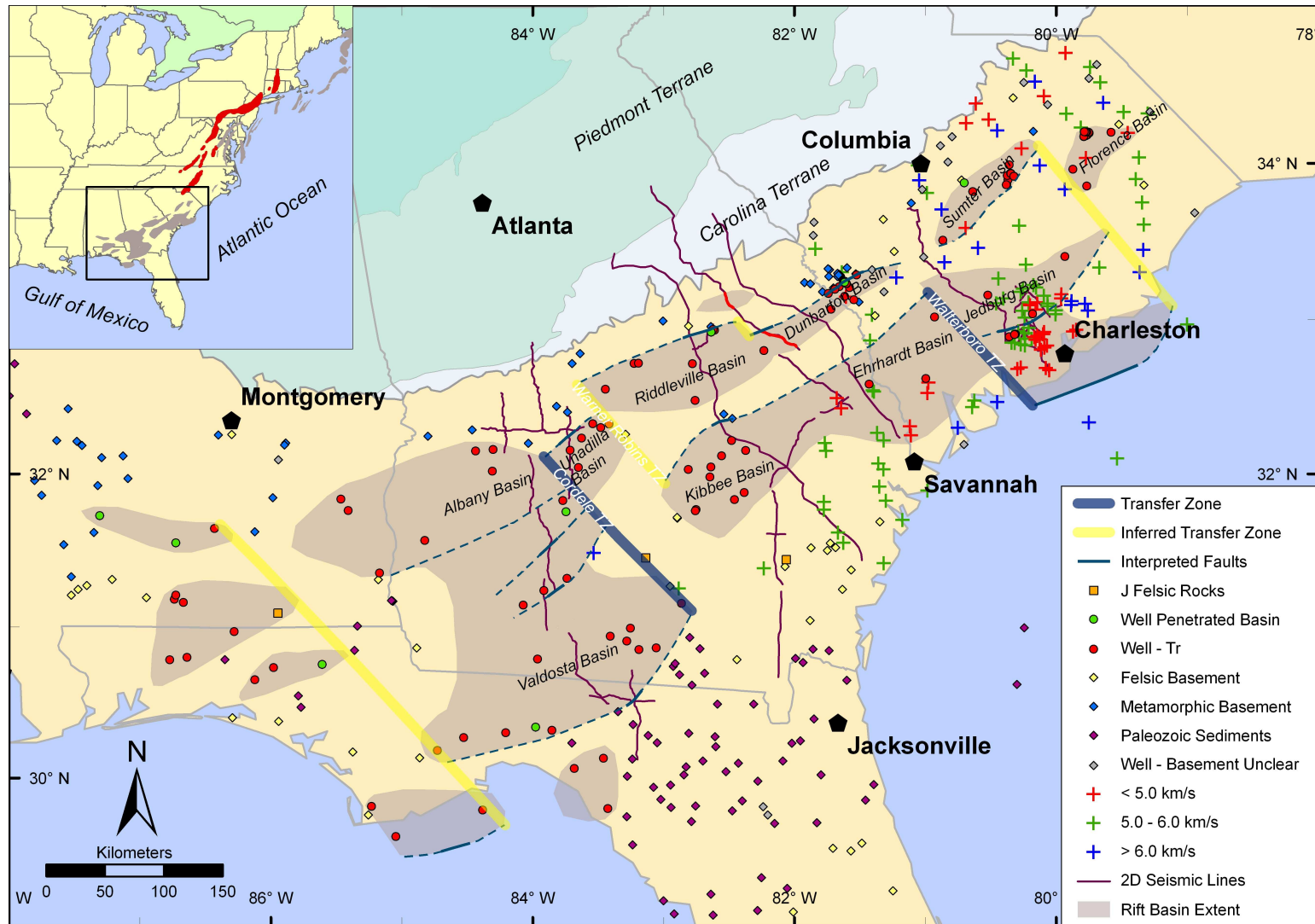
Figure 3.2. Major structures of the South Georgia Rift (SGR). Wells are shown as filled shapes. Crosses are locations where sub-Coastal Plain seismic velocities are reported. Major faults are solid where interpreted and dashed where hypothesized.
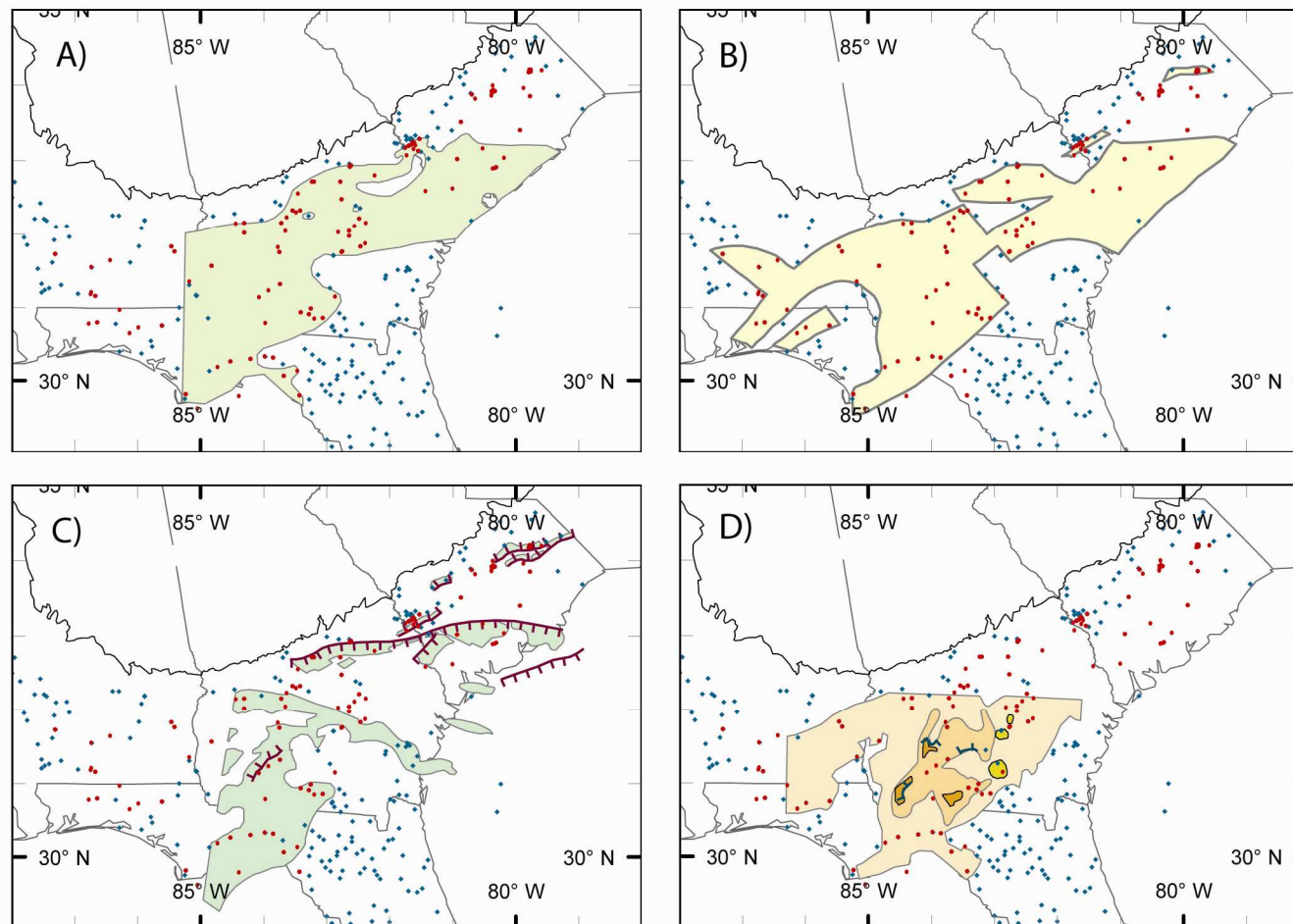
Figure 3.3. Previous interpretations of the extent of the South Georgia Rift (SGR). Blue dots indicate wells outside the SGR and red dots indicated wells inside the SGR. A) Daniels et al. (1983). B) Chowns and Williams (1983). C) Klitgord et al. (1988). D) Sartain and See (1997).

The stratigraphy of the SGR is generalized as a Triassic redbed syn-rift section that is intruded by Jurassic diabase sills and dikes, and locally topped by basalt flows in select locations (Gohn et al., 1978; Chowns and Williams, 1983; Heffner et al., 2012). Although previous studies interpreted a major basalt layer capping the majority of the SGR based on geophysical data, it recently was shown that the basalt is only preserved locally (Heffner et al., 2012). A prominent unconformity separates the Triassic / Jurassic section from the Cretaceous and younger Coastal Plain and is easily identifiable on seismic reflection profiles (Heffner et al., 2012). Sediments generally appear to originate from a fluvial environment, with conglomerates encountered in a few wells near the border faults of the Dunbarton and Riddleville basins, which are interpreted as alluvial fan deposits (Marine and Siple, 1974; Chowns and Williams, 1983).

3.2.2 RIFT GEOMETRY

The geometry of rifts are typically defined either in the sense of structural style (i.e. symmetric vs. asymmetric) or by mode of extension (i.e. wide vs. narrow; Corti et al., 2003; Ziegler and Cloetingh, 2004). Early tectonic studies of rifts were generally more concerned with the structural style in determining the geometry of a rift (Bally, 1982; Gibbs, 1984). Early models of rifting considered the symmetric pure shear model and were successful at predicting the first order effects of rifting on subsidence of a passive margin (McKenzie, 1978). Interpretation of seismic images and observations of field relationships, however, suggested that rift basins were asymmetric (Bally, 1982; Wernicke, 1985; Rosendahl, 1987), and a simple shear detachment model was proposed to explain the asymmetry (Wernicke, 1985). Later studies coupled a simple shear model, to explain shallow brittle deformation, with a pure shear model to explain deep ductile

deformation (Kusznir et al., 1995). Whether or not the entire lithosphere deforms in a pure shear or simple shear mode, the upper crustal expression of rifts is accepted to be asymmetric such that the fundamental building block of a rift is the half-graben (Bally, 1982; Gibbs, 1984; Rosendahl, 1987; Morley et al., 1990; Stewart, 1998; Schlische, 2003; Corti, 2012).

Three end member modes of continental extension are generally recognized on the basis of modeling: narrow rifts, wide rifts, and core complexes (Buck, 1991; Corti et al., 2003 and references therein). Core complexes are often associated with wide rifts and are considered by some authors to be a special case of wide rifts, not a separate mode of extension (e.g. Brun, 1999). Most models demonstrate that the strength of the lithosphere is the dominant factor determining the mode of rifting, although there is some disagreement as to which specific parameters exhibit primary control (Corti et al., 2003, and references therein). In general, extension of a thick, weak lithosphere results in a wide rift, whether the weakness is caused by higher than normal heat flow (Buck, 1991; Buck et al., 1999), mechanically weak layers within the lithosphere (Brun, 1999), or changes in mantle composition (Lizarralde et al., 2007). Narrow rifts are generally thought to occur when a strong lithosphere is extended (Buck, 1991; Buck et al., 1999; Brun, 1999; Corti et al., 2003, and references therein). Extension of pre-existing weaknesses has been observed to play an important role in localizing extension (Morley, 1999a; Ziegler and Cloetingh, 2004; Corti, 2012), even when the initial thermal conditions may favor a wide rift (Keranen et al., 2009).

One important parameter that can have an effect on both the structural style and mode of rifting is the obliquity of extension relative to a pre-existing structural fabric

(Withjack and Jamison, 1986; Morley, 1999a; Ziegler and Cloetingh, 2004; Brune et al., 2012; Corti, 2012). Oblique extension can result in a diffuse zone of deformation which eventually localizes into distinct en-echelon shear zones reflecting the direction of principal stresses (Withjack and Jamison, 1986; Corti et al., 2003; Brune et al., 2012), and may ultimately be the cause of alternating, asymmetric rift geometries (Morley et al., 1990; Morley, 1999a; van Wijk, 2005; Corti, 2012). If the angle of obliquity is too high, either new normal faults will form cross-cutting the old structural fabric in a symmetric structural style (Ziegler and Cloetingh, 2004), or strike-slip deformation may occur (Brune et al., 2012; Corti, 2012).

3.2.3 TRANSFER ZONES

Transfer zones are rift transverse structures that transfer extensional strain between major normal faults, and accommodate differences in extensional strain and strain rate through structures within the transfer zone (Gibbs, 1984; Rosendahl, 1987; Morley et al., 1990; Faulds and Varga, 1998; Morley, 1999b). These structures can range from discrete faults to more complex zones of deformation consisting of ramps, overlapping normal faults, en echelon strike-slip faults, and folds (Gibbs, 1984; Rosendahl, 1987; Morley et al., 1990; Faulds and Varga, 1998; Morley, 1999b).

There are a number of different proposed classification schemes and terminologies for describing transfer zones (Rosendahl, 1987; Morley et al., 1990; Faulds and Varga, 1998; Schlische and Withjack, 2009). For this paper, the generic term "transfer zone" is used (Morley, 1999b), since the spatial resolution of the data is too sparse to truly constrain the style of these structures.

Rift system asymmetry has been observed in many rifts, where the bounding normal faults of adjacent sub-basins are found on opposite flanks of the rift (Rosendahl, 1987; Faulds and Varga, 1998). These reversals in basin polarity require a transfer zone to accommodate and transfer the strain between normal faults. Many discrete transfer faults have been identified in extensional terranes; however, it is generally thought that diffuse accommodation zones are most common (Rosendahl, 1987; Morley et al., 1990; Faulds and Varga, 1998). While the largest transfer zones and cross-rift faults separate structural zones with opposite dip, synthetic transfer zones, where displacement is transferred between faults that dip in the same direction, are perhaps the most common (Morley et al., 1990; Faulds and Varga, 1998).

Oblique rifting of a pre-existing structural fabric has been observed through field relations and demonstrated through modeling to result in reversals of sub-basin polarity and subsequent development of transfer zones (Morley, 1999a; Corti et al., 2003; van Wijk, 2005; Corti, 2012). In addition to oblique rifting, modeling has shown that differences in rheology across a major crustal boundary can stall rift propagation, resulting in the formation of a transfer zone at the crustal discontinuity (van Wijk and Blackman, 2005).

3.3. DATA

Data used in this study consisted largely of seismic reflection profiles and well data compiled from numerous sources. The seismic reflection profiles were not reprocessed and for the most part were unmigrated. Geophysical logs from the wells were primarily available only in raster format. Results from some seismic refraction

studies were used to assist in interpretation of basin extent and, in a few cases, basin thickness.

3.3.1 WELL DATA

Well data were compiled from a variety of sources including scientific journals, federal and state government publications, and well logs (Appendix A). In all cases, reported latitude and longitudes were used when available, and location information from primary sources was preferred. Only wells that penetrated the unconformity beneath the Coastal Plain were recorded in the database. The locations of the 321 wells are shown in Figure 3.4, with the encountered lithology indicated by the shape and color of the markers.

Dip logs were available for only three of the wells in Georgia: GGS-3122, GGS-3456, and GGS-3457. Dip angles, relative to a horizontal plane, and dip azimuths, relative to north, are reported on the logs at approximately 1 meter intervals. The dip azimuths for the upper 100 meters of the Triassic sedimentary section for wells GGS-3456 and GGS-3457 were cataloged as one of the secondary intercardinal directions (i.e. north-north east). Only 76 m of sub-Coastal Plain section for well GGS-3122 were logged, the entirety of which was cataloged as one of the secondary intercardinal directions. The resultant rose diagrams, which indicate the most frequently reported dip azimuths, are shown in Figure 3.4.
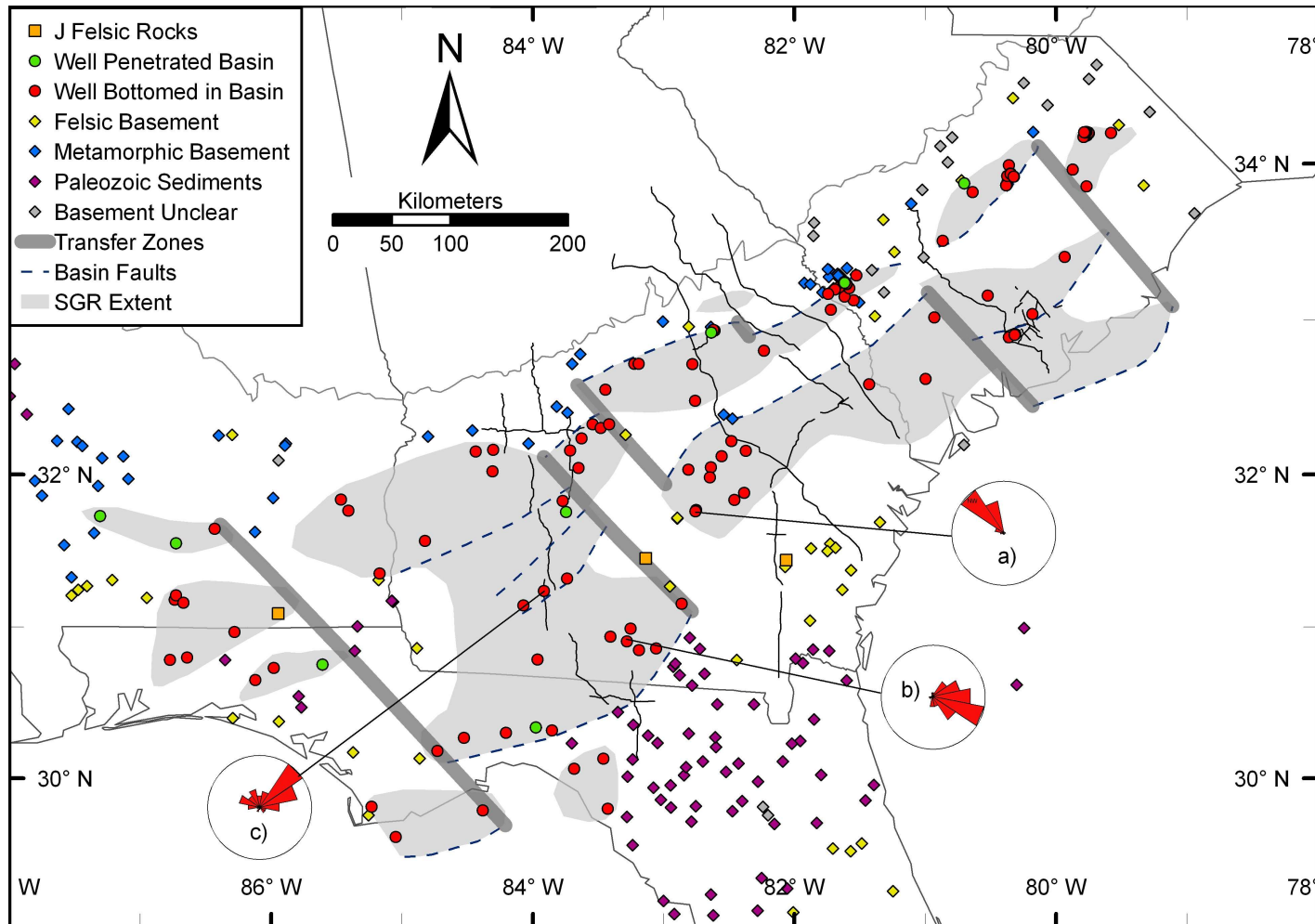
Figure 3.4. South Georgia Rift well data. Wells are shown as filled shapes, with circles representing wells inside the basin, diamonds representing wells outside the basin, and the orange squares marking felsic Jurassic rocks (possibly inside or outside) (Neathery and Thomas, 1975; Heatherington et al., 1999; Heatherington and Mueller, 2003). Rose diagrams derived from ~100m of Triassic basin fill for wells: a) GGS-3457, b) GGS-3122, c) GGS-3456.

3.3.2 SEISMIC REFLECTION DATA

With the exceptions of the Charleston, South Carolina area and the Savannah River National Lab (SRNL), publicly available seismic reflection data acquired across the SGR are sparse and are limited to regional-scale programs such as COCORP and three regional profiles acquired by SeisData Services (Cook et al., 1981; Nelson et al., 1985; Behrendt, 1985; McBride, 1991). The COCORP program across Georgia consisted of a series of 15 lithospheric-scale profiles across the Coastal Plain province spanning the south-central and southeastern portion of that state totaling ~1000 km (Cook et al., 1981; McBride, 1991). Velocity analysis for COCORP GA-5 indicates the possibility of sub-Coastal Plain reflectors with velocities ranging from 4 to 5 km/s beneath portions of this line, shown as red lines in Figure 3.5 (Cook et al., 1981).

The SeisData lines, numbered 4, 6, and 8 from east to west, run from the northwest to southeast in central South Carolina (SeisData 4) and eastern Georgia (SeisData 6 and 8). The Coastal Plain portions of the SeisData lines span ~700 km in total. SeisData 4 and 6 were recorded to a two-way travel time of 6s, and SeisData 8 was recorded to 8s. The Coastal Plain portion of SeisData 6 recently was reprocessed by Akintunde et al. (2013).

Several focused programs to investigate possible seismogenic faults involved collection of active source seismic data in the Charleston, South Carolina area, and at SRNL (Hamilton et al., 1983; Schilt et al., 1983; Yantis et al., 1983; Domoracki, 1995). Four seismic reflection studies in the Charleston, South Carolina area include three onshore 2D seismic reflection programs, the data for some of which have been recently reprocessed (Chapman and Beale, 2010), and an offshore 2D seismic program (Behrendt

42

et al., 1983). A program to investigate reactivation of rift related faults near SRNL was carried out in the 1990s and included 2D seismic profiles acquired by Conoco over the Dunbarton sub-basin (Domoracki, 1995).

3.3.3 SEISMIC REFRACTION DATA

There have been several programs to collect seismic refraction data throughout the region since the 1950s (Appendix B). Bonini and Woollard (1960) is perhaps the best known and most widely cited seismic refraction study of this region. They used dynamite to collect data at 57 different locations throughout North Carolina and South Carolina with 12 stations over line spreads of ~360 meters and varying shot distances. Similar data collection parameters also were used by the same research group for refraction studies in Central Georgia and near the coast of Georgia and South Carolina (Woollard et al., 1957; Pooley, 1960).

Two other seismic refraction programs were carried out in the late 1970s and early 1980s to investigate the velocity structure around Charleston, South Carolina (Amick, 1979; Ackermann, 1983). Amick (1979) used quarry blasts as an energy source with long offset station spacing. Ackerman's (1983) study used dynamite as an energy source and had shorter station spacing of 120 m and total spread lengths of 2760 m.

Smith and Talwani (1986) and Luetgert et al. (1994) reported on two other seismic refraction studies in South Carolina investigating the shallow crustal structure. Smith and Talwani (1986) were investigating the hypothesized presence of a Triassic basin in the Bowman Seismogenic zone. They used long offsets of about 1 to 3 km per station and a long spread length of 12 to 20 km per line. Luetgert et al. (1994) used a
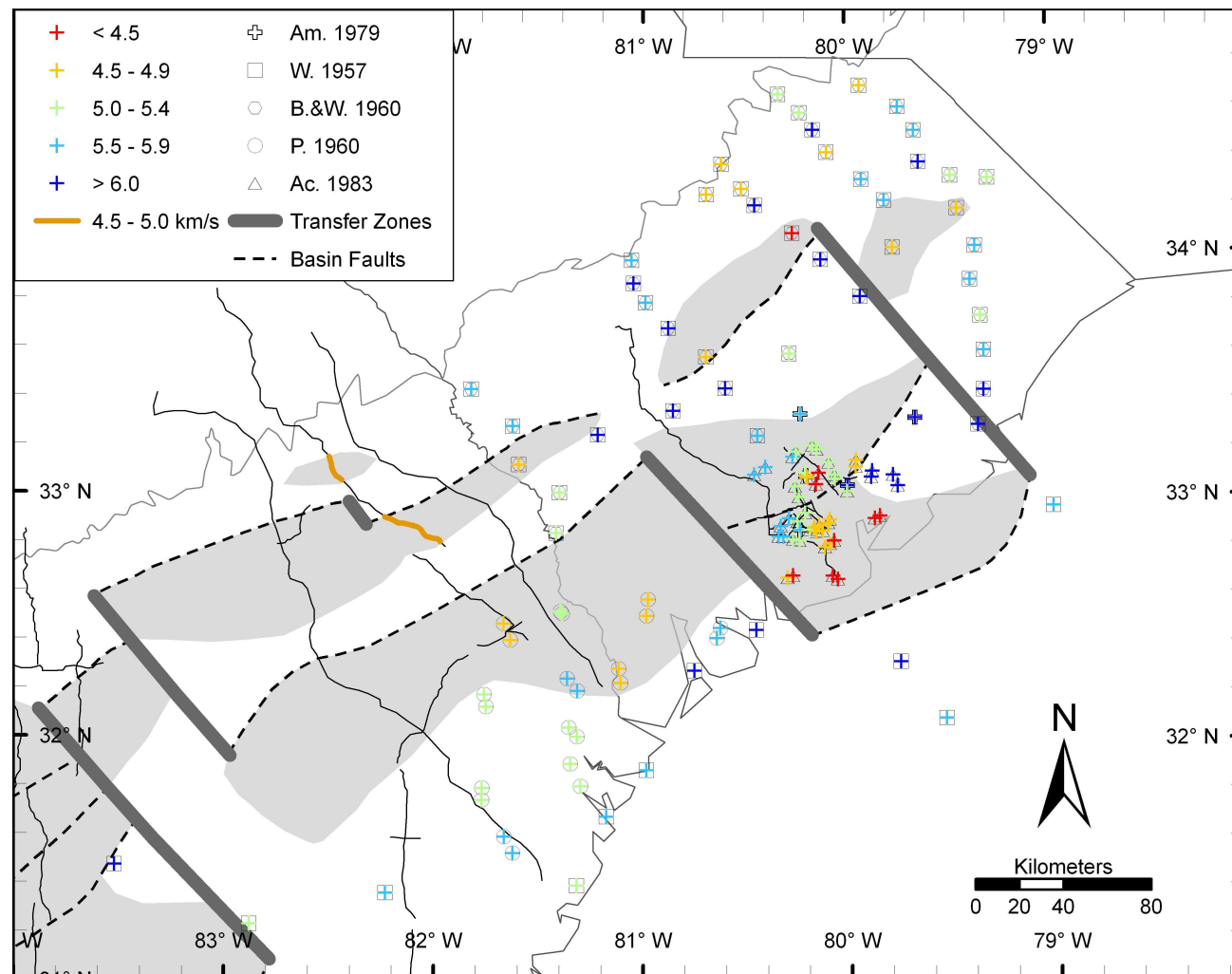
Figure 3.5. Map of sub-Coastal Plain seismic velocities in South Carolina and Georgia. The color of the cross indicates the seismic velocity in km/s. The shape surrounding the cross indicates the study of origin. Colored line segments are derived from analysis of seismic reflection data (Cook et al., 1981). Am. 1979 - Amick (1979), W. 1957 - Woollard et al. (1957), B&W 1960 - Bonini and Woollard (1960), P. 1960 - Pooley (1960), Ac. 1983 - Ackermann (1983).

44

similarly distant station spacing of 1 km and investigated a profile starting 20 kilometers north of the Dunbarton basin running 120 kilometers to the southeast. Luetgert et al. (1994) used sophisticated ray path modeling software to interpret their results, which predict a uniform 3.5 km/s layer underlain by a uniform 5.5 km/s layer running continuously from north of the Dunbarton basin all the way through the town of Walterboro, South Carolina.

The velocities reported at the base of the Coastal Plain from some of the studies (Woollard et al., 1957; Bonini and Woollard, 1960; Pooley, 1960; Amick, 1979; Cook et al., 1981; Ackermann, 1983) are shown in Figure 3.5. The shape of the markers denotes the different studies, and the color of the markers denote the reported velocity with warm colors representing slower velocities and the cool colors representing faster velocities. True velocities are plotted here where lines were reversed; however, where no true velocities were reported, apparent velocities from unreversed lines are plotted.

3.4. OBSERVATIONS

3.4.1 NORTHEASTERN SOUTH GEORGIA RIFT

There are 35 wells in Florence and Sumter counties of South Carolina reported to have encountered rocks correlated with the Triassic Newark Supergroup (Figure 3.6; Darton, 1896; Steele and Colquhoun, 1985). A sub-Coastal Plain velocity of 6 km/s separates the well clusters into two groups: one identified in previous studies as the Florence basin (Marine and Siple, 1974; Chowns and Williams, 1983; Steele and Colquhoun, 1985), and the other referred to here as the Sumter basin. Within the Sumter basin, well ORG-393 encountered a conglomeratic layer, and RIC-543 encountered a 3m thick layer of redbeds between the Coastal Plain sediments and weathered gneiss.
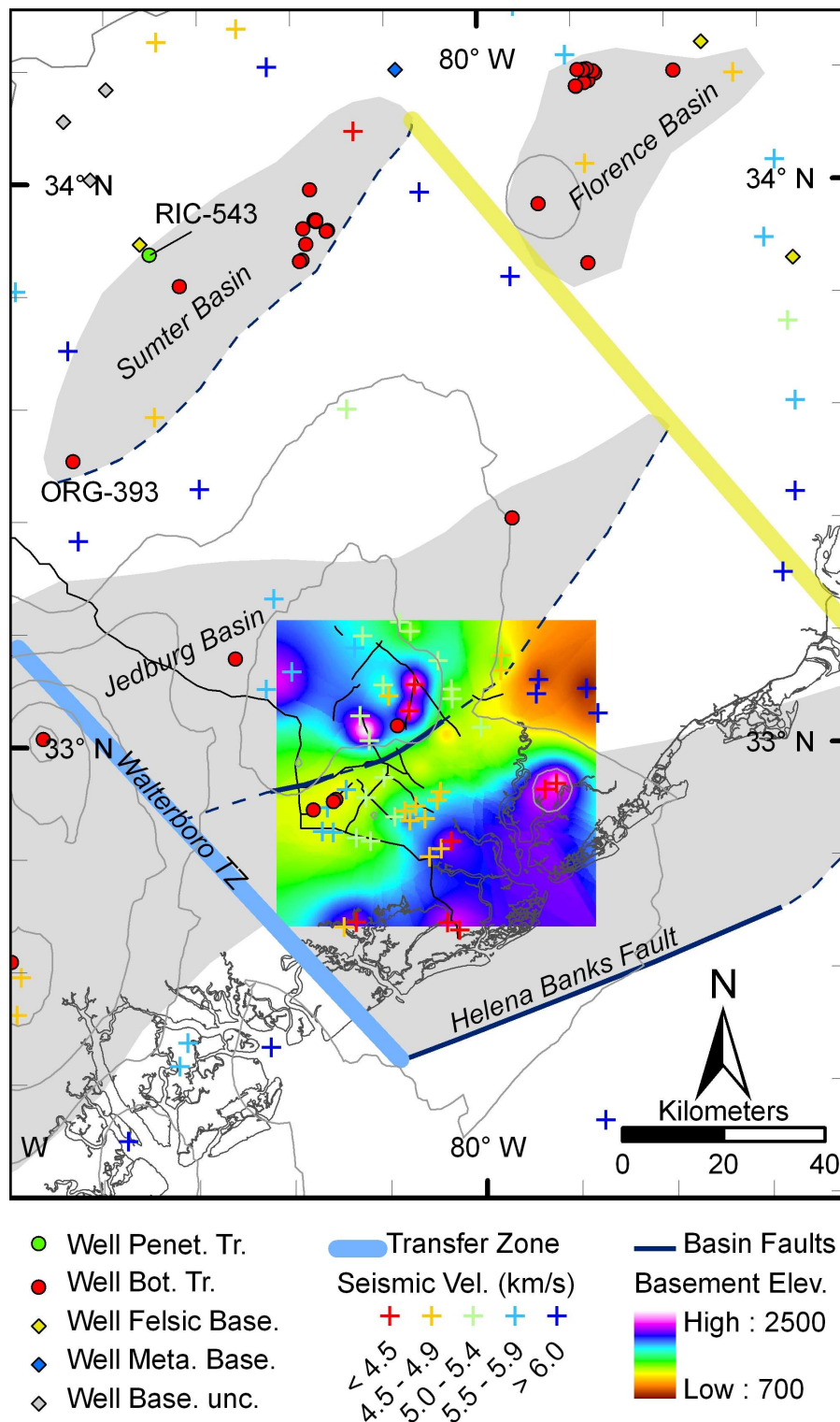
Figure 3.6. Map of the Northeast South Georgia Rift structural domain. Contour lines are derived from the isopach and mark every 500 meters of basin thickness. Grid of basement elevation in meters below sea level is derived from Ackermann (1983).

In the vicinity of Summerville, South Carolina (northwest of Charleston), it has been long established that a Triassic basin is present directly underneath the Coastal Plain, later referred to as the Jedburg basin (Cooke, 1936; Mansfield, 1937; Behrendt, 1985). The Jedburg basin has a defined boundary on the southeast, where sub-Coastal Plain seismic velocities on the order of 4-5 km/s are separated from seismic velocities greater than 6.0 km/s. This southeastern boundary correlates with a steep gradient in the elevation of a high velocity layer observed in a series of seismic refraction surveys (Figure 3.6; Ackermann, 1983). This abrupt change in the elevation of a high velocity layer correlates with a change in reflective character on seismic reflection line SeisData 4 where southeast dipping reflections beneath the Coastal Plain terminate against a zone of low reflectivity (Figure 3.7). Within the mapped boundaries of the Jedburg basin, the geometry of sub-Coastal Plain reflections on SeisData 4 are dipping to the South, and the deeper reflections appear to have an increased dip angle relative to the shallower sub-Coastal Plain reflections. To the South of the Jedburg basin, redbeds beneath a layer of Jurassic basalt were encountered in the Clubhouse Crossroads wells (Gohn et al., 1978). Seismic refraction velocities in the vicinity of the Clubhouse Crossroads wells are on the order of 4 - 5 km/s. The depth from the base of the Coastal Plain to the high velocity layer steadily increases southwards towards the offshore Helena Banks Fault (Behrendt, 1981; Ackermann, 1983).
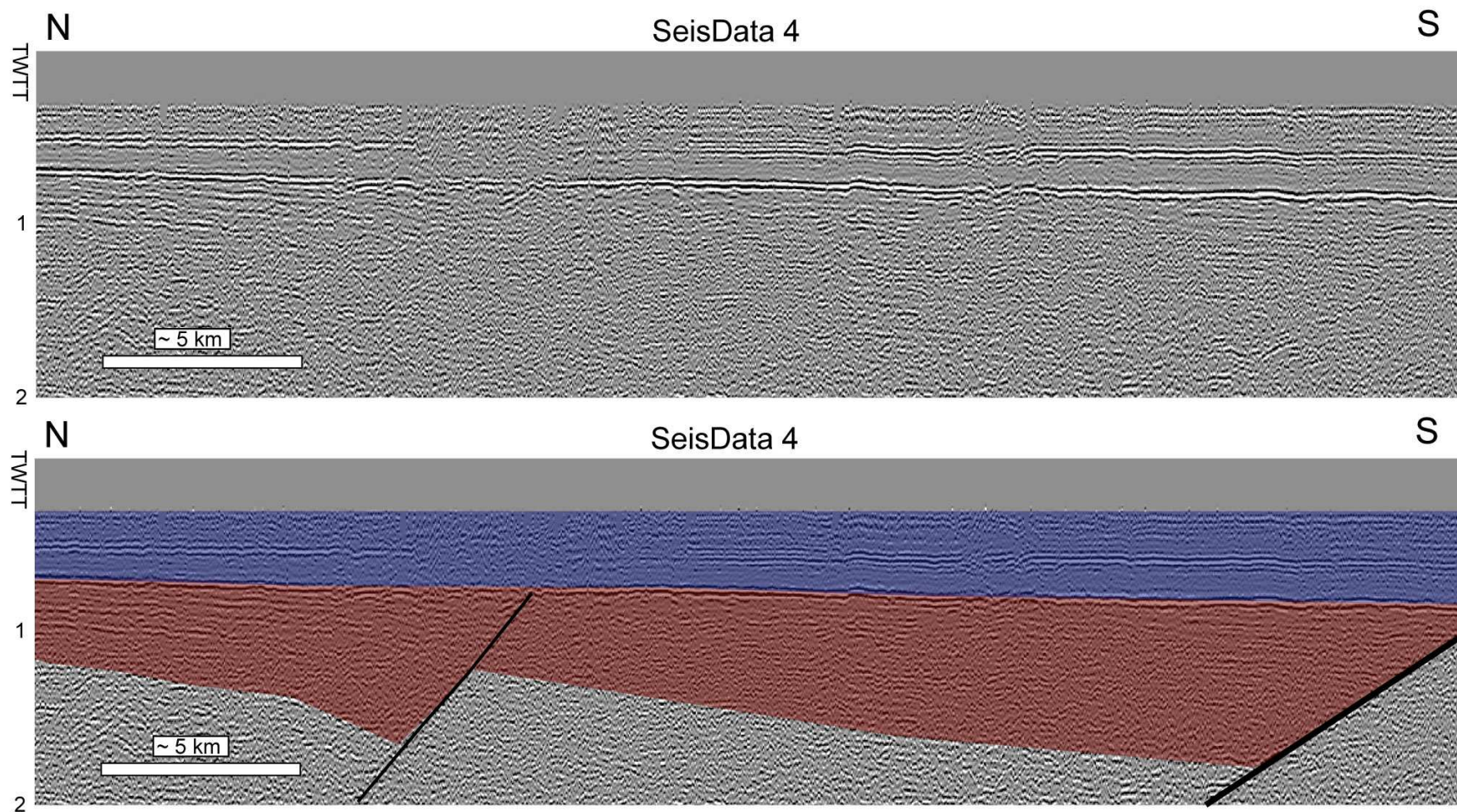
Figure 3.7. Portion of seismic line SeisData 4 shown in two-way travel time (twtt). Uninterpreted section on top. The Coastal Plain is marked in blue and the Triassic basin is marked in red with a basin normal fault as a dark black line. SeisData seismic lines licensed and provided courtesy of Geophysical Pursuit, Inc.

3.4.2 CENTRAL SOUTH GEORGIA RIFT

The Penbranch Fault has been well studied in South Carolina and has been shown through seismic imaging and other geophysical techniques to be the major normal fault bounding the Dunbarton basin on the north (Figure 3.8; Cumbest et al., 1992; Domoracki, 1995). Well DRB-9, just to the south of the Penbranch fault, penetrated 470 m of reddish-brown breccia below the Coastal Plain before bottoming in metamorphic rocks (Marine and Siple, 1974). The Dunbarton basin is an asymmetric basin, thickening towards the northwest and reaching a maximum thickness on the order of 2 km (Domoracki, 1995). The Penbranch Fault projects along strike into Georgia where the Magruder Fault was identified on COCORP GA-5 (Petersen et al., 1984).

The Riddleville basin, first identified by aeromagnetic data, thickens towards the north and reaches a maximum thickness of roughly 2 km (Daniels et al., 1983; Petersen et al., 1984). The northern boundary fault is tightly constrained by a series of boreholes (Figure 3.8). Well GGS-3441 encountered 1.4 km of conglomerate beneath the Coastal Plain, and well GGS-3447 penetrated 2.2 km of the basin fill (Figure 3.9).

To the south of the Dunbarton basin, the Norris-Lightsey well (COL-241) encountered Triassic redbeds (Traverse, 1987) in a basin referred to here as the Ehrhardt basin. The Norris-Lightsey well was drilled through 3.5 km of intercalated redbeds and diabase. Seismic refraction work within this basin indicates a basin thickness ranging from 1.5 – 2.5 km near the center of the basin and a thickness of 0.2 km near the southern end (Pooley, 1960).

South of the Riddleville basin, seismic profile SeisData 8 crossed over a basin referred to as the Kibbee basin by Behrendt (1985). A south-dipping band of reflectivity

49
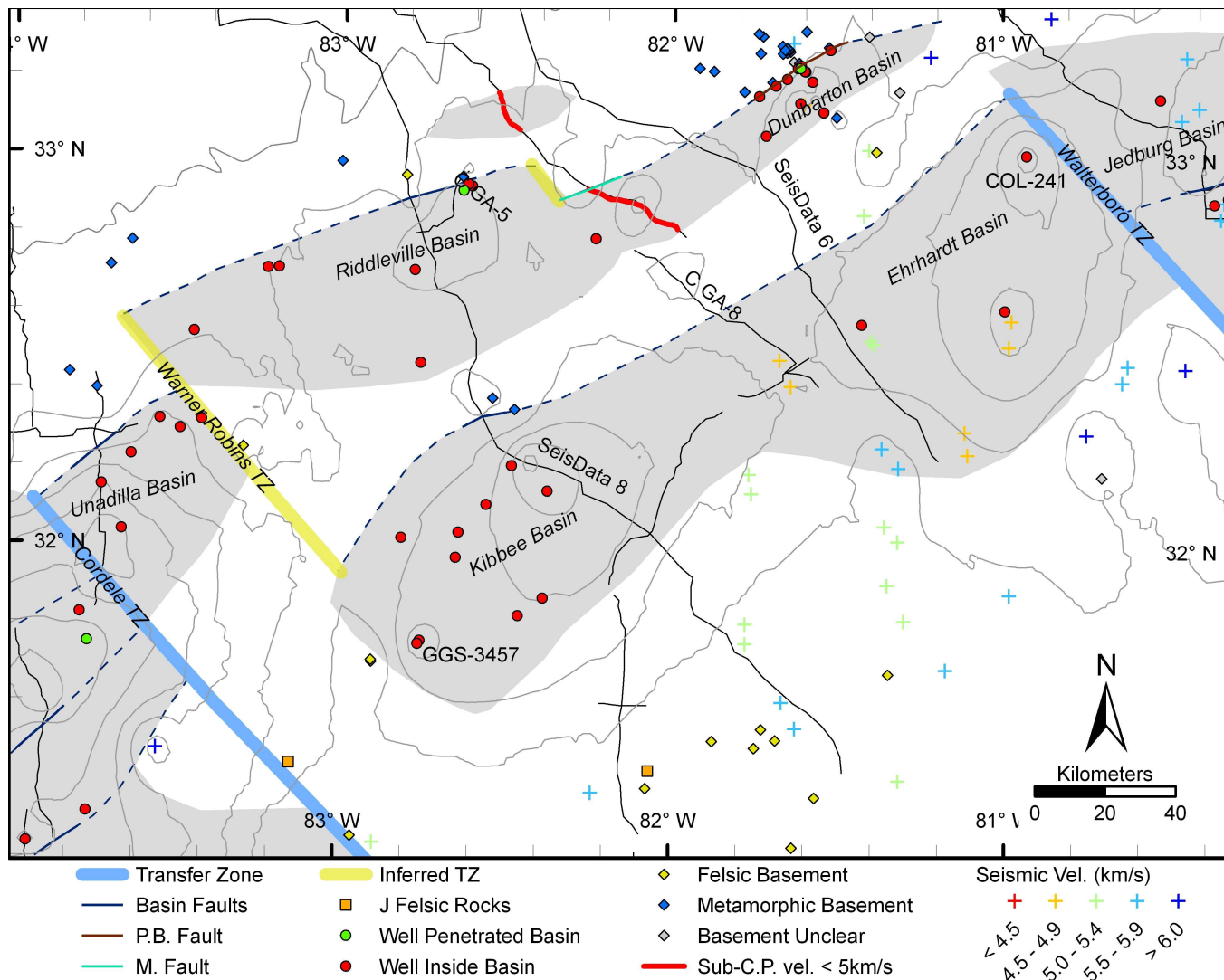
Figure 3.8. Map of the Central South Georgia Rift structural domain. Contour lines derived from the isopach mark every 500 meters of basin thickness. P.B. Fault - Pen Branch Fault, M. Fault - Magruder Fault.
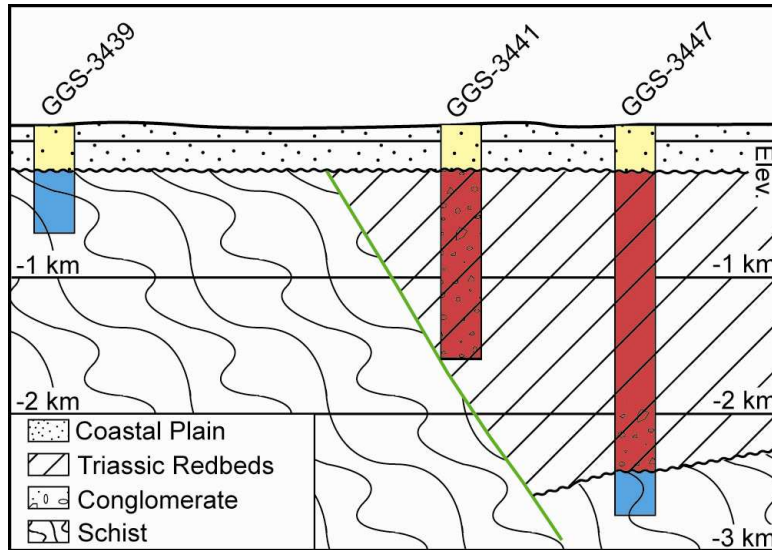
Figure 3.9. Cross-section of wells crossing northern border fault of the Riddleville basin.

is observed on SeisData 8, immediately beneath a dim zone of an otherwise high-amplitude, sub-horizontal reflection at ~0.8 s (Figure 3.10). This band of reflectivity dips south for 5 km to a depth equivalent of ~1.5 s, where the dip of this reflective package reverses. To the south of this reflective package, low-angle, north-dipping reflections are observed beneath sub-horizontal reflections. Approximately 60 km southwest of SeisData 8, the A. P. Snipes well (GGS-3457) was drilled to a total depth of 3.5 km, bottoming in redbeds. A dip log from the A. P. Snipes well indicates that the upper 100 m of redbed section are dipping to the northwest (Figure 3.4).

A high-amplitude reflection is observed on COCORP GA-19 at 0.5 s on the north end of the line continuing to 1.0 s on the south (Figure 3.11). Beneath this prominent reflection, a wedge of south-dipping reflectivity thickens southward from station 250, reaching a maximum depth equivalent of 2.2 s beneath station 500. Beneath the zone of south-dipping reflectivity, between stations 500 and 650, a wedge of north-dipping reflections thickens northward.
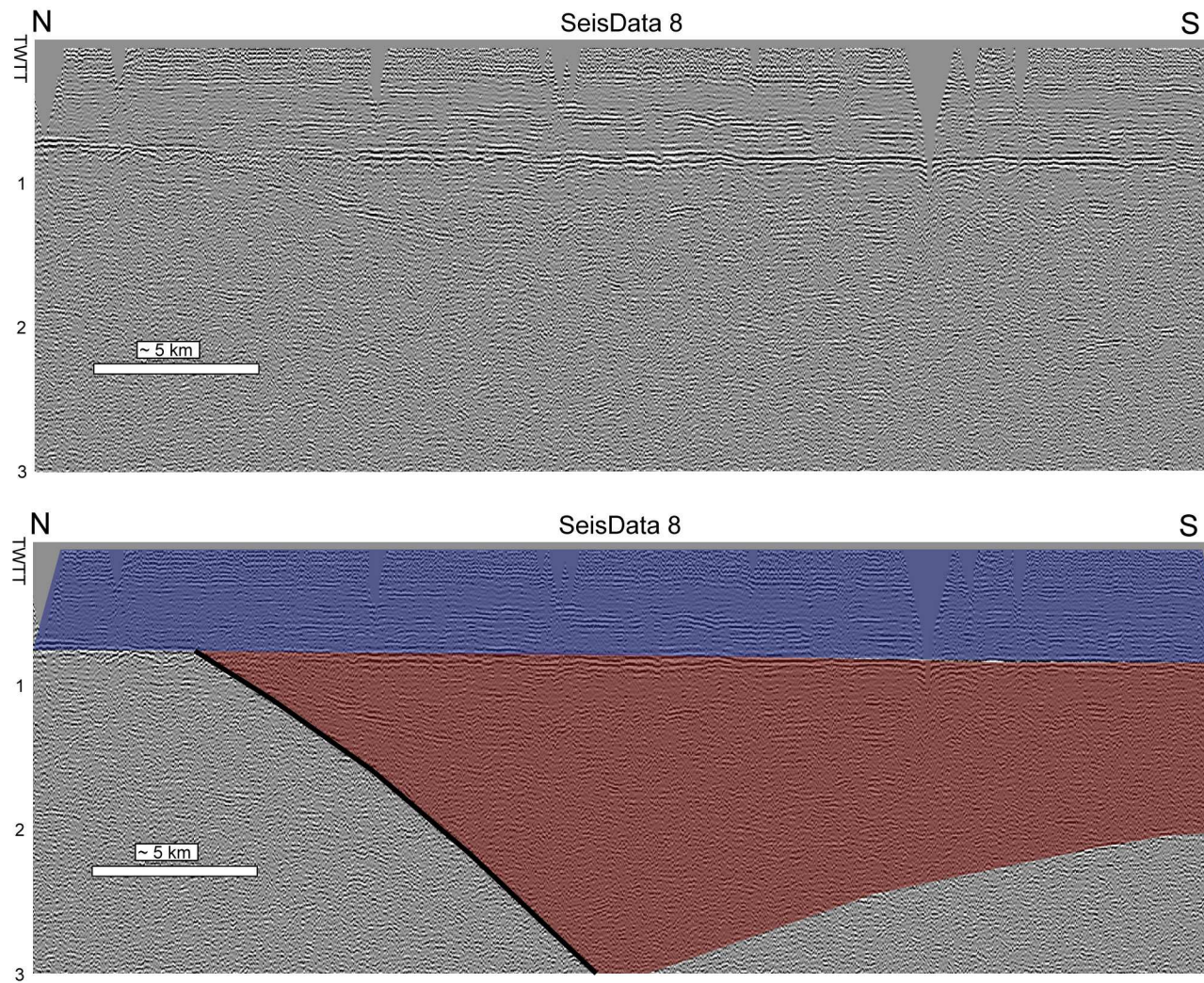
Figure 3.10. Portion of seismic line SeisData 8 shown in two-way travel time (twtt). The Coastal Plain is marked in blue and the Triassic basin is marked in red with a basin normal fault as a dark black line. SeisData seismic lines licensed and provided courtesy of Geophysical Pursuit, Inc.
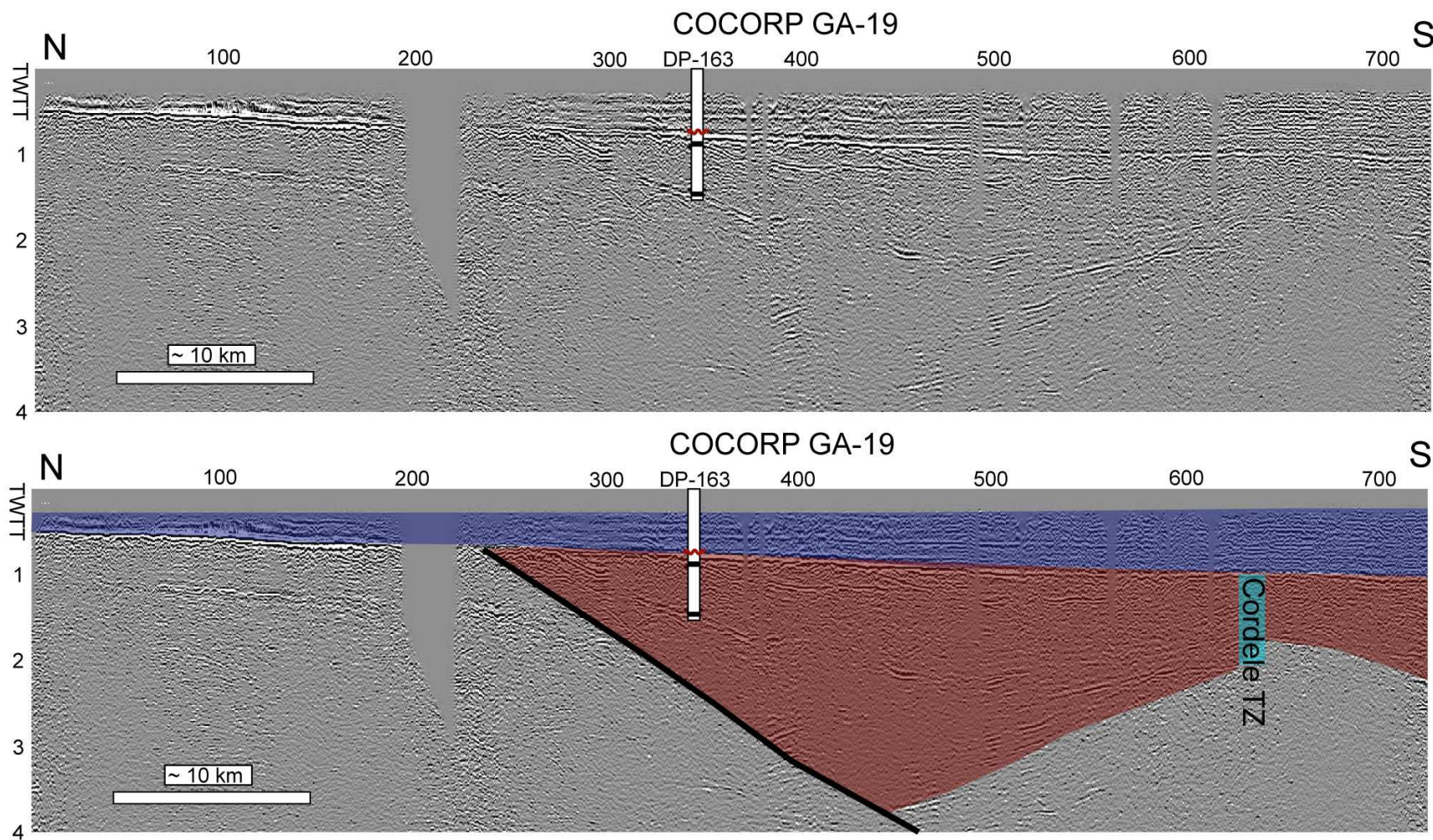
Figure 3.11. Seismic section COCORP GA-19 shown in two-way travel time (twtt) (after McBride, 1991). The Coastal Plain is marked in blue and the Triassic basin is marked in red with a basin normal fault as a dark black line.

3.4.3 SOUTHWESTERN SOUTH GEORGIA RIFT

In southern Georgia, a number of deep wells encountered arkosic redbeds in what is referred to here as the Valdosta basin (Figure 3.12; Barnett, 1975). A dip log from well GGS-3122 indicates that the upper 100 m of redbeds dip to the southeast (Figure 3.4). Prominent south-dipping reflections beneath the sub-horizontal reflection package are observed on COCORP FL-1 between stations 150 and 250 (McBride, 1991). These south dipping reflections terminate abruptly against a zone of low reflectivity (McBride, 1991).

Northwest of the Valdosta basin, a 4-5 km thick basin, referred to here as the Albany Basin, has been partially imaged by COCORP seismic data and penetrated by several deep wells (Figure 3.12; Cook et al., 1981; Nelson et al., 1985; McBride, 1991). Approximately 10 km south of GA-19, well DP-161 penetrated 3.9 km of redbeds and diabase before bottoming in diorite.

On COCORP GA-11, there is a high-amplitude, low-frequency reflection at ~1.25s that marks the bottom of a sub-horizontal package of reflected energy (Figure 3.13). Below this horizon, there are two packages of reflectivity with a maximum time of ~3.5s separated by a zone of low reflectivity. The first package is between stations 580 and 390 and is bottomed by a reflection which dips southward from 2.7s to 3.6s. The second package is between stations 300 and 100 with a maximum time of about 3.8s.

The SGR widens to the southwest, and the sub-basins are of a smaller scale both laterally and in thickness (Figure 3.12). This southwestern part of the SGR has been interpreted to have a complex horst-and-graben structural style (McBride, 1991; Sartain and See, 1997).
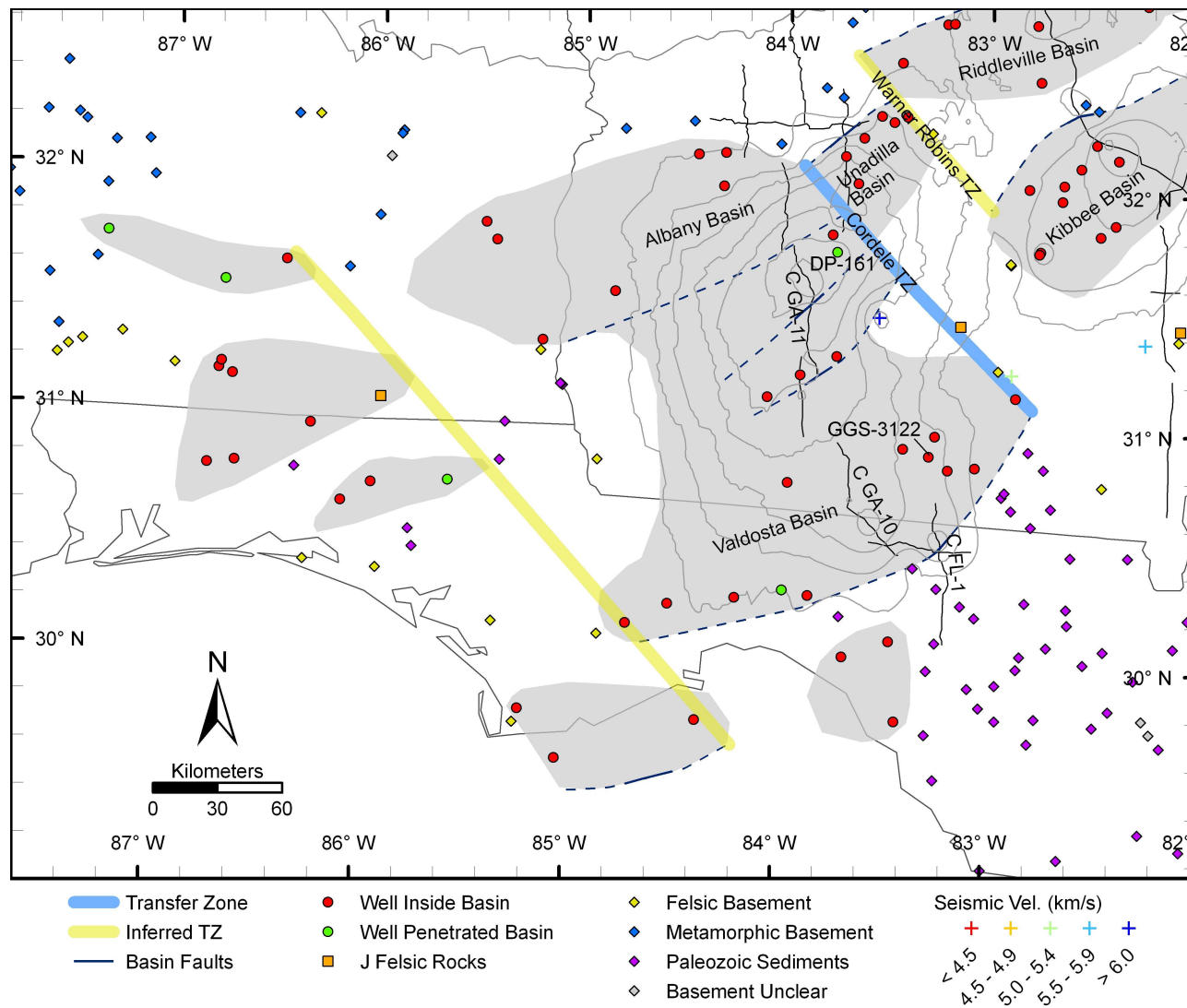
Figure 3.12. Map of the Southwest South Georgia Rift structural domain. Contour lines are derived from the isopach map and mark every 500 meters of basin thickness.
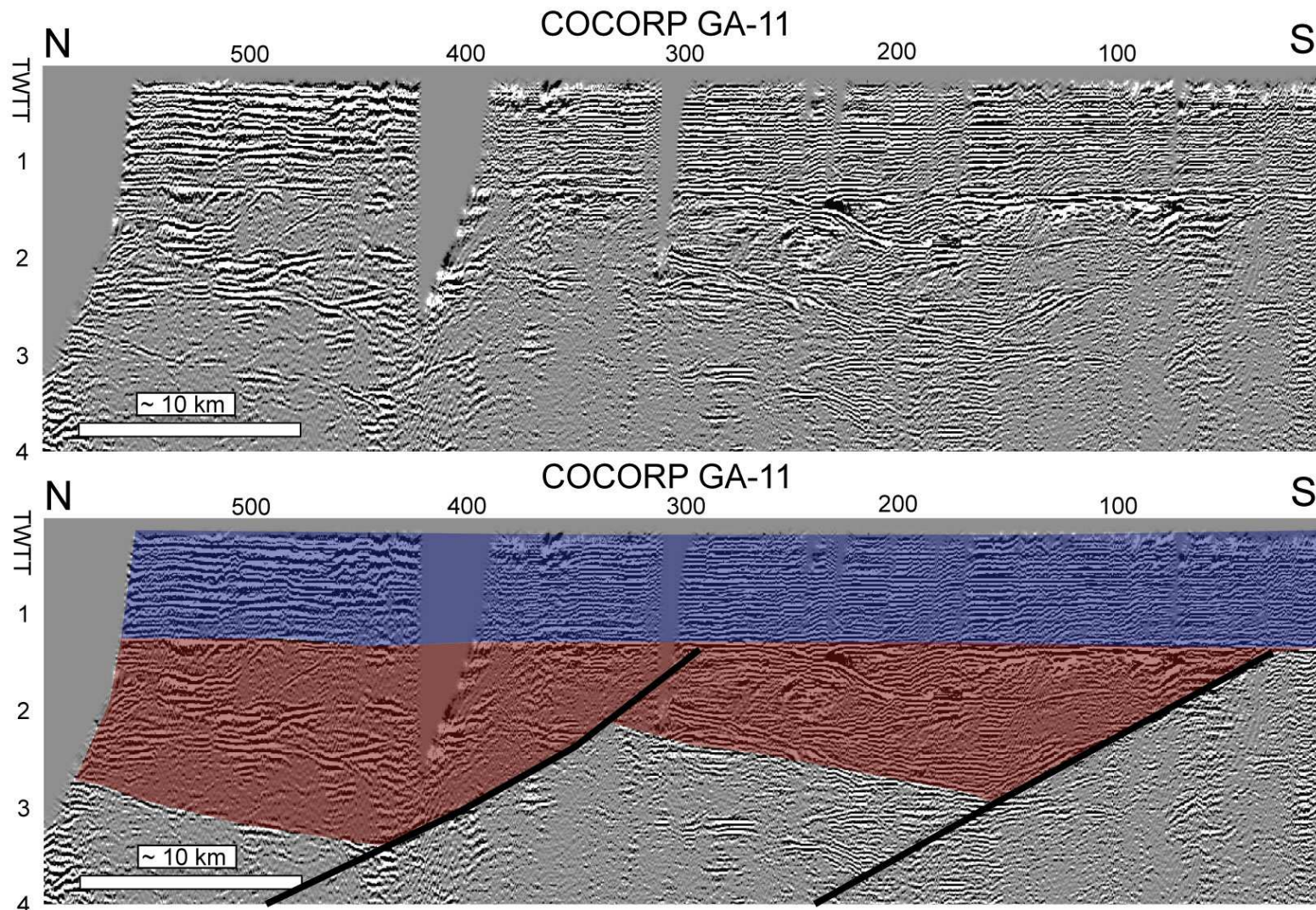
Figure 3.13. Seismic section COCORP GA-11 shown in two-way travel time (twtt) (after McBride, 1991). The Coastal Plain is marked in blue and the Triassic basin is marked in red with a basin normal fault as a dark black line.

3.5. INTERPRETATION

3.5.1 GENERAL APPROACH

The approach to mapping the structure and geometry of the SGR has been based on regional correlation of major structures from seismic reflection profiles, seismic refraction results, and well data. Potential field data has not been used in this study. The reason for not using that data is because studies based solely on potential field data are in disagreement with well data (Figure 3.3A and 3.3C). Studies based solely on potential field data have also interpreted the Dunbarton basin to have an opposite polarity and to be thinner than shown through seismic imaging (Daniels et al., 1983; Klitgord et al., 1988; Domoracki, 1995).

Seismic velocities observed from directly below the Coastal Plain give a good first order indication of the lithology. Coastal Plain velocities typically range from 1.8 - 2.4 km/s, and Triassic redbeds are observed to have velocities from 3.5 - 5.0 km/s (Bonini and Woollard, 1960; Cook et al., 1981; Ackermann, 1983). Velocities ranging between 5 - 6 km/s are the least discriminating of rock type as these velocities correlate with many different lithologies observed in this region including: granitic rocks, Paleozoic sedimentary rocks, and basalt. Velocities greater than 6 km/s are generally interpreted to be crystalline basement rocks (Bonini and Woollard, 1960; Cook et al., 1981; Ackermann, 1983), but these higher velocities are not unreasonable for diabase.

Seismic refraction results from Smith and Talwani (1986) indicate that the estimated depth to true basement varies up to 1 km for co-located stations. The results from Luetgert et al. (1994) indicate a uniform 3.5 km/s layer underlain by a uniform 5.5 km/s layer running continuously from north of the Dunbarton basin all the way through

the town of Walterboro, South Carolina. These results disagree with Bonini and

Woollard (1960) and are contradicted by nearby well data which indicate a variation of

lithology and velocity inside and outside the Dunbarton basin. For these reasons neither

the results from Smith and Talwani (1986) nor Luetgert et al. (1994) are used for

interpreting the extent or thickness of the SGR.

Interpretations of seismic reflection data are complicated by the presence of

numerous diabase sills, which through a high velocity and density contrast with basin

sediments can produce a strong reflection obscuring the surrounding signal (Withjack et

al., 2012). Sills may not conform to the general stratigraphy, and may cross-cut the older

basin faults. Additionally, interpretation of the seismic lines can be complicated by

inversion structures (Withjack et al., 1998; Clendenin et al., 2011).

Basin thickness was estimated across the SGR to assist in the interpretation of the

major structures (Figure 3.14). A database of stratigraphic thicknesses was compiled

from: wells that bottomed in pre-Triassic rocks, interpretations of seismic refraction data,

and interpretations of seismic reflection data (Appendix C). Additional points were

estimated from deep wells which bottomed in the basin. Although the basin thickness at

those points is unclear, these wells provide a minimum thickness of the basin. Seismic

refraction studies which reported a thickness to the basin were taken straight from the

appropriate studies (Pooley, 1960; Ackermann, 1983). Seismic refraction studies that

reported a sub-Coastal Plain velocity greater than 6 km/s are assumed to be outside the

basin.
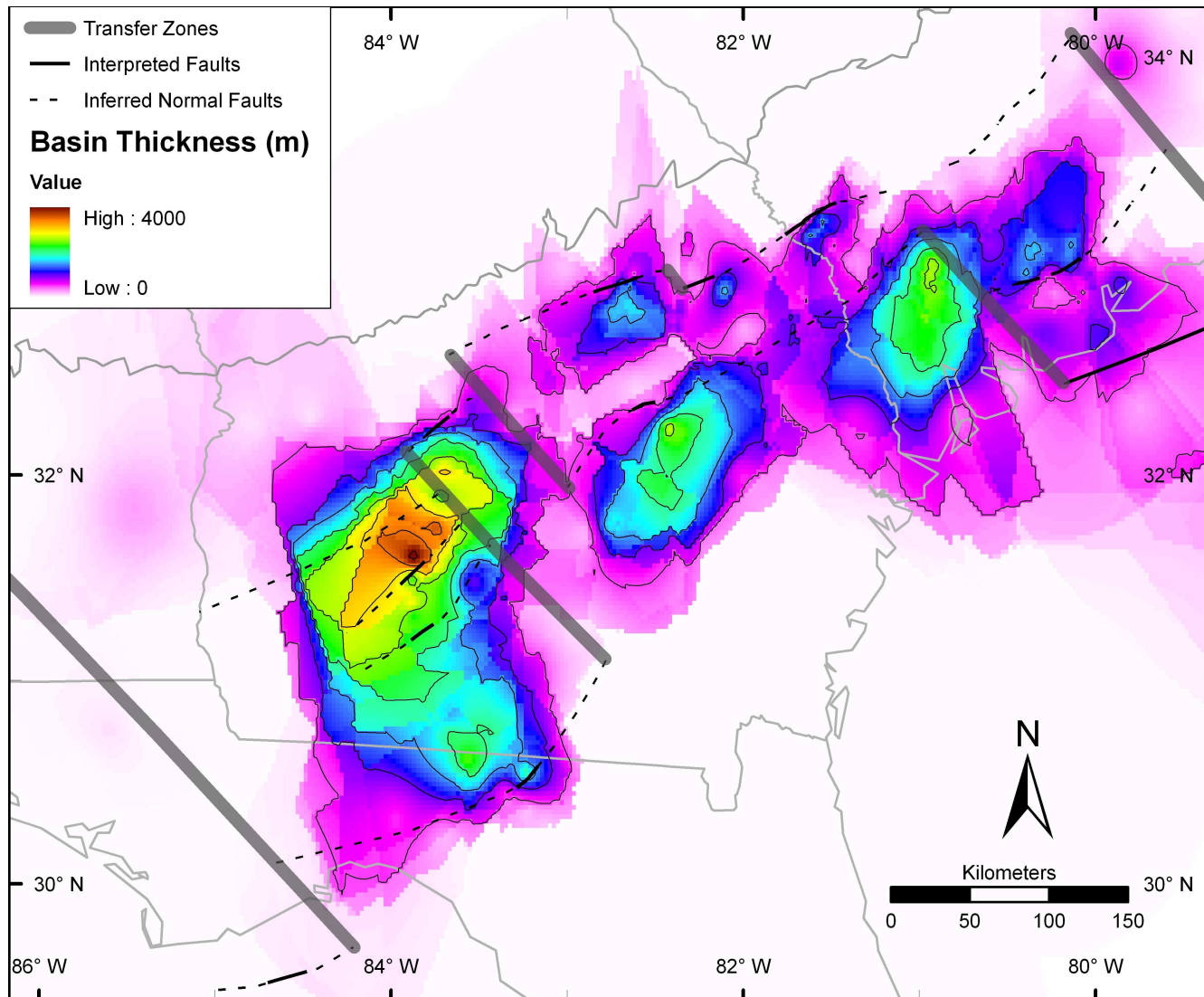
Figure 3.14. Isopach map indicating estimated basin thickness.

Distant points were taken from interpretations of seismic reflection lines to avoid clustering of the data and biasing of the gridding algorithms. The two-way time of the base of the Coastal Plain was subtracted from the interpretation of basin bottom to get an isochron value, and this value was converted to thickness using a constant interval velocity of 4.5 km/s. Values derived from analysis of potential field data (Daniels et al., 1983; Sartain and See, 1997) were not used because of conflicts with known points from wells. Two grids were created: one from a kriging algorithm, and the other using an inverse distance weighted algorithm. The two resultant grids were averaged together to reduce the biases inherent to each algorithm.

Integration of previous studies with observations of well data and interpretation of seismic reflection and refraction data gives a general picture of the SGR geometry and structure (Figures 3.2 and 3.14). The SGR doesn't appear to be one very large rift basin, but rather a segmented series of smaller, northeast striking sub-basins that exhibit a half-graben geometry in seismic profiles (Figures 3.7, 3.10, 3.11, and 3.13). These sub-basins also appear to be separated into three structural domains, with the basins in the northeastern SGR thickening towards the southeast, the basins of the Central SGR thickening towards the northwest, and the basins of the southwestern SGR thickening towards the southeast.

These polarity reversals require two transfer zones which separate the different sub-basin domains: one in South Carolina crossing near the town of Walterboro, and one in Georgia, crossing near the town of Cordele. Both of these transfer zones are similar in geometry and location to the Blake Spur and Jacksonville transfer zones proposed by Tauvers and Muehlberger (1987). Because the relationship of these transfer zones with

60

oceanic fracture zones is unclear, they are referred to here as the Walterboro and Cordele transfer zones. Additional transfer zones are inferred from apparent abrupt changes in basin thickness along strike and offsets in basin bounding normal faults (Figure 3.14).

3.5.2 NORTHEASTERN SOUTH GEORGIA RIFT

A south-bounding normal fault is interpreted on the Sumter basin because well ORG-393 encountered a conglomeratic layer, and well RIC-543 only encountered a 3m thick layer of redbeds between the Coastal Plain sediments and weathered gneiss, indicating it may be right on the feather edge where the basin pinches-out. Only wells near the border faults in the Riddleville and Dunbarton basins encountered conglomeratic strata.

The Jedburg basin is interpreted to have a bounding normal fault on the southeast as indicated from a steep gradient in the gridded refraction data (Figure 3.6; Ackermann, 1983). This fault crosses seismic reflection line SeisData 4 where southeast-dipping reflections beneath the Coastal Plain terminate against a zone of low reflectivity (Figure 3.7). This interpretation is consistent with the geometry of sub-Coastal Plain reflections that are dipping to the south. To the south of the Jedburg basin, redbeds beneath a layer of Jurassic basalt were encountered in the Clubhouse Crossroads wells (Gohn et al., 1978). The presence of redbeds and basalt are further indicated from seismic refraction velocities in the 4 - 5 km/s range and a depth to basement that steadily increases towards the offshore Helena Banks Fault (Behrendt, 1981; Ackermann, 1983).

3.5.3 CENTRAL SOUTH GEORGIA RIFT

The Riddleville basin has been interpreted to have an east-west striking northern border fault (referred to as the Magruder fault by Petersen et al., 1984) and to be a

separate entity from the Dunbarton basin (Daniels and Zietz, 1978; Chowns and Williams, 1983; Daniels et al., 1983). This interpretation is based on a long wavelength east-west trends in the magnetic data and interpretations that the Dunbarton basin is shallower and has an opposite sense polarity (Daniel et al., 1983). The Dunbarton basin has been shown through seismic imaging to also have a north bounding fault, and to have a similar thickness as the Riddleville basin (Domoracki, 1995). Because of the similarities in the basin architectures and because the Penbranch fault projects directly into the Magruder fault on COCORP GA-5, the Dunbarton and Riddleville basins are interpreted to be connected. The long wavelength magnetic trends are suggested here to originate from deeper in the crust.

The south-dipping reflections on SeisData 8 are interpreted to be related to basin inversion against a south dipping fault (Figure 3.10; See Withjack et al., 1998 and Clendenin et al., 2011). To the south of this interpreted fault, below a time of 0.7s, the reflectivity dips slightly towards the north. There are several bright amplitude events that approximate a north-dipping line interpreted to be the basement. The north-dipping reflections and the triangular shape of the reflectivity indicate that the Kibbee basin has a general half-graben geometry with a northern boundary fault. The north-dipping reflections are consistent with north-dipping sedimentary layers indicated from the log of the A.P. Snipes well. Just south of where SeisData 8 crosses COCORP GA-17, the interpreted basement line intersects the base of the Coastal Plain. This pinch-out of the basin is coincident with a change in reflective character below 0.75s.

The Unadilla basin is clearly imaged by COCORP GA-19 (Figure 3.11). Below the sub-horizontal reflection package associated with the Coastal Plain is a triangular

zone of reflectivity that is characterized by south-dipping reflections near the border fault and north-dipping reflections between stations 400 and 600. This zone is correlated with Triassic basin fill in well DP-163, with the brightest reflections correlating with diabase. This interpreted Triassic section is thickest at station 450 and thins towards station 620, south of where the reflectivity dips gently southward. The south-dipping reflections north of station 400 are interpreted to be related to basin inversion of a south-dipping fault (See Withjack et al., 1998 and Clendenin et al., 2011). The south-dipping reflectivity south of station 620 is interpreted to be reflections from the Albany sub-basin.

3.5.4 SOUTHWESTERN SOUTH GEORGIA RIFT

The Albany basin is interpreted to be the thickest of the SGR sub-basins (Figure 3.14). The basin increases in thickness south of GA-19 where well DP-161 penetrates 3.9 km of basin sediments. A basin thickness of ~4 km is in agreement with the interpretation of COCORP GA-11 presented in Figure 3.13. Two major normal faults are interpreted on COCORP GA-11, where south-dipping reflectivity is truncated against a zone of low reflectivity.

The Valdosta basin is interpreted to be distinct from the Albany basin largely because of a reduced thickness, although the Triassic section may be continuous between these two basins. The Valdosta basin is interpreted to be bounded on the southeast by a major normal fault, indicated by an increasing basin thickness to the south on COCORP GA-10, and COCORP FL-1 (McBride, 1991). A bounding fault on the southeast is consistent with the dip log from well GGS-3122, which indicates the Triassic section is dipping towards the southeast.

3.6. DISCUSSION

No transfer zones are observed separating the exposed basins of the eastern North American rift system (Schlische, 2003), yet several studies have proposed their existence in the SGR (Tauvers and Muehlberger, 1987; Etheridge et al., 1989). The proposed transfer faults of Tauvers and Muehlberger (1987) are similar to two of the proposed transfer zones in this study, though their fault interpretations are on the basis of projecting oceanic fracture zones onshore through rift orthogonal boundaries on the map of Chowns and Williams (1983). This interpretation has been criticized for the lack of data supporting the existence of the proposed faults including no observations of reversals in sub-basin polarity (McBride and Nelson, 1988; McBride, 1991), even though an along-strike disparity in basin architecture has been suggested (McBride, 1991).

The interpreted reversals of sub-basin polarity presented in this study require some sort of intervening structures and provide support to the hypothesis that transfer zones are present within the SGR. The major bounding normal faults of the East African rift are approximately 50 - 200 km in length and terminate at transfer zones where the strain is accommodated and transferred to other major normal fault systems either of the same polarity or different polarity (Rosendahl, 1987; Morley et al., 1990; Kusznir et al., 1995; Morley, 1999b). In the Basin and Range extensional province of western North America, regional tilt domains range from several hundred to 1000 km long (Stewart, 1998). The length scale observed for the South Georgia Rift is between these suggested end-member extensional settings, with structural domains on the order of 200 km (Figure 3.2). The data are too sparse to constrain whether the transfer zones in this study are diffuse accommodation zones or discrete transfer faults; however, the wide nature of the

many sub-basins of the South Georgia Rift indicate a high degree of extension, which is consistent with the transfer zone structures tending toward discrete transfer faults (Withjack at al., 2002).

Interestingly, the mapped transfer zones appear to correlate with pockets of encountered basalt and Jurassic felsic rocks (Figure 3.15). This relationship between off-axis rift volcanism and transfer zones has been observed in the East African Rift (Corti, 2012) and suggests the possibility that flood basalts were not terribly pervasive in the SGR.

The presence of transfer zones in the SGR and their absence in the more northerly eastern North American Triassic rift system indicates one of two possibilities: 1) Transfer zones are present in the north, but due to difficulties in mapping (Bally, 1982) have remained unidentified as such; or 2) the SGR has some fundamental difference with the more northerly rift system. Option 1 seems unlikely since the northern rift basins, and in particular the Newark basin, have been very well studied for many years (Olsen, 1997, Schlische, 2003, and references therein). Option 2 is reasonable since the South Georgia Rift is known to straddle the Laurentia - Gondwana suture (Figure 3.16; Chowns and Williams, 1983; Tauvers and Muehlberger, 1987; McBride, 1991) unlike the more northerly Triassic rift system. The transfer zones may be inherited from previous transform faults or weaknesses in the Gondwanan lithosphere (Thomas, 2006), or perhaps are original structures resultant from oblique rifting (van Wijk, 2005). Modeling studies and observations of the East African Rift indicate that alternating, asymmetric rift geometries occur when extensional forces are oblique to a pre-existing zone of weakness (Morley et al., 1990; Morley, 1999a; van Wijk, 2005; Corti, 2012). There have been
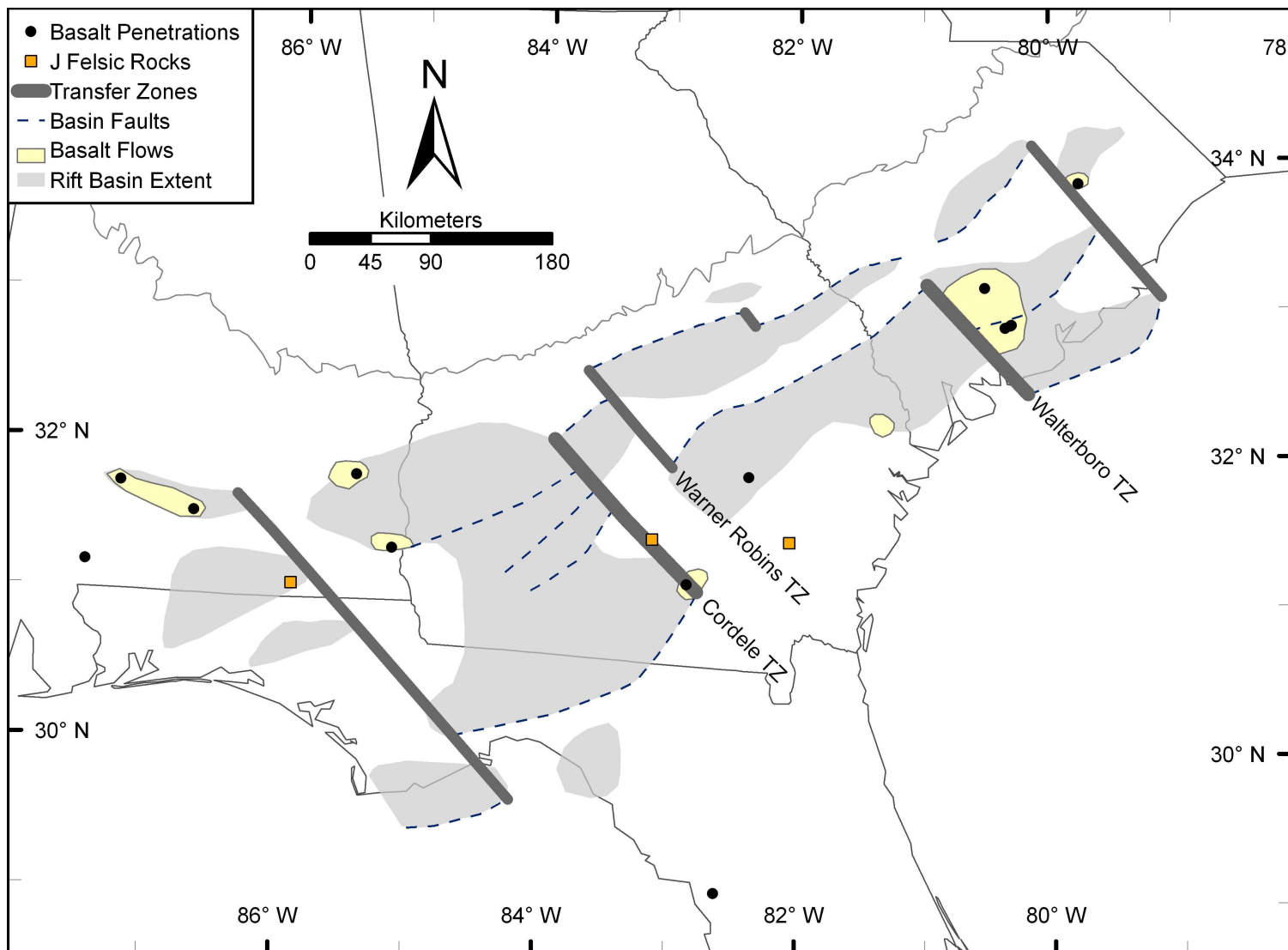
Figure 3.15. Map of preserved basalt flows (after Heffner et al., 2012) in relationship to major structures of the South Georgia Rift.
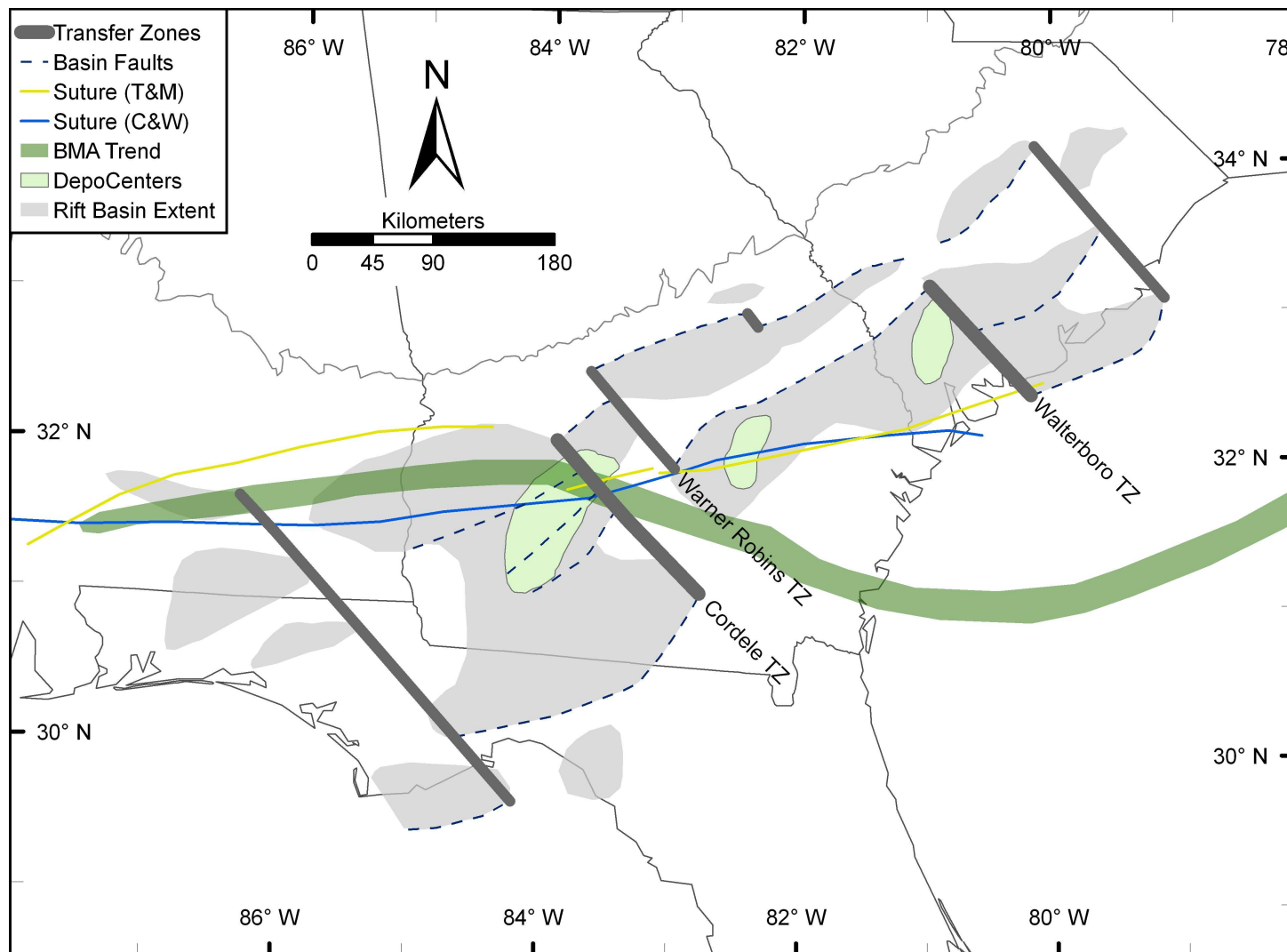
Figure 3.16. Spatial Relationship of South Georgia Rift (SGR) and Laurentia - Gondwana suture. T&M - Tauvers and Muehlberger (1987), C&W - Chowns and Williams (1983), BMA - Brunswick Magnetic Anomaly.

several proposed locations for the Laurentia - Gondwana suture, all of which underlie the major sub-basins of the SGR (Figure 3.16). The approximate trend of the proposed locations for the suture ranges from 60 – 70 degrees to the main northwest-southeast direction of extension (Schlische, 2003).

A narrow rift may form where oblique extension occurs along pre-existing faults (Keranen et al., 2009; Brune et al., 2012). Although Buck's (1991) model suggested that a wide rift would develop in a thick, warm lithosphere, observations of the Ethiopian Rift suggest that inherited structures and lithospheric weaknesses localized deformation in a hot craton (Keranen et al., 2009). Whereas the lower crustal and upper mantle lithosphere is extended over a broad area in the Ethiopian Rift, the upper crustal expression of the rift remains in a narrow valley (Keranen et al., 2009). Oblique extension also has been shown through modeling to result in a diffuse zone of deformation which eventually localizes into distinct en-echelon shear zones reflecting the direction of principal stresses (Brune et al., 2012).

The southwestern SGR is the widest part of the rift and contains the thickest of the SGR sub-basins, indicating that strain was greater in this segment of the rift. Rifting is suggested here to have begun in the southwest, in the Gondwanan lithosphere, and to have progressed towards the northeast. As the rift approached the Laurentian crust, differences in rheology across the suture stalled rift propagation (van Wijk and Blackman, 2005). The Cordele transfer zone formed as deformation was distributed on the Gondwanan crust. Eventually rifting continued across the suture oblique to the deep east-west lithospheric fabric. This pattern of oblique rifting resulted in the reversal of sub-basin polarity (van Wijk, 2005) across the Walterboro transfer zone.

3.7. CONCLUSIONS

The SGR comprises a series of smaller sub-basins that reverse polarity across

transfer zones. Although Triassic rifting of Pangea occurred over a wide area, in the

SGR the upper crustal expression of the rifting was pronounced proximal to the

Alleghanian suture. The weak lithosphere in concert with oblique rifting resulted in a

wide rift with thicker basins forming over the ancient suture.

3.8. REFERENCES

Ackermann, H.D., 1983, Seismic-refraction study in the area of the Charleston, South Carolina, 1886 earthquake, *in* Gohn, G.S., ed., Studies Related to the Charleston, South Carolina, Earthquake of 1886—Tectonics and Seismicity: U.S. Geological Survey Professional Paper 1313, p. F1–F20.

Akintunde, O.M., Knapp, C.C., Knapp, J.H., and Heffner, D.M., 2013, New constraints on buried Triassic basins and regional implications for subsurface CO_2 storage from the SeisData6 seismic profile across the Southeast Georgia Coastal Plain: Environmental Geosciences, v. 20, p. 1-13.

Amick, D.C., 1979, Crustal structure studies in the South Carolina Coastal Plain, M.S. thesis, University of South Carolina, 81 p.

Ball, M.M., Martin, R.G., Foote, R.Q., and Applegate, A.V., 1988, Structure and stratigraphy of the Western Florida Shelf, Part I, Multichannel reflection seismic data: US Geological Survey Open File Report 88-439.

Bally, A.W., 1982, Musings over sedimentary basin evolution: Philosophical Transactions of the Royal Society of London A., v. 305, p. 325-337.

Behrendt, J.C., Hamilton, R.W., Ackermann, H.D., and Henry, V.J., 1981, Cenozoic faulting in the vicinity of the Charleston, S.C., 1886 earthquake: Geology, v. 9, p. 117-122.

Behrendt, J.C., Hamilton, R.M., Ackermann, H.D., Henry, V.J., and Bayer, K.C., 1983, Marine multichannel seismic-reflection evidence for Cenozoic faulting and deep crustal structure near Charleston, South Carolina, *in* Gohn, G.S., ed., Studies Related to the Charleston, South Carolina, Earthquake of 1886—Tectonics and Seismicity: U.S. Geological Survey Professional Paper 1313, p. J1–J29.

Behrendt, J.C., 1985, Interpretations from multichannel seismic-reflection profiles of the deep crust crossing South Carolina and Georgia from the Appalachian mountains to the Atlantic coast: U.S. Geological Survey U.S. Misc. Field Studies, Map MF-1656.

Bonini, W.E., and Woollard, G.P., 1960, Subsurface geology of North Carolina – South Carolina Coastal Plain from seismic data: Bulletin of the American Association of Petroleum Geologists, v. 44, p. 298-315.

Brun, J.-P., 1999, Narrow rifts versus wide rifts: inferences for the mechanics of rifting from laboratory experiments: Philosophical Transactions of the Royal Society London A, v. 357, p. 695-712.

Brune, S., Popov, A.A., and Sobolev, S.V., 2012, Modeling suggests that oblique extension facilitates rifting and continental break-up: Journal of Geophysical Research, v. 117, B08402, doi:10.1029/2011JB008860.

Buck, W.R., 1991, Modes of continental lithospheric extension: Journal of Geophysical Research, v. 96, p. 20161-20178.

Buck, W.R., Lavier, L.L., and Poliakov, A.N.B., 1999, How to make a rift wide: Philosophical Transactions of the Royal Society London A, v. 357, p. 671-693.

Chapman, M.C., and Beale, J.N., 2010, On the Geologic Structure at the Epicenter of the 1886 Charleston, South Carolina, Earthquake: Bulletin of the Seismological Society of America, v. 100, p. 1010–1030, doi:10.1785/0120090231.

Chowns, T.M., and Williams, C.T., 1983, Pre-Cretaceous rocks beneath the Georgia Coastal Plain—Regional Implications, *in* Gohn, G.S., ed., Studies Related to the Charleston, South Carolina, Earthquake of 1886—Tectonics and Seismicity: U.S. Geological Survey Professional Paper 1313, p. L1–L42.

Clendenin, C.W. Jr., Waddell, M.G., and Addison, A.D., 2011, Reactivation and overprinting of South Georgia Rift extension: Geological Society of America Abstract with Programs, v. 43, no. 5, p. 551.

Cook, F.A., Brown, L.D., Kaufman, S., Oliver, J.E., Petersen, T.A., 1981, COCORP seismic profiling of the Appalachian orogen beneath the Coastal Plain of Georgia: Geological Society of America Bulletin, Part I, v. 92, p. 738 – 748.

Cooke, C.W., 1936, Geology of the Coastal Plain of South Carolina: U.S. Geological Survey, Bulletin 867, 196 p.

Corti, G., Bonini, S., Conticelli, S., Innocenti, F., Manetti, P., and Sokoutis, D., 2003, Analogue modeling of continental extension: A review focused on the relations between the patterns of deformation and the presence of magma: Earth Science Reviews, v. 63, p. 169-247.

Corti, G., 2012, Evolution and characteristics of continental rifting: Analog modeling-inspired view and comparison with examples from the East African Rift System: Tectonophysics, v. 522-523, p. 1-33.

Cumbest, R.J., Price, V., and Anderson, E.E., 1992, Gravity and magnetic modeling of the Dunbarton Triassic basin, South Carolina: Southeastern Geology, v. 33, p. 37-51.

Daniels, D.L. and Zietz, I., 1978, Geologic interpretation of aeromagnetic maps of the Coastal Plain region of South Carolina and parts of North Carolina and Georgia: US Geological Survey Open File Report 78-261.

Daniels, D.L., Zietz, I., and Popenoe, P., 1983, Distribution of subsurface lower Mesozoic rocks in the southeastern United States as interpreted from regional aeromagnetic and gravity maps, *in* Gohn, G.S., ed., Studies Related to the Charleston, South Carolina, Earthquake of 1886—Tectonics and Seismicity: U.S. Geological Survey Professional Paper 1313, p. K1–K24.

Darton, N.H., 1896, Artesian wells on the Atlantic Coast: U.S. Geological Survey Bulletin 138, p. 218.

Domoracki, W.J., 1995, A Geophysical investigation of geologic structure and regional tectonic setting at the Savannah River Site, South Carolina, PhD thesis, Virginia Polytechnic Institute & State University, Blacksburg, 236 p.

Etheridge, M.A., Symonds, P.A., and Lister, G.A., 1989, Application of the detachment model to reconstruction of conjugate passive margins, *in* Tankard, A.J. and Balkwill, H.R., eds., Extensional tectonics and stratigraphy of the North Atlantic margins: American Association of Petroleum Geologists Memoir 46, p. 23-40.

Faulds, J.E. and Varga, R.J., 1998, The role of accommodation zones and transfer zones in the regional segmentation of extended terranes, *in* Faulds, J.E. and Stewart, J.H., eds., Accommodation zones and transfer zones: The regional segmentation of the Basin and Range Province: Geological Society of America Special Paper 323, p. 1-45.

Gibbs, A.D., 1984, Structural evolution of extensional basin margins: Journal of the Geological Society of London, v. 141, p. 609-620.

Gohn, G.S., Gottfried, D., Lanphere, M.A., and Higgins, B.B., 1978, Regional implications of Triassic or Jurassic age for basalt and sedimentary red beds in the South Carolina Coastal Plain: Science, v. 202, no. 4370, p. 887-890.

Hamilton, R.M., Behrendt, J.C., and Ackermann, H.D., 1983, Land multichannel seismic-reflection evidence for tectonic features near Charleston, South Carolina, *in* Gohn, G.S., ed., Studies Related to the Charleston, South Carolina, Earthquake of 1886—Tectonics and seismicity: U.S. Geological Survey Professional Paper 1313, p. I1–I18.

Heatherington, A.L., Mueller, P.A., and Nutman, A.P., 1999, A Jurassic granite from Southern Georgia, U.S.A.: silicic, extension-related magmatism along the Southeastern Coastal Plain: Journal of Geology, v. 107, p. 375-384.

Heatherington, A.L., and Mueller, P.A., 2003, Mesozoic Igneous Activity in the Suwannee Terrane, Southeastern USA: Petrogenesis and Gondwanan affinities: Gondwana Research, v. 6, no. 2, p. 296-311.

Heffner, D.M., Knapp, J.H., Akintunde, O.M., and Knapp, C.C., 2012, Preserved extent of Jurassic flood basalt in the South Georgia Rift: A new interpretation of the J horizon: Geology, v. 40, p. 167−170.

Keranen, K.M., Klemperer, S.L., Julia, J., Lawrence, J.F., and Nyblade, A.A., 2009, Low lower crustal velocity across Ethiopia: Is the Main Ethiopian Rift a narrow rift in a hot craton?: Geochemistry Geophysics Geosystems, v. 10, Q0AB01, doi:10.1029/2008GC002293.

Kusznir, J.R., Roberts, A.M., and Morley, C.K., 1995, Forward and reverse modeling of rift basin formation: Geological Society of London Special Publication, v. 80, p. 33-56.

Klitgord, K.D., Hutchinson, D.R.., and Schouten, H., 1988, U.S. Atlantic continental margin; Structural and tectonic framework, *in*, Sheridan, R.W., and Grow, J.A., eds., The Atlantic Continental Margin, U.S.: Geological Society of America, The Geology of North America, V. I-2, p. 19-55.

Luetgert, J.H, Benz, H.M., and Madabhushi, S., 1994, Crustal structure beneath the Atlantic Coastal Plain of South Carolina: Seismological Research Letters, v. 65, p. 180 − 191.

Lizarralde, D., et al., 2007, Variation in styles of rifting in the Gulf of California: Nature, v. 448, p. 466-469, doi:10.1038/nature06035.

Mansfield, W.C., 1937, Some deep wells near the Atlantic coast in Virginia and the Carolinas, U.S. Geological Survey, Prof. Paper 186-I, p. 159-161.

Marine, L.W., and Siple, G.E., 1974, Buried Triassic basin in the central Savannah River area, South Carolina and Georgia: Geological Society of America Bulletin, v. 85, p. 311-320.

McBride, J.H. and Nelson, K.D., 1988, Is the Brunswick magnetic anomaly really the Alleghanian suture? – Comment: Tectonics, v. 7, p. 343-346.

McBride, J.H., 1991, Constraints on the structure and tectonic development of the early Mesozoic South Georgia Rift, southeastern United States; seismic reflection data processing and interpretation: Tectonics, v. 10, p. 1065–1083, doi:10.1029/90TC02682.

McKenzie, D., 1978, Some remarks on the development of sedimentary basins: Earth and
Planetary Science Letters, v. 40, p. 25-32.

Morley, C.K., Nelson, R.A, Patton, T.L., and Munn, S.G., 1990, Transfer zones in the
East African Rift System and their relevance to hydrocarbon exploration in rifts:
AAPG Bulletin, v. 74, p. 1234-1253.

Morley, C.K., 1999a, Influence of preexisting fabrics on rift structure, *in* Morley, C.K.,
ed., Geoscience of Rift Systems—Evolution of East Africa: AAPG Studies in
Geology No. 44, p. 151-160.

Morley, C.K., 1999b, Aspects of transfer zone geometry and evolution in East African
Rifts, *in* Morley, C.K., ed., Geoscience of Rift Systems—Evolution of East
Africa: AAPG Studies in Geology No. 44, p. 161-171.

Neathery, T.L., and Thomas, W.A., 1975, Pre-Mesozoic basement rocks of the Alabama
Coastal Plain: Transactions of the Gulf Coast Association of Geological Societies,
v. 25, p. 86-97.

Nelson, K.D., Arnow, J.A., McBride, J.H., Willemin, J.H., Huang, J., Zheng, L., Oliver,
J.E., Brown, L.D., and Kaufman, S., 1985, New COCORP profiling in the
southeastern United States. Part I: Late Paleozoic suture and Mesozoic rift basin:
Geology, v. 13, p. 714 − 718.

Olsen, P.E., 1997, Stratigraphic record of the early Mesozoic breakup of Pangea in the
Laurasia-Gondwana rift system: Annual Review of Earth and Planetary Sciences,
v. 25, p. 337–401, doi:10.1146/annurev.earth.25.1.337.

Petersen, T.A., Brown, L.D., Cook, F.A., Kaufman, S., and Oliver, J.E., 1984, Structure
of the Riddleville basin from COCORP seismic data and implications for
reactivation tectonics: Journal of Geology, v. 92, p. 261-271.

Pooley, R.N., 1960, Basement configuration and subsurface geology of eastern Georgia
and southern South Carolina as determined by seismic-refraction measurements,
MS Thesis, University of Wisconsin, 47 p.

Rosendahl, B.R., 1987, Architecture of continental rifts with special reference to East
Africa: Annual Review of Earth and Planetary Science, v. 15, p. 445-503.

Sartain, S.M., and See, B.E., 1997, The South Georgia Basin: An integration of Landsat,
gravity, magnetics and seismic data to delineate basement structure and rift basin
geometry: Gulf Coast Association of Geological Society Transactions, v. 47, p.
493-498.

Schilt, F.S., Brown, L.D., Oliver, J.E., and Kaufman, S., 1983, Subsurface structure near Charleston, South Carolina – Results of COCORP reflection profiling in the Atlantic Coastal Plain, *in* Gohn, G.S., ed., Studies Related to the Charleston, South Carolina, Earthquake of 1886—Tectonics and seismicity: U.S. Geological Survey Professional Paper 1313, p. H1–H19.

Schlische, R.W., 2003, Progress in Understanding the Structural Geology, Basin Evolution, and Tectonic History of the Eastern North American Rift System, *in* LeTourneau, P.M., and Olsen, P.E., eds., The Great Rift Valleys of Pangea in Eastern North America: New York, Columbia University Press, p. 21−64.

Schlische, R.W., and Withjack, M.O., 2009, Origin of fault domains and fault-domain boundaries (transfer zones and accommodation zones) in extensional provinces: Result of random nucleation and self-organized fault growth: Journal of Structural Geology, v. 31, p. 910-925.

Smith, W.A., and Talwani, P., 1987, Results of a refraction survey in the Bowman seismogenic zone, South Carolina: South Carolina Geology, v. 31, p. 83 − 98.

Steele, K.B., and Colquhoun, D.J., 1985, Subsurface evidence of the Triassic Newark Supergroup in the South Carolina Coastal Plain: South Carolina Geology, v. 28, no. 2, p. 11 – 22.

Stewart, J.H., 1998, Regional characteristics, tilt domains, and extensional history of the late Cenozoic Basin and Range province, western North America, *in* Faulds, J.E. and Stewart, J.H., eds., Accommodation zones and transfer zones: The regional segmentation of the Basin and Range Province: Geological Society of America Special Paper 323, p. 47-74.

Tauvers, P.R. and Muehlberger, W.R., 1987, Is the Brunswick magnetic anomaly really the Alleghanian suture?: Tectonics, v. 3, p. 331-342.

Tauvers, P.R. and Muehlberger, W.R., 1988, Is the Brunswick magnetic anomaly really the Alleghanian suture? – Reply: Tectonics, v. 7, p. 347-349.

Thomas, W. A., 2006, Tectonic inheritance at a continental margin: GSA Today, v. 16, p. 4-11.

Traverse, A., 1987, Pollen and spores date origin of rift basins from Texas to Nova Scotia as early late Triassic: Science, v. 236, p. 1469–1472, doi:10.1126/science.236.4807.1469.

van Wijk, J.W., 2005, Role of weak zone orientation in continental lithosphere extension: Geophysical Research Letters, v. 32., L02302, doi:10.1029/2004GL022192.

van Wijk, J.W., and Blackman, D.K., 2005, Dynamics of continental rift propagation: the end-member modes: Earth and Planetary Science Letters, v. 229, p. 247-258.

Wernicke, B., 1985, Uniform-sense normal simple shear of the continental lithosphere: Canadian Journal of Earth Science, v. 22, p. 108-125.

Withjack, M.O., and Jamison, W.R., 1986, Deformation produced by oblique rifting: Tectonophysics, v. 126, p. 99-124.

Withjack, M.O., Schlische, R.W., and Olsen, P.E., 1998, Diachronous Rifting, Drifting, and Inversion on the Passive Margin of Central Eastern North America: An Analog for Other Passive Margins: The American Association of Petroleum Geologists Bulletin, v. 82, p. 817–835.

Withjack, M.O., Schlische, R.W., and Olsen, P.E., 2002, Rift-basin structure and its influence on sedimentary systems: Sedimentation in Continental Rifts, SEPM Special Publication No. 73, p 57-81.

Withjack, M.O., Schlische, R.W., and Olsen, P.E., 2012, Development of the passive margin of Eastern North America: Mesozoic rifting, igneous activity, and breakup, *in* Roberts, D.W., and Bally, A.W., eds., Phanerozoic Rift Systems and Sedimentary Basins, Elsevier, Amsterdam, p. 301 − 335.

Woollard, G.P., Bonini, W.E., and Meyer, R.P., 1957, A seismic refraction study of the sub-surface geology of the Atlantic Coastal Plain and continental shelf between Virginia and Florida: Madison, University of Wisconsin Geophysics Section, technical report contract no. N7onr-28512, 128 p.

Yantis, B.R., Costain, J.K., and Ackermann, H.D., 1983, A reflection seismic study near Charleston, South Carolina, *in* Gohn, G.S., ed., Studies Related to the Charleston, South Carolina, Earthquake of 1886—Tectonics and Seismicity: U.S. Geological Survey Professional Paper 1313, p. G1–G20.

Ziegler, P.A., and Cloetingh, S., 2004, Dynamic processes controlling evolution of rifted basins: Earth-Science Reviews, v. 64, p. 1 – 50.

CHAPTER 4

THE STRUCTURE OF THE CENTRAL ATLANTIC: IS IT THE RIFT'S FAULT?

It has long been thought that the structures of an ocean basin, and in particular oceanic transform faults, are inherited from the initial continental rift (Wilson, 1965). A prime candidate for the precursors of transform faults are rift-transverse structures referred to as transfer zones and identified in many of Earth's active and ancient rifts (Gibbs, 1984; Rosendahl, 1987; Morley et al., 1990; Faulds and Varga, 1998; Morley, 1999). Previous studies have projected Central Atlantic oceanic fracture zones onto the eastern North American continental margin based on the assumption that the pole of rotation remained approximately constant from the rift phase, at about 230 Ma, through to 154 Ma (Sykes, 1978; Klitgord et al., 1984; Tauvers and Muehlberger, 1987; Etheridge et al., 1989). Two recent studies have interpreted a new kinematic history for the breakup of Pangea and formation of the Central Atlantic Ocean (Schettino and Turco, 2009; Labails et al., 2010). Small circles predicted from these studies are plotted to test the hypothesis that Central Atlantic oceanic structures are inherited from a pre-cursor rift. Recently mapped transfer zones in the South Georgia Rift correlate with oceanic structures. Interestingly though, there is an apparent aliasing of the projections based on the newer studies (Schettino and Turco, 2009; Labails et al., 2010) relative to previous predictions (Klitgord and Schouten, 1986).

4.1 INTRODUCTION

Oceanic transform faults and their corresponding fracture zones are one of the most striking structural expressions of ocean basins. Because successful continental rifts ultimately result in the formation of ocean basins, it has long been thought that oceanic transform faults are inherited from the initial continental rift (Wilson, 1965). A prime candidate for the precursors of transform faults are rift-transverse structures referred to as transfer zones and identified in many of Earth's active and ancient rifts (Gibbs, 1984; Rosendahl, 1987; Morley et al., 1990; Faulds and Varga, 1998; Morley, 1999). Structural studies of continental margins have suggested a direct tectonic inheritance of transfer zones by oceanic crust (Tamsett, 1984; Cochran and Martinez, 1988; Fantozzi, 1996; d'Acremont et al., 2005). Thomas (2006) has even argued that transform faults are tectonically inherited through multiple Wilson cycles, taken up both as compressive and then subsequently extensional structures. Recent modeling and geophysical studies, however, have suggested that oceanic transforms are not inherited from continental rift structures, but rather form only after sea-floor spreading has begun (Taylor et al., 1999, 2009; Gerya, 2010, 2012).

There has been a long history of researchers projecting Central Atlantic fracture zones onto the North American continental margin (Figure 4.1; Sykes, 1978; Klitgord et al., 1984; Tauvers and Muehlberger, 1987; Etheridge et al., 1989). Strong evidence for the proposed continental transfer zones, however, has been lacking until now (Chapter 3; McBride and Nelson, 1988; Tauvers and Muehlberger, 1988). The hypothesis that North American transfer zones correlate with fracture zones of the Central Atlantic is tested here through small projections of the continental and oceanic features.
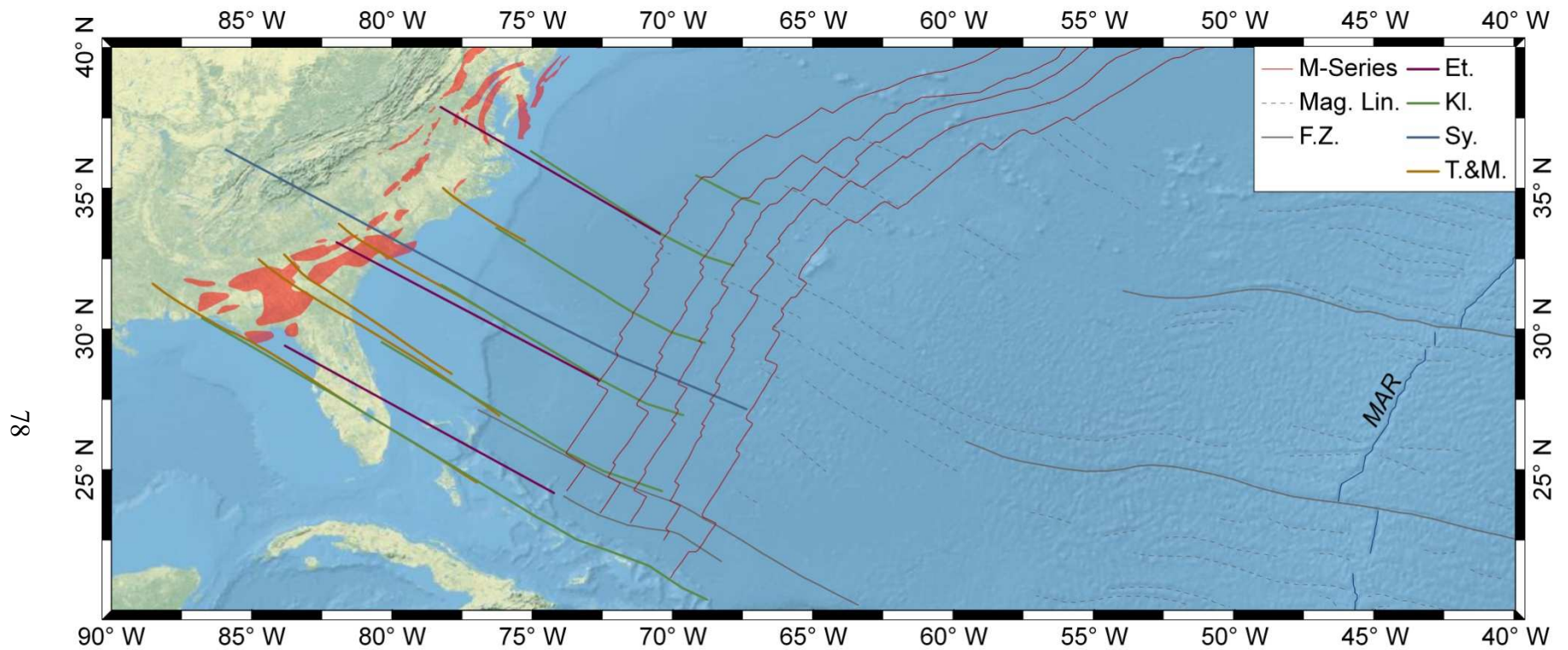
Figure 4.1. Map of the West Central Atlantic Ocean showing onshore projections of oceanic fracture zones from the M-25 magnetic isochron. Triassic rift basins shown in red (after Olsen, 1997; Withjack et al., 1998). M-series isochrons, magnetic lineaments, and fracture zones (F.Z.) after Labails et al. (2010). Fracture zone projections: Et. - Etheridge et al. (1989), K.&S. - Klitgord and Schouten (1986), Sy. - Sykes (1978), T.&M. - Tauvers and Muehlberger (1987).

4.2. BACKGROUND

4.2.1 TRANSFORM FAULTS

In one of his classic papers, Wilson (1965) defined a new class of faults, which he termed transform faults since displacement across these faults could change form and direction. Transform faults are a special class of strike-slip faults that act as conservative plate boundaries. These faults are most abundant in the ocean basins, where they separate actively spreading mid-ocean ridge segments (Gerya, 2012). Oceanic transform faults are only active plate boundaries between ridge segments, where the two plates slide past each other.

Beyond the spreading centers, the relict transform faults are preserved as through going fracture zones. These fracture zones are striking bathymetric features near the mid-ocean ridges and can be mapped from discontinuities in the magnetic lineation patterns of the oceanic crust (Figure 4.2; Klitgord and Schouten, 1986). The fracture zones preserve the flow line of the plate and trend approximately along the small circles of a stage pole for their given time, providing a sort of road map for the kinematic history of the oceanic plates (Klitgord and Schouten, 1986).

4.2.2 TRANSFER ZONES

Transfer zones are rift-transverse structural features that transmit and accommodate extensional strain between normal faults of adjacent extensional basins (Gibbs, 1984; Rosendahl, 1987; Faulds and Varga, 1998; Morley, 1999). Transfer zones range from discrete faults to structurally complex zones of faults and ramps (Gibbs, 1984; Rosendahl, 1987; Morley et al., 1990; Faulds and Varga, 1998). While transfer zones are
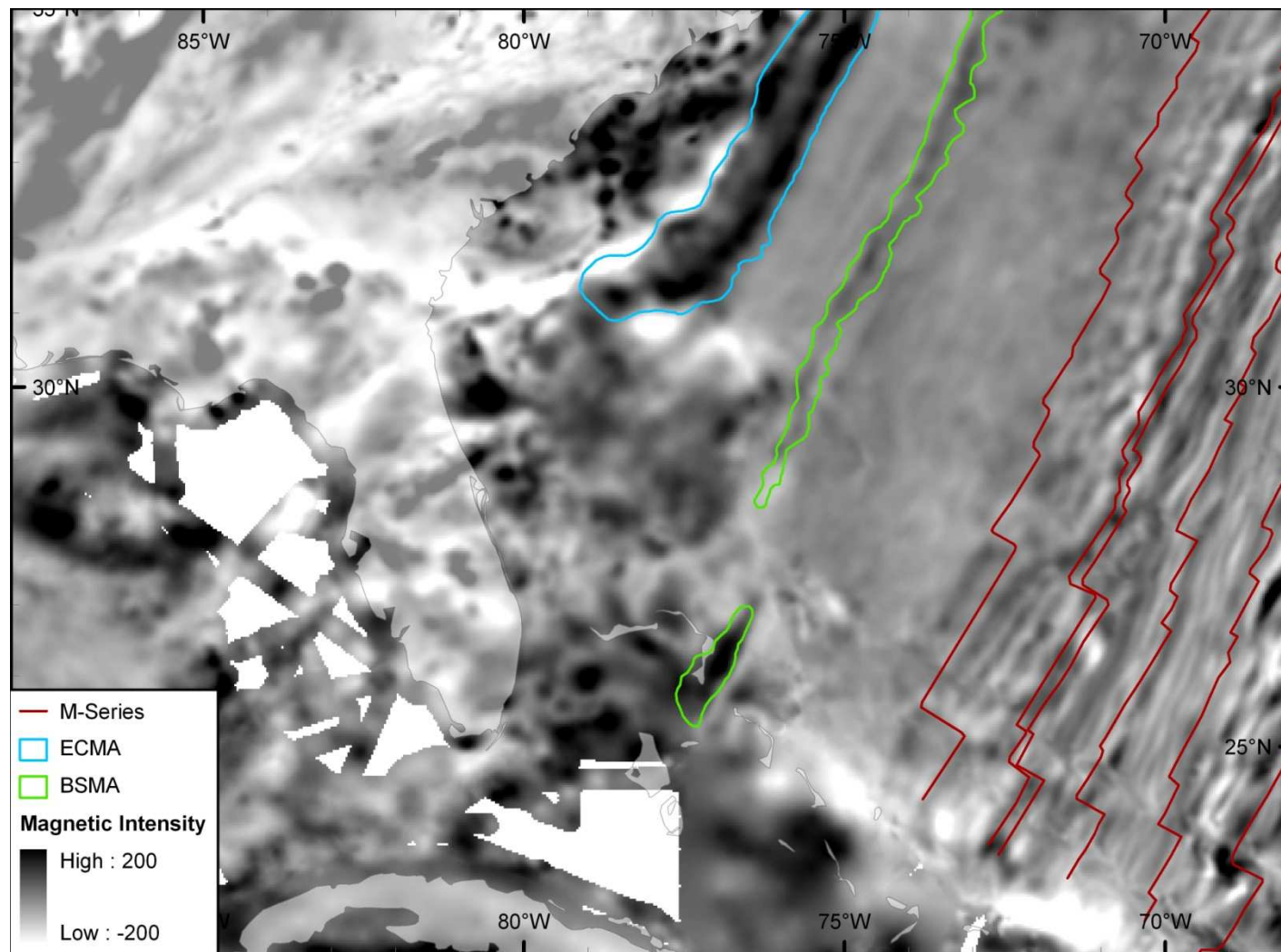
Figure 4.2. Magnetic anomaly map of the southeast North American margin and the western Central Atlantic. Magnetic anomaly grid from EMAG2 (Maus et al., 2009). M-series isochrons are marked in red (after Labails et al., 2010). The East Coast Magnetic Anomaly (ECMA) is outlined in blue and the Blake Spur Magnetic Anomaly (BSMA) is outlined in green (after Labails et al., 2010).

not active plate boundaries, these structures function very similarly to oceanic transform faults that separate mid-ocean ridge spreading centers (Faulds and Varga, 1998).

Transfer zones have been hypothesized to be present on the eastern North American margin (Tauvers and Muehlberger, 1987; Etheridge et al., 1989); however, only recently have reversals in sub-basin polarity been observed, confirming their existence (Chapter 3). The Cordele and Walterboro transfer zones are constrained by reversals in sub-basin polarity and other transfer zones are inferred from changes in basin geometry and offsets in faults (Figure 4.3).

4.2.3 KINEMATIC HISTORY OF THE CENTRAL ATLANTIC

Fracture zones in the Atlantic Ocean are fairly well constrained from the present day back to the M-25 isochron at ca.154 Ma; however, beyond this magnetic feature fracture zones are not well constrained because of the difficulty of mapping isochrons within the Jurassic quiet zone (Klitgord and Schouten, 1986; Schettino and Turco, 2009; Labails et al., 2010). Klitgord and Schouten (1986) predicted an extension of fracture zones beyond the M-25 magnetic anomaly into the Jurassic quiet zone. These fracture zone extensions were traced using contoured aero-magnetic data with the assumption that the divergent plate trajectory was approximately constant (Klitgord and Behrendt, 1979). Two recent studies, however, have reconstructed Pangea based on fitting prominent magnetic anomalies at the edge of the Atlantic oceanic crust (Schettino and Turco, 2009; Labails et al., 2010).

Several authors have argued that a ridge jump took place during the earliest part of the opening of the Atlantic and that the oldest oceanic crust should be found adjacent to North America (Vogt, 1973; Klitgord and Schouten, 1986; Schettino and Turco, 2009).

81
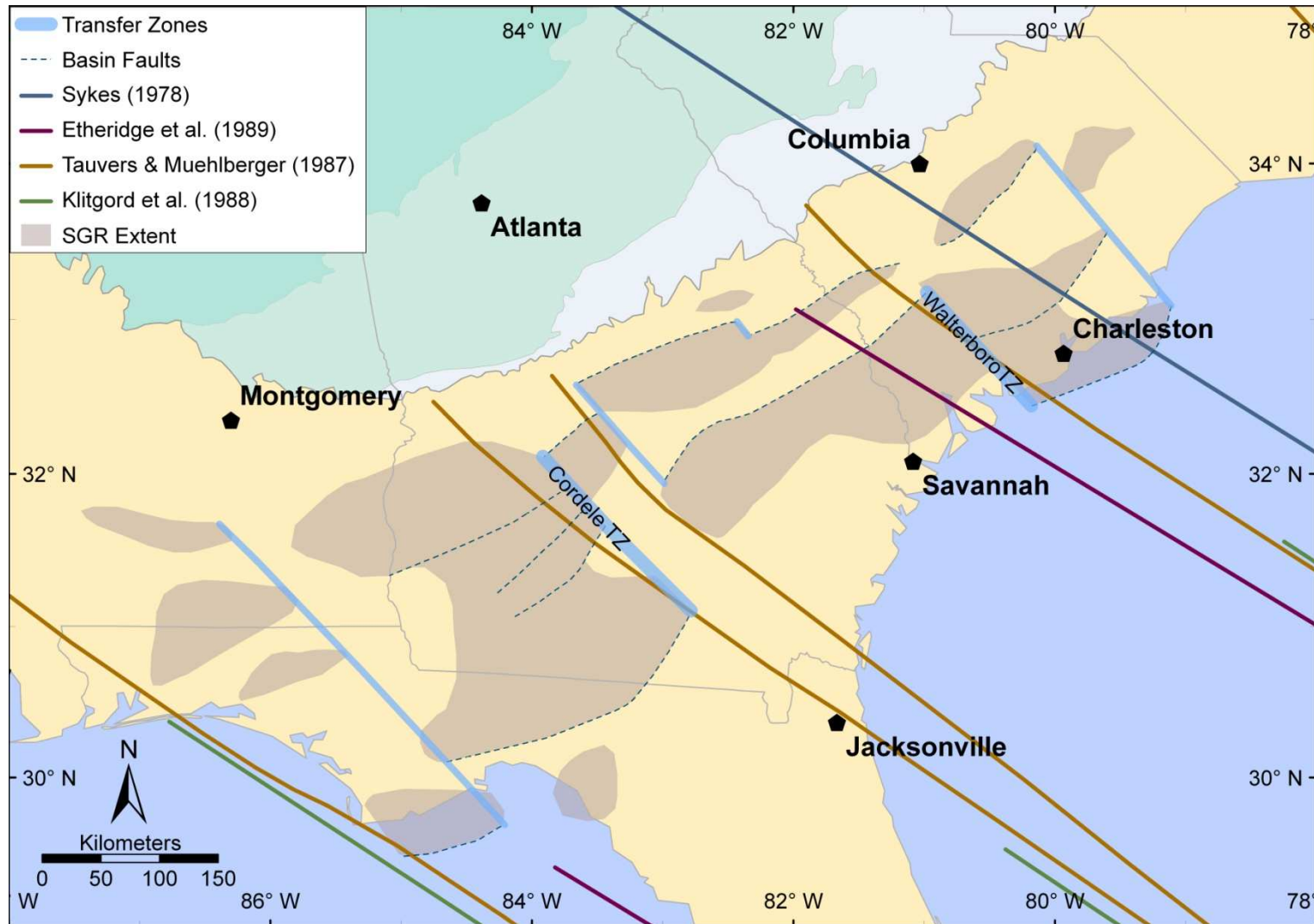
Figure 4.3. Map of major structures of the South Georgia Rift.

Based on this argument, Schettino and Turco (2009) reasoned that the prominent East
Coast Magnetic Anomaly (ECMA) and Blake Spur Magnetic Anomaly (BSMA)
represented the edges of this first Atlantic crust and used a best-fit algorithm to fit the two
magnetic anomalies together. From this fit, Schettino and Turco (2009) calculated a pole
of rotation to represent the earliest opening of the Atlantic (Table 4.1).

Table 4.1. Stage Euler poles for North America.

Reference	Stage	Time (Ma)	Latitude (degrees)	Longitude (degrees)
Klitgord and Schouten (1986)	Rift			
	ECMA – BSMA	175 - 170	60.00	0.00
	BSMA – M-25	170 – 154	60.00	0.00
Schettino and Turco (2009)	Rift	230 - 200	24.51	47.00
	ECMA – BSMA	200 - 185	24.51	47.00
	BSMA – M-25	185 - 154	60.70	30.60
Labails et al. (2010)	Rift	203 - 190	52.44	1.08
	ECMA – BSMA	190 - 170	42.95	-42.47
	BSMA – M-25	170 - 154	62.00	-1.09

Labails et al. (2010) also fit prominent magnetic anomalies to reconstruct Pangea;
however, they worked on fitting magnetic anomalies from the African side of the Atlantic
with the North American side. Labails et al. (2010) interpreted two of the African
magnetic anomalies to be the conjugates to the BSMA and ECMA. They reasoned that
the presence of these conjugate magnetic anomalies precludes a ridge jump and explained
the difference in oceanic crust by asymmetric spreading.

4.3. METHODS

If oceanic transforms are inherited features of the rift, continental transfer zones should project along small circles to the ends of oceanic fracture zones. Since plate movements on a sphere are described as rotations about an Euler pole, transverse features such as oceanic fracture zones follow the approximate path of small circles plotted from these poles (Klitgord and Schouten, 1986).

In order to test the hypothesis that Central Atlantic transform faults are inherited from North American transfer zones, stage poles were compiled from previous studies, either directly where reported (Klitgord and Schouten, 1986; Schettino and Turco, 2009) or calculated from total reconstruction poles (Labails et al., 2010). The compiled stage poles were from Triassic rifting through ca. 154 Ma, for a fixed North American continent relative to Africa (Table 4.1).

Small circles calculated from the rift stage poles were first compared with the geometry against the Cordele and Walterboro Transfer Zones to see if there is a comparable geometry. While Klitgord and Schouten (1986) did not explicitly derive a rift stage pole of rotation, other studies have used similar small circles to project fracture zones onto the continental margin and so assumed that the rift stage was not much different from the early drift stage (Sykes, 1978; Klitgord et al., 1984; Etheridge et al., 1989).

Small circles were then plotted based on the poles of rotation to see if oceanic fracture zones do project into transfer zones. Rift stage small circles for Schettino and Turco (2009) and Labails et al. (2010) were plotted at a close fit to the transfer zones. Small circles from Klitgord and Schouten (1986) were plotted from fracture zones at the

M-25 isochron. Drift stage small circles were plotted at the appropriate location for each study.

For Schettino and Turco (2009), there is no change between the rift stage and first drift stage when they considered oceanic crust to be accreting between the ECMA and BSMA. The change from drift stage 1 to drift stage 2 was considered to take place at the easterly end of the BSMA.

Labails et al. (2010) calculated a different pole of rotation between the rift and first drift stage. Their first drift stage was considered to have occurred at the North American hinge line, which marks the transition from continent to ocean basin. The results from Labails et al. (2010) suggest another change in the pole of rotation at BSMA time, so small circles for their drift 2 stage were plotted from the western edge of the BSMA. The process was reversed for projecting the Jacksonville and Blake Spur Fracture Zones onshore.

4.4. RESULTS

The small circles from Klitgord and Schouten (1986) trend slightly east-west relative to the transfer zones, with a misfit of about 13 degrees to the Cordele transfer zone (Figure 4.4A) and a misfit of 11 degrees to the Walterboro transfer zone (Figure 4.4B). The small circles of Schettino and Turco (2009) have the best fit, off by about 1 degree from the trend of each transfer zone, and are wholly contained within the mapped zone itself. The rift stage small circles from Labails et al. (2010) have a misfit of about 5 degrees for the Cordele transfer zone and 3 degrees for the Walterboro transfer zone.
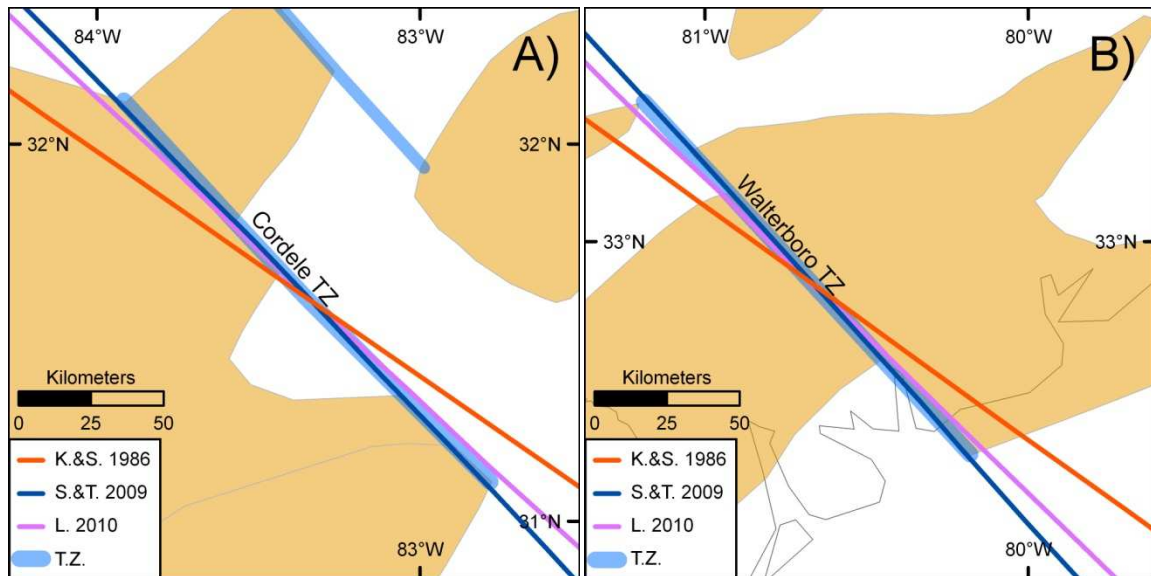
Figure 4.4. Comparison of rift stage small circles with: A) the geometry the Cordele transfer zone in Georgia; and B) the geometry of the Walterboro transfer zone in South Carolina. K.&S. - Klitgord and Schouten (1986), S.&T. - Schettino and Turco (2009), L. - Labails et al. (2010).

Small circle projections of oceanic fracture zones based on Klitgord and Schouten (1986) make similar correlations to previous studies (Figure 4.5; Tauvers and Muehlberger, 1987). The Blake Spur Fracture Zone projects towards the Walterboro transfer zone. The Jacksonville Fracture Zone projects towards the Cordele transfer zone.

Small circle projections from both Schettino and Turco (2009) and Labails et al. (2010) correlate similar features onshore to the M-25 isochron (Figure 4.6 and 4.7). The Cordele transfer zone projects approximately into the 15° 20' fracture zone. The Jacksonville Fracture Zone projects onshore into a transfer zone inferred through an offset on the rift basin border fault system, and a thinning of the basin. Unlike the other projections, the Walterboro transfer zone doesn't appear to project into a prominent fracture zone at M-25. The projection does, however, mark a break in both the ECMA and BSMA. The Blake Spur Fracture Zone projects into an inferred transfer zone northeast of where previous studies have projected its continental extension.
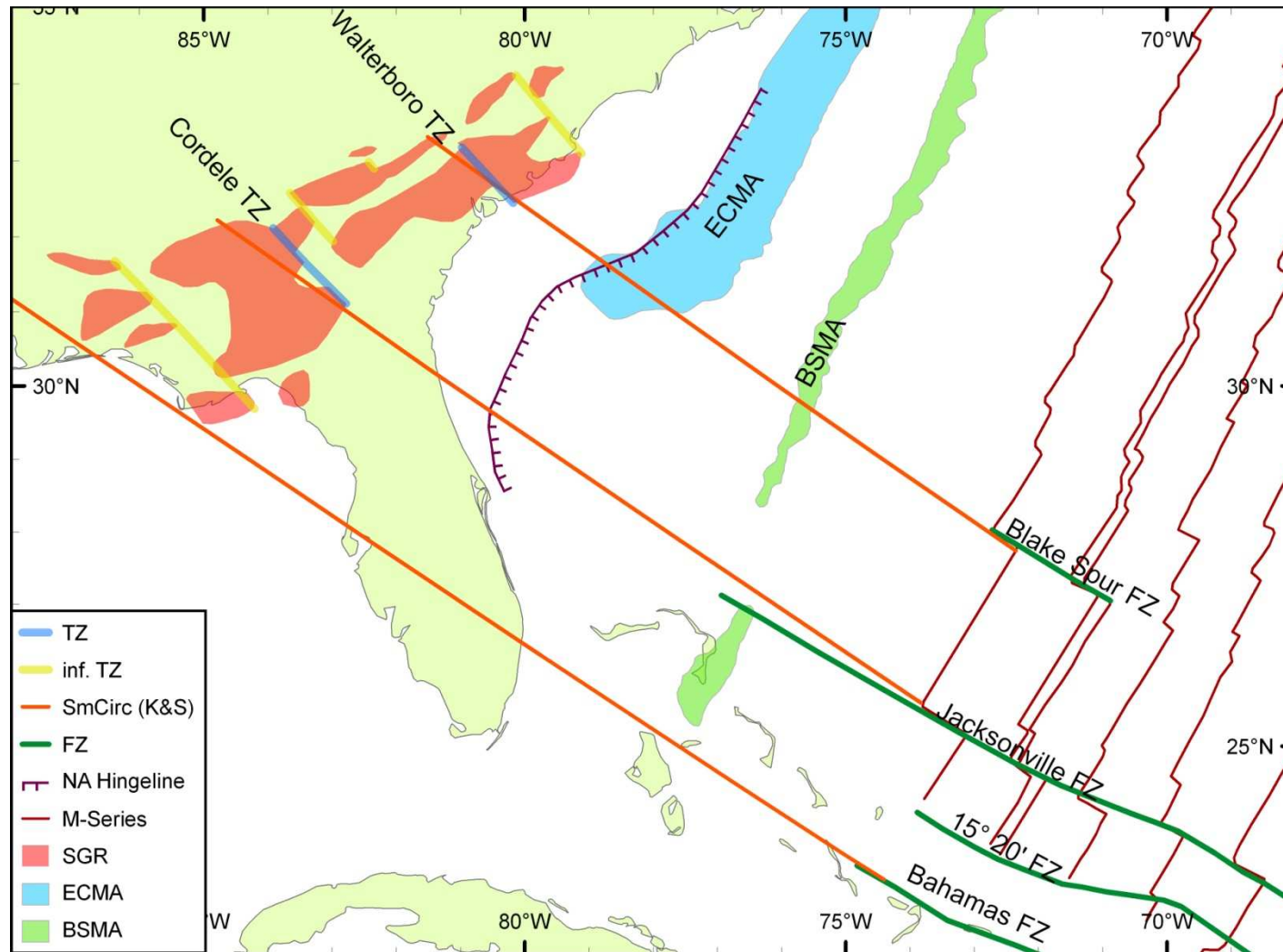
Figure 4.5. Projection of oceanic fracture zones from the M-25 isochron based on Klitgord and Schouten, 1986 (K&S). North American (NA) Hingeline, M-Series isochrons, East Coast Magnetic Anomaly (ECMA), and Blake Spur Magnetic Anomaly (BSMA), after Labails et al., 2010. Fracture zones (FZ) after Klitgord and Schouten, 1986, and Labails et al., 2010.
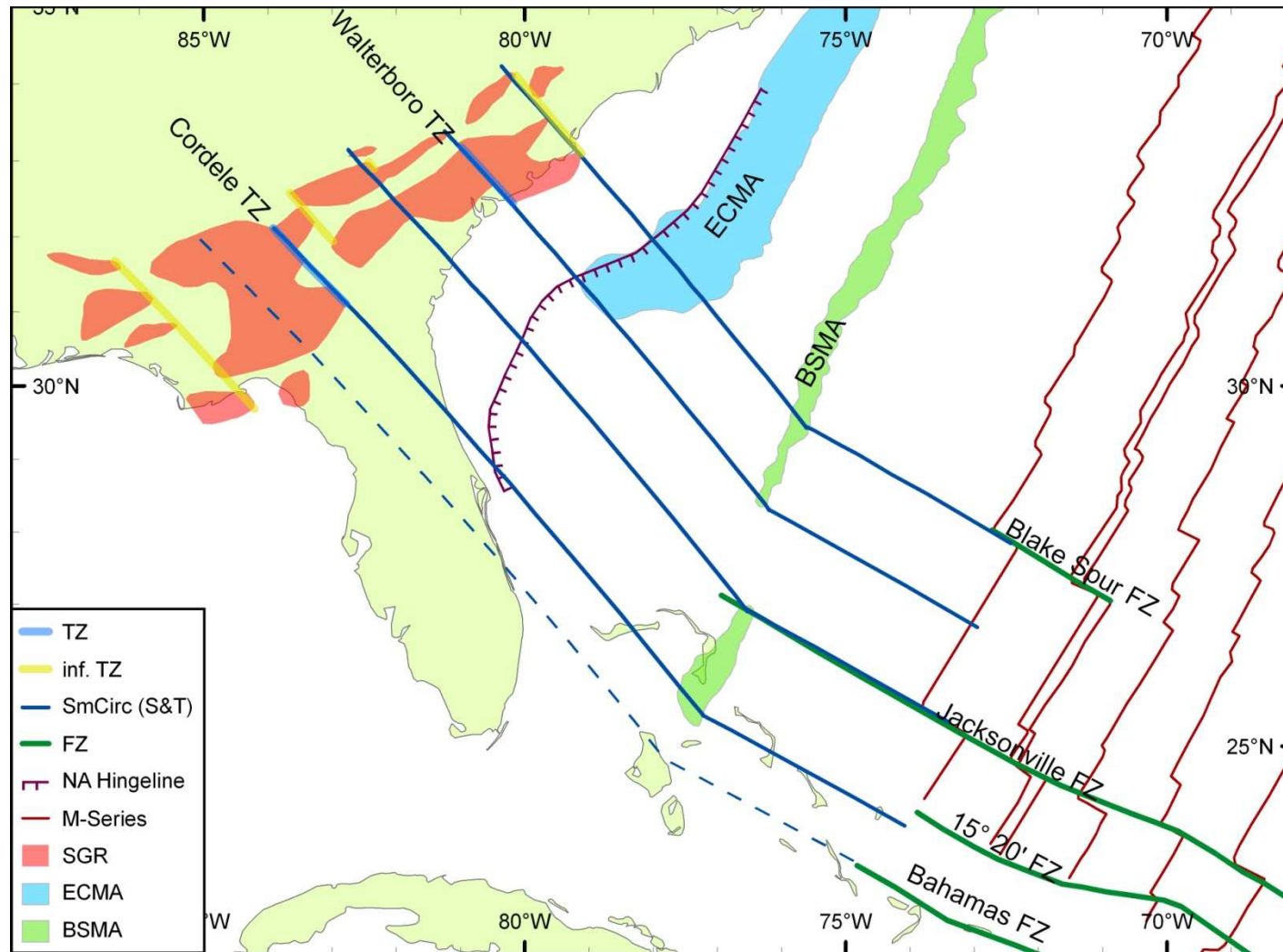
Figure 4.6. Projection of oceanic fracture zones onshore, and transfer zones offshore based on Schettino and Turco, 2009 (S&T). North American (NA) Hingeline, M-Series isochrons, East Coast Magnetic Anomaly (ECMA), and Blake Spur Magnetic Anomaly (BSMA), after Labails et al., 2010. Fracture zones (FZ) after Klitgord and Schouten, 1986, and Labails et al., 2010.
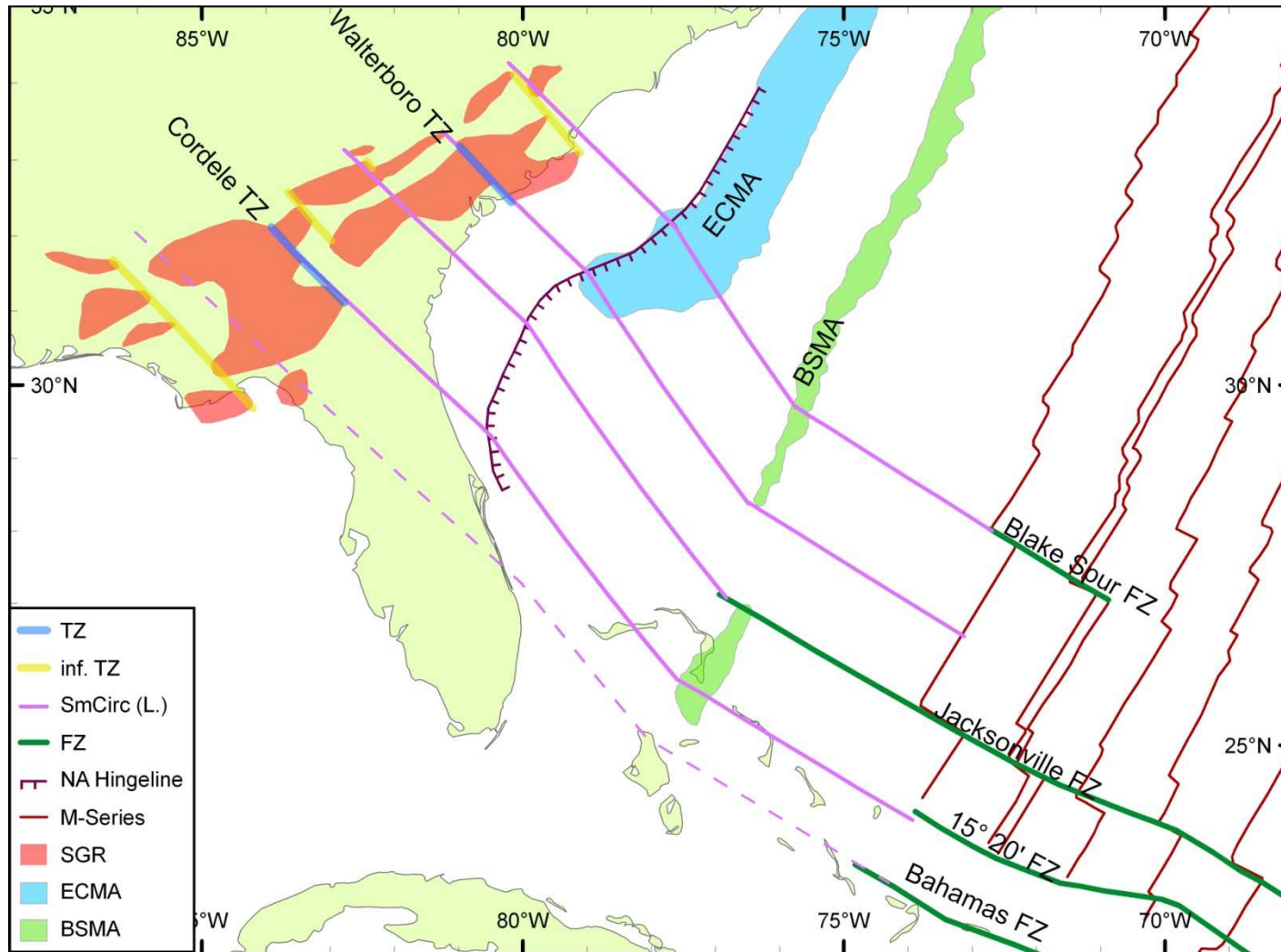
Figure 4.7. Projection of oceanic fracture zones onshore, and transfer zones offshore based on Labails et al., 2010 (L.). North American (NA) Hingeline, M-Series isochrons, East Coast Magnetic Anomaly (ECMA), and Blake Spur Magnetic Anomaly (BSMA), after Labails et al., 2010. Fracture zones (FZ) after Klitgord and Schouten, 1986, and Labails et al., 2010.

4.5. DISCUSSION

The small circle projections based on Klitgord and Schouten (1986) do appear to correlate oceanic fracture zones with mapped transfer zones, in a similar manner as previously suggested (Figure 4.5; Tauvers and Muehlberger, 1987). The small circle projections based on the newer studies (Schettino and Turco, 2009; Labails et al., 2010) also seem to correlate some oceanic features with the continental transfer zones, but not quite the same correlation as has previously been suggested (Tauvers and Muehlberger, 1987). The Cordele transfer zone does not project into the Jacksonville Fracture Zone, but instead into the 15° 20' Fracture Zone. Unlike the other projections, the Walterboro transfer zone does not appear to project into a prominent fracture zone at M-25. The projection does, however, mark a break in both the ECMA and BSMA (Figure 4.6 and 4.7) suggesting it was an important oceanic structure prior to 154 Ma.

Small circles from the newer studies (Schettino and Turco, 2009; Labails et al., 2010) have a closer fit to the mapped transfer zones than small circles from Klitgord and Schouten (1986), indicating that a change in pole of rotation likely occurred between rifting and ca. 154 Ma. Interestingly the small circle projections based on the newer studies do not distinguish between a change in plate motion at BSMA time (Schettino and Turco, 2009) or the earliest drift stage (Labails et al., 2010). The same approximate correlation is made between transfer zones in the SGR and fracture zones at the M-25 isochron.

The Bahamas Fracture Zone is one of the major structural features of the Central Atlantic, bounding the southern margin. It was proposed by Klitgord et al. (1984) to cut through Florida and bound the southwestern end of the SGR. The BSMA and ECMA are

90

not mapped this far south, so the Bahamas Fracture Zone is tentatively projected into an inferred transfer zone based on the newer studies (Figures 4.6 and 4.7; Schettino and Turco, 2009; Labails et al., 2010).

Although the small circle projections of both Schettino and Turco (2009) and Labails et al. (2010) result in a similar onshore – offshore correlation (Figure 4.6 and 4.7), the location of the poles of rotation make different predictions for rift extension and early formation of the Atlantic Ocean basin. The rift and initial drift pole from Schettino and Turco (2009) predicts that extension in the ENA rift system would be slightly greater towards the northeast which is closer to the 90 degree small circle (Figure 4.8A). Their model also predicts that opening of the Central Atlantic would be approximately synchronous along the margin. This prediction is in contrast to the diachronous southwest to northeast opening argued by Withjack et al. (1998). The rotational model of Labails et al. (2010), however, predicts that extension should be greatest towards the southwest (Figure 4.8B), and that opening of the Central Atlantic would be diachronous, opening from the south to the north (Figure 4.8C). This prediction is in better agreement with the SGR widening and thickening towards the southwest.
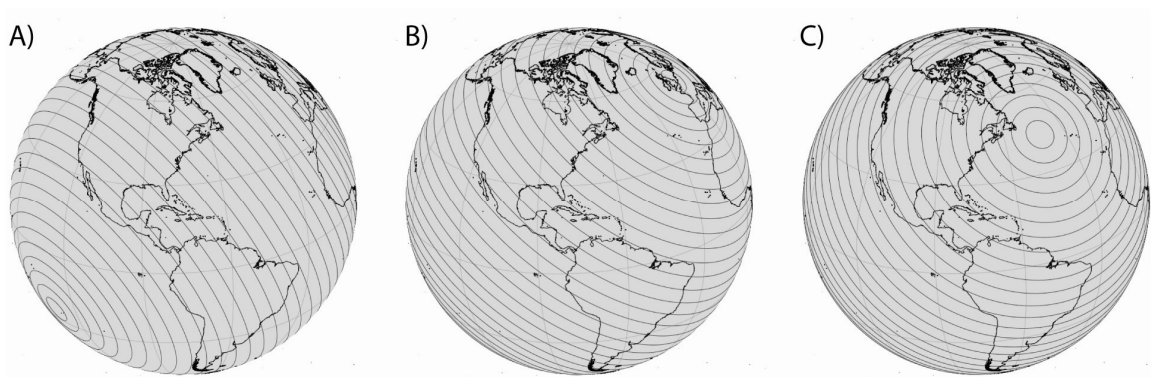
Figure 4.8. Western hemisphere of Earth with small circles from three different stage Euler poles. A) Small circles from Schettino and Turco (2009) rift stage plotted every 5 et al. (2010) result in a similar onshore – offshore correlation (Figure 4.6 and 4.7) the location of the et al. (2010) earliest drift stage plotted every 5°.

4.6. CONCLUSIONS

A first order test, projecting rift related transfer zones and oceanic fracture zones along small circles, indicates that there was likely a change in plate motion and the resultant stress fields between the Triassic rifting of Pangea and the formation of the Central Atlantic Ocean. This study also provides weak support for the hypothesis that oceanic structures are inherited from the preceding continental rift. Small circles from the work of Klitgord and Schouten (1986) project the Jacksonville and Blake Spur Fracture Zones near the Cordele and Walterboro transfer zones, but not into these rift structures. Schettino and Turco (2009) interpret a change in the pole of rotation at BSMA time. Labails et al. (2010) interpret a change in the pole of rotation between the rift stage and the earliest opening of the Atlantic. Small circles from Schettino and Turco (2009) and Labails et al. (2010) project oceanic fracture zones into inferred continental transfer zones.

Small circles from the work of Schettino and Turco (2009) and Labails et al. (2010) also suggest a different correlation than those from Klitgord and Schouten (1986); projecting the Cordele transfer zone into the 15° 20' Fracture Zone. The small circles based on Schettino and Turco (2009) and Labails et al. (2010) do not project the Walterboro transfer zone into a known fracture zone; however, the projection does correspond with terminations of the East Coast and Blake Spur magnetic anomalies. The apparent aliasing of older studies (Klitgord et al., 1984; Klitgord and Schouten, 1986; Tauvers and Muehlberger, 1987) relative to the projections based on Schettino and Turco (2009) and Labails et al. (2010) illustrates the need for more data to constrain Central Atlantic fracture zones within the Jurassic crust.

4.7 REFERENCES CITED

Cochran, J.R., and Martinez, F., 1988, Evidence from the northern Red Sea on the transition from continental to oceanic rifting: Tectonophysics, v. 153, p. 25-53.

d'Acremont, E., Leroy, S., Beslier, M.-O., Bellahsen, N., Fournier, M., Robin, C., Maia, M., and Gente, P., 2005, Structure and evolution of the eastern Gulf of Aden conjugate margins from seismic reflection data: Geophysical Journal International, v. 160, p. 869-890, doi: 10.1111/j.1365-246X.2005.02524.x.

Etheridge, M.A., Symonds, P.A., and Lister, G.A., 1989, Application of the detachment model to reconstruction of conjugate passive margins, *in* Tankard, A.J. and Balkwill, H.R., eds., Extensional tectonics and stratigraphy of the North Atlantic margins: American Association of Petroleum Geologists Memoir 46, p. 23-40.

Fantozzi, P.L., 1996, Transition from continental to oceanic rifting in the Gulf of Aden: structural evidence from field mapping in Somalia and Yemen: Tectonophysics, v. 259, p. 285-311.

Faulds, J.E. and Varga, R.J., 1998, The role of accommodation zones and transfer zones in the regional segmentation of extended terranes, *in* Faulds, J.E. and Stewart, J.H., eds., Accommodation zones and transfer zones: The regional segmentation of the Basin and Range Province: Geological Society of America Special Paper 323, p. 1-45.

Gerya, T., 2010, Dynamical instability produces transform faults at mid-ocean ridges: Science v. 329, p. 1047-1050.

Gerya, T., 2012, Origin and models of oceanic transform faults: Tectonophysics, v. 522-523, p. 34-54.

Gibbs, A.D., 1984, Structural evolution of extensional basin margins: Journal of the Geological Society of London, v. 141, p. 609-620.

Klitgord, K.D., and Behrendt, J.C., 1979, Basin structure of the U.S. Atlantic margin, *in* Watkins, J.S., Montadert, L, and Dickerson, P.W., eds., Geological and Geophysical Investigations of Continental Margins: American Association of Petroleum Geologists Memoir 29, p. 85-112.

Klitgord, K.D., Popenoe, P., and Schouten, H., 1984, Florida: A Jurassic Transform plate boundary: Journal of Geophysical Research v. 89, p. 7753-7772.

Klitgord, K.D. and Schouten, H., 1986, Plate kinematics of the central Atlantic, *in* Vogt, P.R., and Tucholke, B.E., eds., The Geology of North America, Volume M, The Western North Atlantic Region: Geological Society of America, p. 351-425.

Labails, C., Olivet, J.-L., Aslanian, D., and Roest, W.R., 2010, An alternative early opening scenario for the Central Atlantic Ocean: Earth and Planetary Science Letters, v. 297, p. 355 – 368.

Maus, S., et al., 2009, EMAG2: A 2—arc min resolution Earth Magnetic Anomaly Grid compiled from satellite, airborne, and marine magnetic measurements: Geochemistry, Geophysics, Geosystems, v. 10, Q08005, doi:10.1029/2009GC002471.

McBride, J.H. and Nelson, K.D., 1988, Is the Brunswick magnetic anomaly really the Alleghanian suture? – Comment: Tectonics, v. 7, p. 343-346.

Morley, C.K., Nelson, R.A, Patton, T.L., and Munn, S.G., 1990, Transfer zones in the East African Rift System and their relevance to hydrocarbon exploration in rifts: AAPG Bulletin, v. 74, p. 1234-1253.

Morley, C.K., 1999, Aspects of transfer zone geometry and evolution in East African Rifts, *in* Morley, C.K., ed., Geoscience of Rift Systems—Evolution of East Africa: AAPG Studies in Geology No. 44, p. 161-171.

Rosendahl, B.R., 1987, Architecture of continental rifts with special reference to East Africa: Annual Review of Earth and Planetary Science, v. 15, p. 445-503.

Schettino, A. and Turco, E., 2009, Breakup of Pangea and plate kinematics of the central Atlantic and Atlas regions: Geophysical Journal International, v. 178, p. 1078-1097.

Sykes, L.R., 1978, Intraplate seismicity, reactivation of preexisting zones of weakness, alkaline magmatism, and other tectonism postdating continental fragmentation: Review of Geophysics v. 16, p. 621-688.

Tamsett, D., 1984, Comments on the development of rifts and transform faults during continental breakup; examples from the Gulf of Aden and northern Red Sea: Tectonophysics, v. 104, p. 35-46.

Tauvers, P.R. and Muehlberger, W.R., 1987, Is the Brunswick magnetic anomaly really the Alleghanian suture?: Tectonics, v. 3, p. 331-342.

Tauvers, P.R. and Muehlberger, W.R., 1988, Is the Bruswick magnetic anomaly really the Alleghanian suture? – Reply: Tectonics, v. 7, p. 347-349.

Taylor, B., Goodliffe, A.M., and Martinez, F., 1999, How continents break up: Insights from Papua New Guinea: Journal of Geophysical Research, v. 104, p. 7497-7512.

Taylor, B., Goodliffe, A., and Martinez, F., 2009, Initiation of transform faults at rifted continental margins: Comptes Rendus Geoscience, v. 341, p. 428-438.

Thomas, W. A., 2006, Tectonic inheritance at a continental margin: GSA Today, v. 16, p. 4-11.

Vogt, P.R., 1973, Early events in the opening of the North Atlantic, *in* Tarling, D.H., and Runcorn, S.K., eds, Implications of Continental Drift to the Earth Sciences, v. 2: Academic Press, London, p. 693-712.

Wilson, J.T., 1965, A new class of faults and their bearing on continental drift: Nature, v. 207, p. 343-347.

Withjack, M.O., Schlische, R.W., and Olsen, P.E., 1998, Diachronous Rifting, Drifting, and Inversion on the Passive Margin of Central Eastern North America: An Analog for Other Passive Margins: The American Association of Petroleum Geologists Bulletin, v. 82, p. 817–835.

CHAPTER 5

CONCLUSIONS

The South Georgia Rift (SGR) provides an excellent natural laboratory for studying the effects of continental rifting. It was thought that much of the history of the rifting of Pangea was preserved in the SGR, as it was suggested to have been covered by basalt (McBride et al., 1989; Schlische et al., 2003). Additionally, while the SGR is known to overlie the Alleghanian suture (Chowns and Williams, 1983; Tauvers and Muehlberger, 1987), the apparent lithospheric weakness never fully developed into an ocean basin. Yet despite the SGR ultimately failing to open into an ocean, there has for a long time been attempts to suggest oceanic features could be projected onshore to explain intraplate seismicity and large scale tectonic patterns (Sykes, 1978; Tauvers and Muehlberger, 1987; Etheridge et al., 1989). The studies presented here have attempted to address some of these issues and progress our understanding of continental rifting. The results from Chapters 2, 3, and 4 are summarized and shown in Figure 5.1.

Reanalysis and integration of well and seismic data shows that most sub-Coastal Plain wells in the SGR do not encounter basalt; and in many wells, diabase also is not present. Absence of basalt suggests that the areal extent of basalt flows in the SGR is not as regionally pervasive as previously proposed. On SeisData 8A, a prominent reflection is identified as the J-Horizon, yet adjacent wells didn't encounter mafic igneous rocks. Therefore, the ubiquitous J-Horizon must have a different origin than basalt. On all of the seismic lines with adjacent wells, the J-Horizon corresponds with the base of the
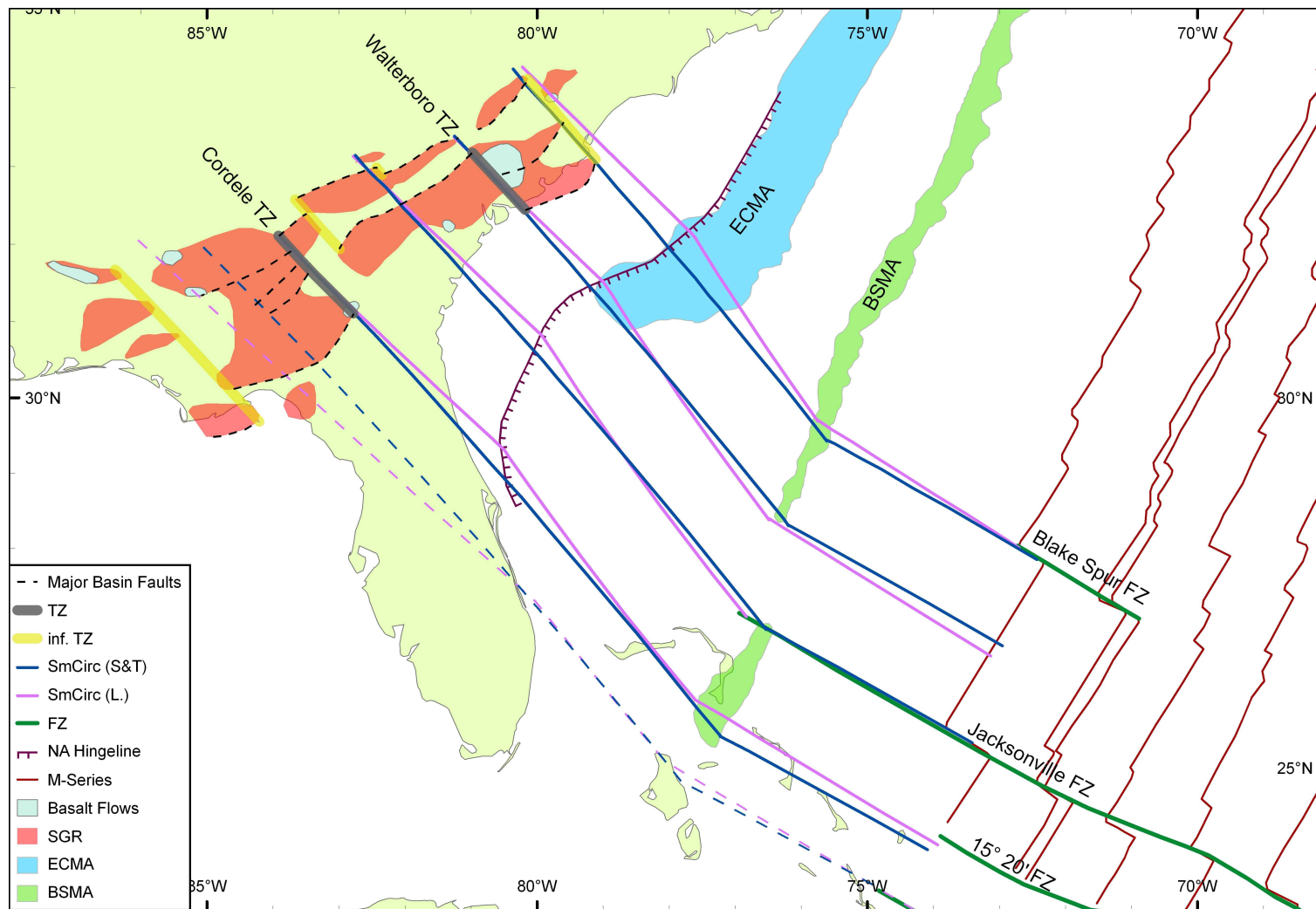
Figure 5.1. Summary figure of the South Georgia Rift. Small circles (SmCirc) based on studies from Schettino and Turco, 2009 (S&T), and Labails et al., 2010 (L.). North American (NA) Hingeline, M-Series isochrons, East Coast Magnetic Anomaly (ECMA), and Blake Spur Magnetic Anomaly (BSMA), after Labails et al., 2010. Fracture zones (FZ) after Klitgord and Schouten, 1986, and Labails et al., 2010.

Coastal Plain irrespective of basalt. Interestingly the local extent of basalt seems to correspond with mapped and inferred transfer zones.

Subsurface mapping of the SGR based on integration of seismic and well data suggests that it comprises a series of smaller sub-basins that reverse polarity across transfer zones. Although Triassic rifting of Pangea occurred over a wide area, in the SGR the upper crustal expression of the rifting was pronounced along the Alleghanian suture. The weak lithosphere in concert with oblique rifting resulted in a wide rift. Multiple rift basins formed within a zone up to 400 km wide, yet a deeper rift valley ~100 km across formed over the ancient suture.

A first order test provides support for the hypothesis that oceanic structures correlate with preceding continental rift features. The Walterboro transfer zone does not project into a known fracture zone; however, the projection does correspond with terminations of the East Coast and Blake Spur magnetic anomalies. The Cordele transfer zone projects close to the 15° 20' Fracture Zone. The Blake Spur and Jacksonville Fracture Zones project onshore to where the South Georgia Rift exhibits abrupt along-strike changes indicating possible transfer zones. The apparent aliasing of previous studies (Klitgord et al., 1984; Klitgord and Schouten, 1986; Tauvers and Muehlberger, 1987) relative to these projections illustrates the need for more data to constrain Central Atlantic fracture zones within the Jurassic crust.

The conclusions of these studies open up some new questions regarding the evolution of the eastern North American continental margin. It is thought that CAMP magmatism was exceedingly wide spread and that it may be linked with the opening of the Atlantic Ocean (McBride et al., 1989; Austin et al., 1990; Oh et al., 1995; Withjack et

98

al., 1998; Schettino and Turco, 2009). The J-Horizon had been used to mark the timing of the so-called seaward dipping reflectors (Austin et al., 1990; Oh et al., 1995), but it is clear now that this reflection does not uniquely correspond with the Club House Crossroads basalt (Heffner et al., 2012). The notion that the eastern North American margin is a volcanic passive margin is not as firm as it used to be. And perhaps we should not expect it to be volcanic in nature, as volcanic passive margins are often associated with narrower margins (White and McKenzie, 1989; Corti et al., 2003), which the eastern North American margin certainly is not. The nature of the seaward dipping reflectors should be re-evaluated, as they may also prove not to be basalt.

Reactivated Triassic normal faults have been suggested to be the primary structures responsible for seismicity in the Charleston, South Carolina region (Talwani and Dura-Gomez, 2009; Chapman and Beale, 2010). Cast in the tectonic framework of this study, previously interpreted northeast striking faults are likely reactivated normal faults while northwest striking faults are likely strike-slip faults of a transfer zone. It is unclear if this relationship of transfer zones to intra-plate seismicity holds further along the eastern margin of North America; however, the Cape Fear Arch, a tectonic feature that has been active through the Cretaceous and Cenozoic (Prowell and Obermeier, 1991), has a very similar geometry, and other northwest striking zones of intra-plate tectonics may be related (Sykes, 1978). This relationship should be further explored as it may prove important for understanding present day intra-plate seismicity.

It is not clear why the structures of the failed South Georgia Rift should be inherited by the Central Atlantic. Perhaps both sets of structures are mutually inherited from older pre-Mesozoic lithospheric weaknesses as argued by Thomas (2006). In either

case, the projection of the continental rift features to oceanic structures suggests that structural inheritance is an important process for the formation of oceanic transforms as originally proposed by Wilson (1965). The apparent aliasing of previous projections (Klitgord et al., 1984; Klitgord and Schouten, 1986; Tauvers and Muehlberger, 1987) relative to the projections based on more recent studies (Schettino and Turco, 2009; Labails et al., 2010) illustrates the need for more data to constrain Central Atlantic fracture zones within the Jurassic crust.

A common theme through these three studies is that tectonic inheritance plays an important role in continental rifting (Thomas, 2006). Triassic rifting oblique to the weak lithospheric suture between Laurentia and Gondwana lead to the formation of transfer zones within the South Georgia Rift. These transfer zones later acted as conduits for volcanism at the beginning of the Jurassic as the Central Atlantic Magmatic Province was emplaced. And although the South Georgia Rift ultimately failed to open, it imparted an early structural framework to the Central Atlantic.

REFERENCES

Aadland, R.K., Gellici, J.A., and Thayer, P.A., 1995, Hydrogeologic framework of west-central South Carolina: South Carolina Department of Natural Resources Water Resources Division Report 5, 200 p.

Ackermann, H.D., 1983, Seismic-refraction study in the area of the Charleston, South Carolina, 1886 earthquake, *in* Gohn, G.S., ed., Studies Related to the Charleston, South Carolina, Earthquake of 1886—Tectonics and Seismicity: U.S. Geological Survey Professional Paper 1313, p. F1–F20.

Akintunde, O.M., Knapp, C.C., Knapp, J.H., and Heffner, D.M., 2013, New constraints on buried Triassic basins and regional implications for subsurface CO_2 storage from the SeisData6 seismic profile across the Southeast Georgia Coastal Plain: Environmental Geosciences, v. 20, p. 1-13.

Amick, D.C., 1979, Crustal structure studies in the South Carolina Coastal Plain, M.S. thesis, University of South Carolina, 81 p.

Applin, P.L., 1951, Preliminary report on buried pre-Mesozoic rocks in Florida and adjacent states: US Geological Survey Circular 91, 28 p.

Applin, E.R., and Applin, P.L., 1964, Logs of selected wells in the Coastal Plains of Georgia: Georgia Geologic Survey Bulletin 74, 229 p.

Austin, J.A., Stoffa, P.L., Phillips, J.D., Oh, J., Sawyer, D.S., Purdy, G.M., Reitet, E., and Makris, J., 1990, Crustal structure of the southeast Georgia Embayment-Carolina Trough: preliminary results of a composite seismic image of a continental suture(?) and a volcanic passive margin: Geology, v. 18, p. 1023–1027, doi:10.1130/0091-7613(1990)018<1023:CSOTSG>2.3.CO;2.

Bailey, D.K., 1977, Lithosphere control of continental rift magmatism: Journal of the Geological Society, v. 133, p. 103-106.

Ball, M.M., Martin, R.G., Foote, R.Q., and Applegate, A.V., 1988, Structure and stratigraphy of the Western Florida Shelf, Part I, Multichannel reflection seismic data: US Geological Survey Open File Report 88-439.

Bally, A.W., 1982, Musings over sedimentary basin evolution: Philosophical Transactions of the Royal Society of London A., v. 305, p. 325-337.

Barnes, A.E., and Reston, T.J., 1992, A study of two mid-crustal bright spots from southeast Georgia (USA): Geophysical Journal International, v. 108, p. 683-691.

Barnett, R.S., 1975, Basement structure of Florida and its tectonic implications: Transactions of the Gulf Coast Association of Geological Societies, v. 25, p. 122-140.

Behrendt, J.C., Hamilton, R.W., Ackermann, H.D., and Henry, V.J., Cenozoic faulting in the vicinity of the Charleston, S.C., 1886 earthquake: Geology, v. 9, p. 117-122.

Behrendt, J.C., Hamilton, R.M., Ackermann, H.D., Henry, V.J., and Bayer, K.C., 1983, Marine multichannel seismic-reflection evidence for Cenozoic faulting and deep crustal structure near Charleston, South Carolina, *in* Gohn, G.S., ed., Studies Related to the Charleston, South Carolina, Earthquake of 1886—Tectonics and Seismicity: U.S. Geological Survey Professional Paper 1313, p. J1–J29.

Behrendt, J.C., 1985, Interpretations from multichannel seismic-reflection profiles of the deep crust crossing South Carolina and Georgia from the Appalachian mountains to the Atlantic coast: U.S. Geological Survey U.S. Misc. Field Studies, Map MF-1656.

Behrendt, J.C., and Yuan, A., 1987, The Helena Banks strike-slip (?) fault zone in the Charleston, South Carolina, earthquake areal: Results from a marine, high-resolution, multichannel, seismic-reflection survey: Geological Society of America Bulletin, v. 98, p. 591-601.

Bonini, W.E., and Woollard, G.P., 1960, Subsurface geology of North Carolina – South Carolina Coastal Plain from seismic data: Bulletin of the American Association of Petroleum Geologists, v. 44, p. 298-315.

Brune, S., Popov, A.A., and Sobolev, S.V., 2012, Modeling suggests that oblique extension facilitates rifting and continental break-up: Journal of Geophysical Research, v. 117, B08402, doi:10.1029/2011JB008860.

Buck, W.R., 1991, Modes of continental lithospheric extension: Journal of Geophysical Research, v. 96, p. 20161-20178.

Chapman, M.C., and Beale, J.N., 2010, On the Geologic Structure at the Epicenter of the 1886 Charleston, South Carolina, Earthquake: Bulletin of the Seismological Society of America, v. 100, p. 1010–1030, doi:10.1785/0120090231.

Chowns, T.M., and Williams, C.T., 1983, Pre-Cretaceous rocks beneath the Georgia Coastal Plain—Regional Implications, *in* Gohn, G.S., ed., Studies Related to the Charleston, South Carolina, Earthquake of 1886—Tectonics and Seismicity: U.S. Geological Survey Professional Paper 1313, p. L1–L42.

Clendenin, C.W. Jr., Waddell, M.G., and Addison, A.D., 2011, Reactivation and overprinting of South Georgia Rift extension: Geological Society of America Abstract with Programs, v. 43, no. 5, p. 551.

Cochran, J.R., and Martinez, F., 1988, Evidence from the northern Red Sea on the transition from continental to oceanic rifting: Tectonophysics, v. 153, p. 25-53.

Cook, F.A., Brown, L.D., Kaufman, S., Oliver, J.E., Petersen, T.A., 1981, COCORP seismic profiling of the Appalachian orogen beneath the Coastal Plain of Georgia: Geological Society of America Bulletin, Part I, v. 92, p. 738 – 748.

Cooke, C.W., 1936, Geology of the Coastal Plain of South Carolina: U.S. Geological Survey, Bulletin 867, 196 p.

Corti, G., Bonini, S., Conticelli, S., Innocenti, F., Manetti, P., and Sokoutis, D., 2003, Analogue modeling of continental extension: A review focused on the relations between the patterns of deformation and the presence of magma: Earth Science Reviews, v. 63, p. 169-247.

Corti, G., 2012, Evolution and characteristics of continental rifting: Analog modeling-inspired view and comparison with examples from the East African Rift System: Tectonophysics, v. 522-523, p. 1-33.

Costain, J.K, Speer, J.A., Glover III, L., Perry, L., Dashevsky, S., and McKinney, M. (1986), Heat flow in the Piedmont and Atlantic Coastal Plain of the Southeastern United States: Journal of Geophysical Research, v. 91, p. 2123-2135.

Cumbest, R.J., Price, V., and Anderson, E.E., 1992, Gravity and magnetic modeling of the Dunbarton Triassic basin, South Carolina: Southeastern Geology, v. 33, p. 37-51.

d'Acremont, E., Leroy, S., Beslier, M.-O., Bellahsen, N., Fournier, M., Robin, C., Maia, M., and Gente, P., 2005, Structure and evolution of the eastern Gulf of Aden conjugate margins from seismic reflection data: Geophysical Journal International, v. 160, p. 869-890, doi: 10.1111/j.1365-246X.2005.02524.x.

Daniels, D.L. and Zietz, I., 1978, Geologic interpretation of aeromagnetic maps of the Coastal Plain region of South Carolina and parts of North Carolina and Georgia: US Geological Survey Open File Report 78-261.

Daniels, D.L., Zietz, I., and Popenoe, P., 1983, Distribution of subsurface lower Mesozoic rocks in the southeastern United States as interpreted from regional aeromagnetic and gravity maps, *in* Gohn, G.S., ed., Studies Related to the Charleston, South Carolina, Earthquake of 1886—Tectonics and Seismicity: U.S. Geological Survey Professional Paper 1313, p. K1–K24.

Darton, N.H., 1896, Artesian wells on the Atlantic Coast: U.S. Geological Survey Bulletin 138, p. 218.

Dillon, W.P., Paull, C.K., Buffler, R.T., and Fail, J.P., 1979, Structure and development of the Southeast Georgia Embayment and northern Blake Plateau – Preliminary analysis, *in* Watkins, J.S., Montadert, L., and Dickerson, P.W., eds., Geological and geophysical investigations of continental margins: American Association of Petroleum Geologists Memoir 29, p. 27-41.

Dillon, W.P., and Popenoe, P., 1988, The Blake Plateau basin and Carolina Trough, *in* Sheridan, R.E., and Grow, J.A., eds., The Atlantic Continental Margin, U.S.: Geological Society of America, Geology of North America, I-2, p. 291-328.

Domoracki, W.J., Stephenson, S.E., Çoruh, C., and Costain, J.K., 1999, Seismotectonic structures along the Savannah River Corridor, South Carolina, U.S.A.: Geodynamics v. 27, p. 97-118.

Domoracki, W.J., 1995, A Geophysical investigation of geologic structure and regional tectonic setting at the Savannah River Site, South Carolina, PhD thesis, Virginia Polytechnic Institute & State University, Blacksburg, 236 p.

Dove, D., Jaume, S.C., and Beutel, E., 2007, Tectonic core of a sedimentary drift: a potential ridge propagation feature beneath the Blake Outer Ridge: Marine Geophysical Research v. 28, p. 1-11.

Etheridge, M.A., Symonds, P.A., and Lister, G.A., 1989, Application of the detachment model to reconstruction of conjugate passive margins, *in* Tankard, A.J. and Balkwill, H.R., eds., Extensional tectonics and stratigraphy of the North Atlantic margins: American Association of Petroleum Geologists Memoir 46, p. 23-40.

Falls, W.F., 1994, Lithologic descriptions of two cores and ground-water-quality data from five counties in the northeastern part of the Coastal Plain of South Carolina, 1988 and 1991: United States Geological Survey Open-File Report 94-58, 49 p.

Falls, W.F., and Prowell, D.C., 2001, Stratigraphy and depositional environments of sediments from five cores from Screven and Burke counties, Georgia: United States Geological Survey Professional Paper 1603-A, 22 p.

Fantozzi, P.L., 1996, Transition from continental to oceanic rifting in the Gulf of Aden: structural evidence from field mapping in Somalia and Yemen: Tectonophysics, v. 259, p. 285-311.

Faulds, J.E. and Varga, R.J., 1998, The role of accommodation zones and transfer zones in the regional segmentation of extended terranes, *in* Faulds, J.E. and Stewart, J.H., eds., Accommodation zones and transfer zones: The regional segmentation of the Basin and Range Province: Geological Society of America Special Paper 323, p. 1-45.

Gawthorpe, R.L., and Hurst, J.M., 1993, Transfer zones in extensional basins—their structural style and influence on drainage development and stratigraphy: Journal of the Geological Society, v. 150, P. 1137-1152.

Gawthorpe, R.L., and Leeder, M.R., 2000, Tectono-sedimentary evolution of active extensional basins: Basin Research, v. 12, p. 195-218.

Gellici, J.A., 2007, Hydrostratigraphy of the ORG-393 core hole at Orangeburg, South Carolina: South Carolina Department of Natural Resources Water Resources Report 42, 40 p.

GeoPRISMS Draft Science Plan, 2010.

Gerya, T., 2010, Dynamical instability produces transform faults at mid-ocean ridges: Science v. 329, p. 1047-1050.

Gerya, T., 2012, Origin and models of oceanic transform faults: Tectonophysics, v. 522-523, p. 34-54.

Gibbs, A.D., 1984, Structural evolution of extensional basin margins: Journal of the Geological Society of London, v. 141, p. 609-620.

Gohn, G.S., Gottfried, D., Lanphere, M.A., and Higgins, B.B., 1978, Regional implications of Triassic or Jurassic age for basalt and sedimentary red beds in the South Carolina Coastal Plain: Science, v. 202, no. 4370, p. 887-890.

Gohn, G.S., 1983, Geology of the basement rocks near Charleston, South Carolina—Data from detrital rock fragments in lower Mesozoic(?) rocks, *in* Clubhouse Crossroads test hole #3, in Gohn, G.S., ed., Studies Related to the Charleston, South Carolina, Earthquake of 1886—Tectonics and Seismicity: U.S. Geological Survey Professional Paper 1313, p. E1–E22.

Gohn, G.S., Houser, B.B., and Schneider, R.R., 1983, Geology of the Lower Mesozoic(?) sedimentary rocks in Clubhouse Crossroads Test Hole #3, near Charleston, South Carolina, in Gohn, G.S., ed., Studies Related to the Charleston, South Carolina, Earthquake of 1886—Tectonics and Seismicity: U.S. Geological Survey Professional Paper 1313, p. D1–D17.

Gregory, J.W., 1896, The Great Rift Valley, Frank Cass & Co. Ltd. ,London, 422 p.

Hames, W.E., Renne, P.R., and Ruppel, C., 2000, New evidence for geologically instantaneous emplacement of earliest Jurassic Central Atlantic magmatic province basalts on the North American margin: Geology, v. 28, p. 859–862, doi:10.1130/0091-7613(2000)28<859:NEFGIE>2.0.CO;2.

Hames, W.E., Salters, V.J., Morris, D., and Billor, M.Z., 2010, The Middle Jurassic flood basalts of southeastern North America: Geological Society of America Abstracts with Programs, v. 42, p. 196.

Hamilton, R.M., Behrendt, J.C., and Ackermann, H.D., 1983, Land multichannel seismic-reflection evidence for tectonic features near Charleston, South Carolina, *in* Gohn, G.S., ed., Studies Related to the Charleston, South Carolina, Earthquake of 1886—Tectonics and seismicity: U.S. Geological Survey Professional Paper 1313, p. I1–I18.

Heatherington, A.L., Mueller, P.A., and Nutman, A.P., 1999, A Jurassic granite from Southern Georgia, U.S.A.: silicic, extension-related magmatism along the Southeastern Coastal Plain: Journal of Geology, v. 107, p. 375-384.

Heatherington, A.L., and Mueller, P.A., 2003, Mesozoic Igneous Activity in the Suwannee Terrane, Southeastern USA: Petrogenesis and Gondwanan affinities: Gondwana Research, v. 6, no. 2, p. 296-311.

Heffner, D.M., Knapp, J.H., Akintunde, O.M., and Knapp, C.C., 2012, Preserved extent of Jurassic flood basalt in the South Georgia Rift: A new interpretation of the J horizon: Geology, v. 40, p. 167–170.

Herrick, S.M., 1961, Well logs of the Coastal Plain of Georgia: Georgia Geological Survey Bulletin 70, 462 p.

Keranen, K.M., Klemperer, S.L., Julia, J., Lawrence, J.F., and Nyblade, A.A., 2009, Low lower crustal velocity across Ethiopia: Is the Main Ethiopian Rift a narrow rift in a hot craton?: Geochemistry Geophysics Geosystems, v. 10, Q0AB01, doi:10.1029/2008GC002293.

Klitgord, K.D., and Behrendt, J.C., 1979, Basin structure of the U.S. Atlantic margin, *in* Watkins, J.S., Montadert, L, and Dickerson, P.W., eds., Geological and Geophysical Investigations of Continental Margins: American Association of Petroleum Geologists Memoir 29, p. 85-112.

Klitgord, K.D., Popenoe, P., and Schouten, H., 1984, Florida: A Jurassic Transform plate boundary: Journal of Geophysical Research v. 89, p. 7753-7772.

Klitgord, K.D. and Schouten, H., 1986, Plate kinematics of the central Atlantic, *in* Vogt, P.R., and Tucholke, B.E., eds., The Geology of North America, Volume M, The Western North Atlantic Region: Geological Society of America, p. 351-425.

Klitgord, K.D., Hutchinson, D.R., and Schouten, H., 1988, U.S. Atlantic continental margin; structural and tectonic framework, *in* Sheridan, R.W., and Grow, J.A., eds., The Geology of North America Volume I-2, The Atlantic Continental Margin, U.S.: Geological Society of America, p. 19-55.

Kusznir, N.J., and Ziegler, P.A., 1992, The mechanics of continental extension and sedimentary basin formation: A simple-shear / pure-shear flexural cantilever model, *in* Ziegler, P.A., ed., Geodynamics of Rifting, Volume III. Thematic Discussions: Tectonophysics, v. 215 p. 117-131.

Kusznir, J.R., Roberts, A.M., and Morley, C.K., 1995, Forward and reverse modeling of rift basin formation: Geological Society of London Special Publication, v. 80, p. 33-56.

Labails, C., Olivet, J.-L., Aslanian, D., and Roest, W.R., 2010, An alternative early opening scenario for the Central Atlantic Ocean: Earth and Planetary Science Letters, v. 297, p. 355 – 368.

Leeder, M.R., and Gawthorpe, R.L., 1987, Sedimentary models for extensional tilt-block / half-graben basins, *in* Coward, M.P., Dewey, J.F., and Hancock, P.L., eds, Continental Extensional Tectonics, Geological Society special Publication No. 28, p. 139 – 152.

Le Pichon, X., and Fox, P.J., 1971, Marginal offsets, fracture zones, and the early opening of the North Atlantic: Journal of Geophysical Research, v. 76, p. 6294-6308.

Leutgert, J.H, Benz, H.M., and Madabhushi, S., 1994, Crustal structure beneath the Atlantic Coastal Plain of South Carolina: Seismological Research Letters, v. 65, p. 180 – 191.

Lister, G.S., Etheridge, M.A., Symonds, P.A., 1986, Detachment faulting and the evolution of passive continental margins: Geology, v. 14, p. 246-250.

Mansfield, W.C., 1937, Some deep wells near the Atlantic coast in Virginia and the Carolinas, U.S. Geological Survey, Prof. Paper 186-I, p. 159-161.

Marine, L.W., and Siple, G.E., 1974, Buried Triassic basin in the central Savannah River area, South Carolina and Georgia: Geological Society of America Bulletin, v. 85, p. 311-320.

Marzoli, A., Renne, P.R., Piccirillo, E.M., Ernesto, M., Bellieni, G., and De-Min, A., 1999, Extensive 200-million-year-old continental flood basalts of the Central Atlantic Magmatic Province: Science, v. 284, p. 616–618, doi:10.1126/science.284.5414.616.

Maus, S., et al., 2009, EMAG2: A 2—arc min resolution Earth Magnetic Anomaly Grid compiled from satellite, airborne, and marine magnetic measurements: Geochemistry, Geophysics, Geosystems, v. 10, Q08005, doi:10.1029/2009GC002471.

McBride, J.H. and Nelson, K.D., 1988, Is the Brunswick magnetic anomaly really the Alleghanian suture? – Comment: Tectonics, v. 7, p. 343-346.

McBride, J.H., Nelson, K.D., and Brown, L.D., 1989, Evidence and implications of an extensive Mesozoic rift basin and basalt/diabase sequence beneath the southeast Coastal Plain: Geological Society of America Bulletin, v. 101, p. 512–520, doi:10.1130/0016-7606(1989)101<0512:EAIOAE>2.3.CO;2.

McBride, J.H., 1991, Constraints on the structure and tectonic development of the early Mesozoic South Georgia Rift, southeastern United States; seismic reflection data processing and interpretation: Tectonics, v. 10, p. 1065–1083, doi:10.1029/90TC02682.

McFadden, S.S., Hetrick, J.H., Kellam, M.F., Rodenbeck, S.A., and Huddlestun, P.F., 1986, Geologic data of the Gulf Trough area, Georgia: Georgia Geological Survey Information Circular, v. 56, p. 211–214.

McHone, J.G., 2000, Non-plume magmatism and rifting during the opening of the central Atlantic Ocean: Tectonophysics, v. 316, p. 287–296, doi:10.1016/S0040-1951(99)00260-7.

McKenzie, D., 1978, Some remarks on the development of sedimentary basins: Earth and Planetary Science Letters, v. 40, p. 25-32.

Milton, C., and Hurst, V.J., 1965, Subsurface "basement" rocks of Georgia: Georgia Geological Survey Bulletin Number 76, 56 p.

Morley, C.K., Nelson, R.A, Patton, T.L., and Munn, S.G., 1990, Transfer zones in the East African Rift System and their relevance to hydrocarbon exploration in rifts: AAPG Bulletin, v. 74, p. 1234-1253.

Morley, C.K., 1999, Aspects of transfer zone geometry and evolution in East African Rifts, *in* Morley, C.K., ed., Geoscience of Rift Systems—Evolution of East Africa: AAPG Studies in Geology No. 44, p. 161-171.

Neathery, T.L., and Thomas, W.A., 1975, Pre-Mesozoic basement rocks of the Alabama Coastal Plain: Transactions of the Gulf Coast Association of Geological Societies, v. 25, p. 86-97.

Nelson, K.D., Arnow, J.A., McBride, J.H., Willemin, J.H., Huang, J., Zheng, L., Oliver, J.E., Brown, L.D., and Kaufman, S., 1985, New COCORP profiling in the southeastern United States. Part I: Late Paleozoic suture and Mesozoic rift basin: Geology, v. 13, p. 714 – 718.

Nomade, S., Knight, K.B., Beutel, E., Renne, P.R., Verati, C., Feraud, G., Marzoli, A., Youbi, N., and Bertrand, H., 2007, Chronology of the Central Atlantic Magmatic Province: implications for the Central Atlantic rifting processes and the Triassic-Jurassic biotic crisis: Palaeogeography, Palaeoclimatology, Palaeoecology, v. 244, p. 326–344, doi:10.1016/j.palaeo.2006.06.034.

Oh, J., Austin, A., Phillips, J.D., Coffin, M.F., and Stoffa, P.L., 1995, Seaward-dipping reflectors offshore the southeastern United States: seismic evidence for extensive volcanism accompanying sequential formation of the Carolina Trough and Blake Plateau basin: Geology, v. 23, p. 9–12, doi:10.1130/0091-7613(1995)023<0009:SDROTS>2.3.CO;2.

Olsen, P.E., 1997, Stratigraphic record of the early Mesozoic breakup of Pangea in the Laurasia-Gondwana rift system: Annual Review of Earth and Planetary Sciences, v. 25, p. 337–401, doi:10.1146/annurev.earth.25.1.337.

Olsen, P.E., Kent, D.V., Et-Touhami, M., and Puffer, J., 2003, Cyclo-, magneto-, and bio-stratigraphic constraints on the duration of the CAMP event and its relationship to the Triassic-Jurassic boundary, *in* Hames, W.E., McHone, J.G., Renne, P.R., and Ruppel, C., eds., The Central Atlantic Magmatic Province Insights from fragments of Pangea: Washington, D.C., American Geophysical Union, p. 7–32.

Petersen, T.A., Brown, L.D., Cook, F.A., Kaufman, S., and Oliver, J.E., 1984, Structure of the Riddleville basin from COCORP seismic data and implications for reactivation tectonics: Journal of Geology, v. 92, p. 261-271.

Pooley, R.N., 1960, Basement configuration and subsurface geology of eastern Georgia and southern South Carolina as determined by seismic-refraction measurements, MS Thesis, University of Wisconsin, 47 p.

Rosendahl, B.R., 1987, Architecture of continental rifts with special reference to East Africa: Annual Review of Earth and Planetary Science, v. 15, p. 445-503.

Salvador, A., 1987, Late Triassic-Jurassic paleogeography and origin of Gulf of Mexico basin: American Association of Petroleum Geologists Bulletin, v. 71, p. 419-451.

Sandwell, D.T., and Smith, W.H.F., 2009, Global marine gravity from retracked Geosat and ERS-1 altimetry: Ridge Segmentation versus spreading rate: Journal of Geophysical Research, v. 114, B01411.

Sartain, S.M., and See, B.E., 1997, The South Georgia Basin: An integration of Landsat, gravity, magnetics and seismic data to delineate basement structure and rift basin geometry: Gulf Coast Association of Geological Society Transactions, v. 47, p. 493-498.

SCDNR, South Carolina Department of Natural Resources Coastal Plain Water Well Records: http://www.dnr.sc.gov/water/hydro/WellRecords/Wells_main.htm

Schettino, A. and Turco, E., 2009, Breakup of Pangea and plate kinematics of the central Atlantic and Atlas regions: Geophysical Journal International, v. 178, p. 1078-1097.

Schilt, F.S., Brown, L.D., Oliver, J.E., and Kaufman, S., 1983, Subsurface structure near Charleston, South Carolina – Results of COCORP reflection profiling in the Atlantic Coastal Plain, *in* Gohn, G.S., ed., Studies Related to the Charleston, South Carolina, Earthquake of 1886—Tectonics and seismicity: U.S. Geological Survey Professional Paper 1313, p. H1–H19.

Schlische, R.W., 2003, Progress in Understanding the Structural Geology, Basin Evolution, and Tectonic History of the Eastern North American Rift System, *in* LeTourneau, P.M., and Olsen, P.E., eds., The Great Rift Valleys of Pangea in Eastern North America: New York, Columbia University Press, p. 21–64.

Schlische, R.W., Withjack, M.O., and Olsen, P.E., 2003, Relative timing of CAMP, rifting continental breakup, and basin inversion: tectonic significance, *in* Hames, W.E., McHone, J.G., Renne, P.R., and Ruppel, C., eds., The Central Atlantic Magmatic Province Insights from fragments of Pangea: Washington, D.C., American Geophysical Union, p. 33–59.

Schlische, R.W. and Withjack, M.O., 2009, Origin of fault domains and fault-domain boundaries (transfer zones and accommodation zones) in extensional provinces: Result of random nucleation and self-organized fault growth: Journal of Structural Geology, v. 31, p. 910-925.

Scholle, P.A., 1979, Geological studies of the COST GE-1 well, United States South Atlantic outer continental shelf area: United States Geological Survey Circular 800, 114 p.

Smith, W.A., and Talwani, P., 1987, Results of a refraction survey in the Bowman seismogenic zone, South Carolina: South Carolina Geology, v. 31, p. 83 – 98.

Snipes, D.S., Kidd, N.B., Warner, R.D., Hodges, R.A., Price, V. Jr., and Temples, T.J., 1995, An initial petrographic and geochemical study of a rhyolitic rock recovered from Test Well #1, Hilton Head, South Carolina: South Carolina Geology, v.38, p. 53-60.

Steele, K.B., and Colquhoun, D.J., 1985, Subsurface evidence of the Triassic Newark Supergroup in the South Carolina Coastal Plain: South Carolina Geology, v. 28, no. 2, p. 11 – 22.

Stewart, J.H., 1998, Regional characteristics, tilt domains, and extensional history of the late Cenozoic Basin and Range province, western North America, *in* Faulds, J.E. and Stewart, J.H., eds., Accommodation zones and transfer zones: The regional segmentation of the Basin and Range Province: Geological Society of America Special Paper 323, p. 47-74.

Suess, E., 1891, Die Bruche des ostlichen Afrika: Denkschriften der Kaiserlichen Akademie der Wissenschaften, Mathematisch-Naturwissenschaftliche Classe, v. 58, p. 555-584.

Sykes, L.R., 1978, Intraplate seismicity, reactivation of preexisting zones of weakness, alkaline magmatism, and other tectonism postdating continental fragmentation: Review of Geophysics v. 16, p. 621-688.

Talwani, P. and Durá-Gómez, I., 2009, Finding faults in the Charleston area, South Carolina: 2. Complementary data: Seismological Research Letters, v. 80, no. 5, p. 901-919.

Tamsett, D., 1984, Comments on the development of rifts and transform faults during continental breakup; examples from the Gulf of Aden and northern Red Sea: Tectonophysics, v. 104, p. 35-46.

Tauvers, P.R. and Muehlberger, W.R., 1987, Is the Brunswick magnetic anomaly really the Alleghanian suture?: Tectonics, v. 3, p. 331-342.

Tauvers, P.R. and Muehlberger, W.R., 1988, Is the Bruswick magnetic anomaly really the Alleghanian suture? – Reply: Tectonics, v. 7, p. 347-349.

Taylor, B., Goodliffe, A.M., and Martinez, F., 1999, How continents break up: Insights from Papua New Guinea: Journal of Geophysical Research, v. 104, p. 7497-7512.

Taylor, B., Goodliffe, A., and Martinez, F., 2009, Initiation of transform faults at rifted continental margins: Comptes Rendus Geoscience, v. 341, p. 428-438.

Thomas, W. A., 2006, Tectonic inheritance at a continental margin: GSA Today, v. 16, p. 4-11.

Traverse, A., 1987, Pollen and spores date origin of rift basins from Texas to Nova Scotia as early late Triassic: Science, v. 236, p. 1469–1472, doi:10.1126/science.236.4807.1469.

van Wijk, J.W., 2005, Role of weak zone orientation in continental lithosphere extension: Geophysical Research Letters, v. 32., L02302, doi:10.1029/2004GL022192.

van Wijk, J.W., and Blackman, D.K., 2005, Dynamics of continental rift propagation: the end-member modes: Earth and Planetary Science Letters, v. 229, p. 247-258.

Vogt, P.R., 1973, Early events in the opening of the North Atlantic, *in* Tarling, D.H., and Runcorn, S.K., eds, Implications of Continental Drift to the Earth Sciences, v. 2: Academic Press, London, p. 693-712.

Wernicke, B., 1985, Uniform-sense normal simple shear of the continental lithosphere: Canadian Journal of Earth Science, v. 22, p. 108-125.

White, R., and McKenzie, D., 1989, Magmatism at rift zones: The generation of volcanic continental margins and flood basalts: Journal of Geophysical Research, v. 94, p. 7685-7729.

Wildermuth, E., 2003, Potential field analysis of the shallow crustal structure in Eastern South Carolina, unpublished MS thesis, University of South Carolina, 190 p.

Wilson, J.T., 1965, A new class of faults and their bearing on continental drift: Nature, v. 207, p. 343-347.

Wilson, J.T., 1966, Did the Atlantic close and then re-open?: Nature, v. 211, p. 676-681.

Withjack, M.O., and Jamison, W.R., 1986, Deformation produced by oblique rifting: Tectonophysics, v. 126, p. 99-124.

Withjack, M.O., Schlische, R.W., and Olsen, P.E., 1998, Diachronous Rifting, Drifting, and Inversion on the Passive Margin of Central Eastern North America: An Analog for Other Passive Margins: The American Association of Petroleum Geologists Bulletin, v. 82, p. 817–835.

Withjack, M.O., Schlische, R.W., and Olsen, P.E., 2002, Rift-basin structure and its influence on sedimentary systems: Sedimentation in Continental Rifts, SEPM Special Publication No. 73, p 57-81.

Withjack, M.O., Schlische, R.W., and Olsen, P.E., 2012, Development of the passive margin of Eastern North America: Mesozoic rifting, igneous activity, and breakup, *in* Roberts, D.W., and Bally, A.W., eds., Phanerozoic Rift Systems and Sedimentary Basins, Elsevier, Amsterdam, p. 301 – 335.

Woollard, G.P., Bonini, W.E., and Meyer, R.P., 1957, A seismic refraction study of the sub-surface geology of the Atlantic Coastal Plain and continental shelf between Virginia and Florida: Madison, University of Wisconsin Geophysics Section, technical report contract no. N7onr-28512, 128 p.

Yantis, B.R., Costain, J.K., and Ackermann, H.D., 1983, A reflection seismic study near Charleston, South Carolina, *in* Gohn, G.S., ed., Studies Related to the Charleston, South Carolina, Earthquake of 1886—Tectonics and Seismicity: U.S. Geological Survey Professional Paper 1313, p. G1–G20.

Ziegler, P.A., and Cloetingh, S., 2004, Dynamic processes controlling evolution of rifted basins: Earth-Science Reviews, v. 64, p. 1 – 50.

APPENDIX A – WELL DATA

Well data was compiled from a variety of sources including state government databases, published reports and articles, geophysical and geological logs, and direct observations of core. 321 wells which reportedly penetrated the entire Coastal Plain are catalogued in Tables A.1, A.2, and A.3.

The 6 columns of Table A.1 are: 1) Well ID – well number based from the reference; 2) Well Name – name of the well where reported; 3) State – US state where the well is located; 4) County – name of the county where the well is located; 5) Latitude – latitude of the well in decimal degrees, north of the equator; 6) Longitude – longitude of the well in decimal degrees, negative denotes west of Greenwich.

The 7 columns of Table A.2 are: 1) Well ID – as described above; 2) Elevation – elevation of the well in meters relative to mean sea level; 3) Elevation Reference – reference for measuring elevation: Surface denotes ground level, KB = Kelly Bushing, DF = Derrick Floor, GL = Ground Level; 4) TD – total depth (TD) of the well in meters; 5) Elevation Base CP – elevation of the base of the Coastal Plain relative to mean sea level; 6) Elevation Basement – elevation of pre-Triassic rocks (considered here to be basement) relative to mean sea level; 7) Reference – reference(s) for well information, "Logs" indicates geophysical or geological logs, "Core" indicates core was directly observed, "SCDNR" refers to the South Carolina Department of Natural Resources.

The 8 columns of Table A.3 are: 1) Well ID – as described above; 2) Jurassic or Triassic Lithology – description of either Jurassic or Triassic rocks, if encountered in the well; 3) Basement Rock – description of pre-Triassic (basement) rocks; 4) Maf. Ign. – classification of mafic igneous (Maf. Ign.) rocks when encountered: B = Basalt, D = Diabase; 5) J/Tr – "*" indicates Jurassic or Triassic (J/Tr) rocks were encountered, "?" if unsure; 6) Pal. Sed. – "*" indicates Paleozoic sedimentary (Pal. Sed.) rocks were encountered, "?" if unsure; 7) Met. Bas. – "*" indicates metamorphic basement (Met. Bas.) rocks were encountered, "?" if unsure; 8) Fel. Ign. – "*" indicates felsic igneous (Fel. Ign.) rocks were encountered, "?" if unsure.

Table A.1. Location information for sub-Coastal Plain wells in South Carolina, Georgia, northern Florida, and eastern Alabama.

Well ID	Well Name	State	County	Latitude (degrees)	Longitude (degrees)
32Y020		GA	Burke	33.0650	-81.7203
36Q318	Pooler #1	GA	Chatham	32.1169	-82.5553
A-19	J.W. Campbell #1	FL	Flagler	29.5650	-81.4850
A-23	Henry N. Camp #1	FL	Marion	29.1040	-82.0080
A-25	H.E. Westbury et al #1	FL	Putnam	29.5310	-81.7060
A-26	Retail Lumber Co. #1	FL	Volusia	29.2460	-81.2470
A-36	R.H. Cato #1	FL	Alachua	29.7800	-82.4740
A-37	Josie Parker #1	FL	Alachua	29.8470	-82.3990
A-38	J.A. Phifer #1	FL	Alachua	29.6960	-82.1520
A-39	H.L. Hunt #1	FL	Baker	30.4900	-82.3100
A-40	M.F. Wiggins #1	FL	Bradford	29.9780	-82.2790
A-41	Foremost Properties Corp',. #1	FL	Clay	30.0210	-81.7960
A-42	J.P. Cone #1	FL	Columbia	30.4900	-82.5880
A-44	W.F. Johnson #1	FL	Columbia	30.1120	-82.7000
A-47	Perpetual Forest, Inc. #1	FL	Dixie	29.5530	-83.2350
A-48	P.C. Crapps "A", well #1	FL	Dixie	29.7420	-83.2800
A-49	Hazel Langston #1	FL	Dixie	29.8040	-82.9430
A-50	Alto Adams #1	FL	Gilchrist	29.7100	-82.7860
A-51	Williams Bros. #1	FL	Gilchrist	29.8130	-82.7540

Well ID	Well Name	State	County	Latitude (degrees)	Longitude (degrees)
A-53	C.W. Tindel #1	FL	Jackson	30.8440	-85.3600
A-54	E.P. Larsh #1	FL	Jefferson	30.3360	-83.9770
A-55	Ronald Sapp #1	FL	Lafayette	29.9520	-82.9460
A-56	Brooks-Scanlon, Inc. Block 49	FL	Lafayette	30.0100	-83.2760
A-57	R.L. Henderson #1	FL	Lafayette	30.1250	-83.2370
A-58	P.C. Crapps #1	FL	Lafayette	29.9380	-83.0770
A-59	J.B. and J.T. Ragland #1	FL	Levy	29.1800	-83.0000
A-60	C.E. Robinson #1	FL	Levy	29.0830	-82.6210
A-61	J.T. Goethe #1	FL	Levy	29.2240	-82.6370
A-62	J.W. Gibson #2	FL	Madison	30.4390	-83.3480
A-63	J.W. Gibson #4	FL	Madison	30.3540	-83.2320
A-64	W.L. Lawson #1	FL	Marion	29.3340	-82.2510
A-65	Clark-Ray-Johnson #1	FL	Marion	29.1140	-82.2820
A-66	H.T. Parker #1	FL	Marion	29.2630	-82.0540
A-67	Hilliard Turpentine Co. #1	FL	Nassau	30.7640	-81.9340
A-68	Q.T. Roberts #1	FL	Putnam	29.7020	-81.8280
A-69	Earl Odom #1	FL	Suwannee	30.0200	-82.8440
A-70	A.B. Russell	FL	Suwannee	30.0740	-82.8280
A-71	J.H. Tillis	FL	Suwannee	30.2970	-82.8070
A-73	A.C. Chandler #1	GA	Early	31.1670	-85.0670
A-81	Brooks-Sclanlon, Inc., Block 33, well #1	FL	Taylor	30.1300	-83.4590
A-82	Brooks-Sclanlon, Inc., Block 42, well #1	FL	Taylor	29.7960	-83.4260
A-83	G.H. Hodges #1	FL	Taylor	30.0620	-83.6820
AIK-2448		SC	Aiken	33.6244	-81.8497
AIK-2449		SC	Aiken	33.5394	-81.8550
AIK-465	DRB-3	SC	Aiken	33.2855	-81.6636
AIK-59		SC	Aiken	33.6419	-81.3208
AIK-593	DRB-6	SC	Aiken	33.2872	-81.6524
AIK-595	DRB-4	SC	Aiken	33.2763	-81.6697
AIK-596	DRB-1	SC	Aiken	33.2963	-81.6708
AIK-603	DRB-7	SC	Aiken	33.2847	-81.6502
AIK-614	P-7R	SC	Aiken	33.3333	-81.5983
AIK-637	DRB-5	SC	Aiken	33.2900	-81.6572
AIK-687	P-6R	SC	Aiken	33.2766	-81.7372
AIK-688	DRB-2	SC	Aiken	33.2791	-81.6580
AIK-689	P-8R	SC	Aiken	33.3266	-81.7433
AIK-690	P-9R	SC	Aiken	33.3197	-81.7308
ALL-324		SC	Allendale	33.1260	-81.5460

Well ID	Well Name	State	County	Latitude (degrees)	Longitude (degrees)
ALL-348	C-10	SC	Allendale	33.0250	-81.3847
ALL-357	C-7	SC	Allendale	33.1133	-81.5061
B-1	Chevron #1 Containe Corp.	FL	Alachua	29.7527	-82.2025
B-10	Mobil Oil Al-St. Lse. 224A	FL	Citrus	28.8301	-82.8074
B-13	Getty Oil Co. #1 Holmes 21-8	FL	Columbia	30.2073	-82.6003
B-14	Getty Oil Co. #1 JC Marsh	FL	Columbia	30.2731	-82.6058
B-17	T.A. Durham #1 Gilman Paper	FL	Duval	30.2466	-81.9542
B-18	T.A. Durham #B1 Gilman Paper	FL	Duval	30.2306	-82.0187
B-19	T.A. Durham #1 Monticello Drug	FL	Duval	30.3905	-81.8507
B-2	Chevron #1 Donaldson	FL	Alachua	29.8086	-82.2387
B-20	Mobil Prod. #1C Lse. 224A	FL	Franklin	29.6081	-85.0458
B-21	Charter Expl. & Prod. #1 St. Joe Paper Co.	FL	Gulf	29.7537	-85.2547
B-22	Charter Expl. Prod. #6 St. Joe Paper	FL	Gulf	29.8094	-85.2313
B-23	Hunt Oil 30 #4 International Paper	FL	Gulf	30.1714	-85.3730
B-28	Sonat Expl. #1 Randall Hughes	FL	Holmes	30.7308	-85.9784
B-29	Amoco Prod. #1 Buckeye	FL	Jefferson	30.3157	-83.8520
B-3	Charter Expl. #2 St. Joe Paper	FL	Bay	30.3757	-85.9401
B-30	Hunt Oil #1A PC Crapps	FL	Lafayette	29.8570	-83.0211
B-34	Phillips Petr. #1 St. Joe A	FL	Leon	30.3001	-84.2054
B-35	Mobil Oil #1B St. Lse 224A	FL	Levy	29.0919	-82.9178
B-36	Placid Oil 26 #1 USA	FL	Liberty	30.1814	-84.7273
B-37	Placid Oil 16-3 USA	FL	Liberty	30.1326	-84.8633
B-4	Inexco Oil Co. Gilman Paper	FL	Bradford	30.1119	-82.0888
B-40	Amoco Prod. #2 ITT Rayonier	FL	Nassau	30.6475	-81.5999
B-41	Cabot Corp. 1 #9 USA	FL	Okaloosa	30.7825	-86.7721
B-42	Sonat Expl. #1 JG Moore 3-11	FL	Okaloosa	30.7983	-86.6402
B-54	Thayer & Davis #1 Johnson Malphure	FL	Putnam	29.5130	-81.5687
B-55	Carolina Resources #1 Cummer Co.	FL	St. Johns	29.9551	-81.3933
B-56	Kerr McGee Corp. #1 H.W. Mizell	FL	St. Johns	29.8523	-81.4573
B-58	Hunt Petr. #1 CR Howes	FL	Suwanee	30.2823	-83.1175
B-59	Hunt Petr. #1 TP Hurst	FL	Suwanee	30.2334	-83.0474
B-60	Amoco Prod. #1 Canal Tbr. Co.	FL	Taylor	30.2316	-83.7001
B-63	Getty Oil Co. #1 W Croft	FL	Union	30.0418	-82.5219
B-64	Getty Oil #1 KO Dicks	FL	Union	30.0971	-82.4271
B-65	Placid Oil Co. #1 USA Unit 27-2	FL	Wakulla	30.2668	-84.5264

Well ID	Well Name	State	County	Latitude (degrees)	Longitude (degrees)
B-66	Charter Oil #4 St. Joe Paper	FL	Walton	30.3993	-86.2922
B-67	Coastal Prod. #1 Brady Belcher	FL	Walton	30.7832	-86.3507
B-68	McCulloch 1DS Rudman #1 Indian Crk Ranch	FL	Walton	30.6504	-86.1213
B-69	Texas Gas Expl. #1 International Paper Co.	FL	Walton	30.9681	-86.2800
B-70	Hunt Petr. #1 International Paper Co.	FL	Washington	30.7520	-85.6070
B-71	R. Mosbacher et al #1 First Nat. Bank of Akron	FL	Washington	30.4693	-85.7692
B-72	Rudman Resources #1 FNB of Akron	FL	Washington	30.5434	-85.7902
B-9	Mobil Oil #1 Harbond	FL	Citrus	28.9741	-82.6484
BFT-2055	Hilton Head Test Well	SC	Beaufort	32.1911	-80.7042
BRK-644	USGS St. Stephen	SC	Berkley	33.4042	-79.9339
BRN-239		SC	Barnwell	33.4367	-81.2369
BRN-245	P5R	SC	Barnwell	33.1492	-81.6158
BRN-336	DRB-8	SC	Barnwell	33.2810	-81.6480
BRN-337	DRB9	SC	Barnwell	33.2390	-81.6161
BRN-338	DRB10	SC	Barnwell	33.2042	-81.5800
BRN-339	DRB-11	SC	Barnwell	33.2300	-81.6010
BRN-340	P-12R	SC	Barnwell	33.2310	-81.6030
BRN-349	C-6 site	SC	Barnwell	33.1783	-81.3153
BRN-357	C-5 site	SC	Barnwell	33.3206	-81.4070
BRN-364		SC	Barnwell	33.2556	-81.6375
BRN-379	P-25-TA	SC	Barnwell	33.2110	-81.6570
BRN-888	PBF-1	SC	Barnwell	33.2930	-81.5300
BRN-889	PBF-2	SC	Barnwell	33.2860	-81.5250
BRN-890	PBF-3	SC	Barnwell	33.2520	-81.6200
BRN-891	PBF-4	SC	Barnwell	33.2030	-81.7010
BRN-892	PBF-5	SC	Barnwell	33.1940	-81.6910
BRN-893	PBF-6	SC	Barnwell	33.1670	-81.7410
BRN-894	PBF-7	SC	Barnwell	33.2390	-81.6240
BRN-895	PBF-8	SC	Barnwell	33.2450	-81.6150
CAL-132		SC	Calhoun	33.8328	-81.0231
CAL-224A		FL		29.7850	-84.3817
CC#1	Clubhouse Crossroads #1	SC	Dorcestor	32.8881	-80.3592
CC#2	Clubhouse Crossroads #2	SC	Dorcestor	32.9067	-80.3111
CC#3	Clubhouse Crossroads #3	SC	Dorcestor	32.9025	-80.3172
COL-241	Norris-Lighstey #1	SC	Colleton	33.0150	-80.9289
COST GE-1				30.6189	-80.2997
CTF-60		SC	Chesterfield	34.5122	-80.2478

Well ID	Well Name	State	County	Latitude (degrees)	Longitude (degrees)
DAR-124		SC	Darlington	34.3731	-80.0650
DIL-121		SC	Dillon	34.3286	-79.2839
DOR-211	USGS St. George	SC	Dorcestor	33.1569	-80.5217
DP-160	Jack & Monk Royal #1	GA	Dooly	32.2333	-83.6256
DP161	McNair et al #1	GA	Turner	31.7536	-83.7453
DP163	Ronnie Leadford #1	GA	Dooly	32.1544	-83.7133
DP39		GA	Macon	32.2000	-84.0333
FLO-103		SC	Florence	34.1697	-79.7883
FLO-123		SC	Florence	34.1967	-79.7522
FLO-124		SC	Florence	34.1967	-79.7522
FLO-125		SC	Florence	34.1928	-79.7478
FLO-126		SC	Florence	34.1961	-79.5800
FLO-127		SC	Florence	34.1997	-79.7719
FLO-139		SC	Florence	34.1797	-79.7619
FLO-140		SC	Florence	34.1758	-79.7711
FLO-146		SC	Florence	34.1697	-79.7883
FLO-149		SC	Florence	34.1967	-79.7522
FLO-154		SC	Florence	34.1992	-79.7847
FLO-262	Dora J. Truluck	SC	Florence	33.9617	-79.8719
FLO-268	USGS Edisto Test Hole	SC	Florence	34.1703	-79.7892
FLO-274		SC	Florence	33.8556	-79.7672
FLO-293		SC	Florence	34.1375	-79.7694
FLO-33		SC	Florence	34.2006	-79.7656
FLO-5		SC	Florence	34.1981	-79.7736
FLO-87		SC	Florence	34.1992	-79.7847
GEO-24		SC	Georgetown	33.3714	-79.2892
GGS-107	Doster Ladson #1	GA	Atkinson	31.2667	-82.9500
GGS-108		GA	Crisp	31.8264	-83.7694
GGS-109	J. H. Pullen #2	GA	Mitchell	31.1417	-84.0708
GGS-1145		GA	Early	31.1708	-85.0736
GGS-119		GA	Pierce	31.3958	-82.0708
GGS-1197		GA	Glynn	31.3736	-81.5667
GGS-1198		GA	Camden	30.8519	-81.8583
GGS-1199		GA	Camden	30.8431	-81.7347
GGS-120	Adams - NC Caskil #1	GA	Pierce	31.4403	-82.0625
GGS-121		GA	Early	31.1722	-85.0778
GGS-131		GA	Burke	33.2375	-81.9231
GGS-144		GA	Clinch	30.9292	-82.7986
GGS-148	Mrs. W.E. Bradley #1	GA	Appling	31.8792	-82.3833

Well ID	Well Name	State	County	Latitude (degrees)	Longitude (degrees)
GGS-150		GA	Echols	30.6153	-82.7819
GGS-153		GA	Camden	31.0417	-81.8800
GGS-158		GA	Echols	30.7389	-82.9250
GGS-166		GA	Echols	30.6833	-82.8778
GGS-169		GA	Echols	30.6931	-82.6861
GGS-172		GA	Emanuel	32.8000	-82.2333
GGS-189		GA	Echols	30.7583	-82.9111
GGS-190		GA	Montgomery	32.2167	-82.4806
GGS-192		GA	Calhoun	31.5658	-84.8239
GGS-193		GA	Houston	32.4403	-83.8167
GGS-194		GA	Houston	32.4014	-83.7333
GGS-223		GA	Washington	32.9903	-83.0042
GGS-296		GA	Sumter	32.1583	-84.3028
GGS-3001		GA	Seminole	30.8606	-84.8858
GGS-3080	Ronnie Towns #1	GA	Wheeler	32.0453	-82.6383
GGS-3099	Jack Cole #1	GA	Lowndes	30.9367	-83.4064
GGS-3105	B & L Farms #1	GA	Dodge	32.2578	-83.2892
GGS-3113	J.T. Stalvey #1	GA	Lowndes	30.9903	-83.2522
GGS-3114	Irene E.W. Sedgewick	GA	Thomas	30.7864	-83.9622
GGS-3115	L.P. Shelton Well #1A	GA	Lowndes	30.8483	-83.1878
GGS-3120	Langsdale #1	GA	Lowndes	30.8597	-83.0564
GGS-3122	E.N. Murray, Jr. #1	GA	Lowndes	30.9058	-83.2811
GGS-3127		GA	Coffee	31.4514	-83.1350
GGS-3128	J.L. Sinclair #1	GA	Jeff Davis	31.7672	-82.7506
GGS-3137		GA	Pulaski	32.3256	-83.5408
GGS-3146		GA	Wayne	31.5175	-81.8733
GGS-3147	GA Craft #1	GA	Twiggs	32.5500	-83.4436
GGS-3154		GA	Worth	31.3178	-83.7369
GGS-3165		GA	Wilkinson	32.7156	-83.2244
GGS-3201		GA	Wayne	31.5481	-81.7264
GGS-3353	T.R. Taylor #1	GA	Washington	32.9308	-82.6100
GGS-336	Jordan Meirs #1	GA	Wheeler	31.9806	-82.6458
GGS-338	Lem Griffis #1	GA	Clinch	30.7833	-82.4389
GGS-341		GA	Chattahoochee	32.2454	-84.7991
GGS-3439	G. Giesbrecht #1	GA	Washington	32.9547	-82.6381
GGS-3441	Malpasse #1	GA	Washington	32.9358	-82.6208
GGS-3447	McCoy #1	GA	Washington	32.9189	-82.6356
GGS-3456	Horace Parker #1	GA	Colquitt	31.2378	-83.9133
GGS-3457	A.P. Snipes #1	GA	Jeff Davis	31.7592	-82.7567

Well ID	Well Name	State	County	Latitude (degrees)	Longitude (degrees)
GGS-3514	Belote #1	GA	Wilkinson	32.7175	-83.1911
GGS-357		GA	Bibb	32.7802	-83.6372
GGS-361		GA	Bibb	32.7802	-83.6372
GGS-363	Jelks-Rogers #1	GA	Liberty	31.6889	-81.3472
GGS-3632	Hobby #1	GA	Johnson	32.7142	-82.7794
GGS-3633	L. Brinson #1	GA	Wayne	31.5000	-81.7472
GGS-3634	ITT-Rayonier #1	GA	Appling	31.8333	-82.4572
GGS-375	Henry Spurlin #1	GA	Telfair	32.0292	-82.8097
GGS-3758		GA	Burke	33.2300	-81.8789
GGS-3794		GA	Burke	33.1783	-81.7861
GGS-442		GA	Sumter	32.0181	-84.3083
GGS-468	Terrell Thurman #1	GA	Coffee	31.7125	-82.8944
GGS-476		GA	Marion	32.2861	-84.4625
GGS-481	Alice Musgrove #1	GA	Clinch	30.8556	-82.7222
GGS-491		GA	Pulaski	32.3014	-83.4797
GGS-496	Timber Products Company #1-A	GA	Clinch	31.1528	-82.8625
GGS-505		GA	Marion	32.1486	-84.4361
GGS-509	C.T. Thurman #2	GA	Coffee	31.7167	-82.8958
GGS-51	Grace McCain #1	GA	Laurens	32.4778	-82.7583
GGS-52		GA	Wayne	31.3911	-81.8061
GGS-619		GA	Dooly	32.0417	-83.6500
GGS-651		GA	Wayne	31.5200	-81.6842
GGS-7		GA	Bibb	32.7157	-83.6993
GGS-719		GA	Glynn	31.2458	-81.6333
GGS-730	Jim L. Gillis, Sr. #1	GA	Treutlen	32.3889	-82.5403
GGS-789	Jim Gillis, Jr	GA	Treutlen	32.3611	-82.4736
GGS-855	Helen Pryor #1	GA	Screven	32.5833	-81.4278
GGS-876		GA	Charlton	30.7917	-81.9917
GGS-94		GA	Washington	32.9573	-82.8081
GGS-95		GA	Toombs	32.1528	-82.3719
GGS-960		GA	Pulaski	32.3250	-83.4153
HOR-547		SC	Horry	33.6842	-78.9422
JAS-426		SC	Jasper	32.6183	-80.9958
KER-100		SC	Kershaw	34.1683	-80.7944
KER-66		SC	Kershaw	34.4161	-80.3294
LEE-75	USGS Lee State Park	SC	Lee	34.2025	-80.1744
LEX-844	USGS Swansea Elementary School	SC	Lexington	33.7461	-81.1075
MLB-112		SC	Marlboro	34.6264	-79.6894
MLB-137		SC	Marlboro	34.5389	-79.7492

Well ID	Well Name	State	County	Latitude (degrees)	Longitude (degrees)
MRN-78		SC	Marion	33.8619	-79.3306
MRN-90		SC	Marion	34.2472	-79.5203
N&T-10	George W. Marott #1 M.G.Larkin	AL	Sumter	32.7215	-88.2050
N&T-11	Harry W. Elliott #1 Pete Perolio	AL	Sumter	32.5068	-87.9981
N&T-12	E.C. Johnston #1 H.O. Peteet	AL	Marengo	32.3901	-87.8667
N&T-13	Hughes and Oglesby #1 H.D. Alexander	AL	Marengo	32.4240	-87.5485
N&T-14	Currey Oil Co. #1 W.M. Glass et al	AL	Marengo	32.2168	-87.6351
N&T-15	J. Keller Henderson #1 Strother Bros. et al	AL	Wilcox	32.2122	-87.4809
N&T-16	Geochemical Surveys #1 Strother Bros.	AL	Wilcox	32.1861	-87.4426
N&T-17	Murphy Oil Co. #1 A.S. Johnson	AL	Clarke	31.9574	-87.8044
N&T-20	Placid Oil Co. #1 A-1 Land et al	AL	Choctaw	32.0198	-88.4198
N&T-23	Rudman and Marr #2 Buchanan	AL	Dallas	32.1173	-87.1282
N&T-24	Gulf Refining Co. #1 H.H. Wilkinson	AL	Wilcox	32.1064	-87.2915
N&T-26		AL	Wilcox	31.9698	-87.0913
N&T-27		AL	Wilcox	31.9249	-87.3214
N&T-28	American Petrofina Co. of Texas #1 Harrigan	AL	Clarke	31.8618	-87.7512
N&T-29		AL	Monroe	31.7276	-87.3065
N&T-30		AL	Monroe	31.6176	-87.3525
N&T-31	Skelly Oil Co. #1 Mabel Hall	AL	Monroe	31.5387	-87.5816
N&T-32	Getty Oil Corp. #1 Rufus Garrett 12-7	AL	Monroe	31.3280	-87.5242
N&T-33	Tenneco Oil Co. #1 Alger Sullivan "A"	AL	Conecuh	31.2705	-87.4056
N&T-34	Getty Oil Corp. #1 Scott Paper Co. et al 9-13	AL	Escambia	31.2454	-87.4723
N&T-35	Shell Oil co. #1 Alger Tenants	AL	Escambia	31.2081	-87.5247
N&T-36	Chevron Oil Co. #1 Cecil Neal et al	AL	Escambia	31.1872	-87.5521
N&T-37		AL	Conecuh	31.3105	-87.2130
N&T-38		AL	Escambia	31.1918	-86.9503
N&T-39	Gulf Refining Co. #1 D.W. Hendrix	AL	Butler	31.5500	-86.7250
N&T-40	S.D. Suggs #2 S.D. Suggs	AL	Montgomery	32.2533	-86.4005
N&T-41	Montgomery Oil Co. #1 Snowdown	AL	Montgomery	32.2563	-86.2979
N&T-42	Capital Oil and Gas Co. #1 E.B. Gholston	AL	Bullock	32.2010	-85.8872
N&T-43	Robert W. Williams #1 Mrs. J.H. Rainer, Sr.	AL	Bullock	32.1881	-85.8948

Well ID	Well Name	State	County	Latitude (degrees)	Longitude (degrees)
N&T-44	Capital Oil and Gas Co. #1 Fred Pickett	AL	Bullock	32.0918	-85.9426
N&T-45		AL	Pike	31.8451	-85.9841
N&T-46		AL	Pike	31.6239	-86.1216
N&T-47		AL	Henry	31.3087	-85.1783
N&T-48		AL	Houston	31.0042	-85.3392
N&T-49		AL	Escambia	31.1804	-86.7370
N&T-50		AL	Conecuh	31.2079	-86.7250
N&T-51		AL	Covington	31.1588	-86.6689
N&T-52		AL	Crenshaw	31.6439	-86.4310
N&T-53		AL	Barbour	31.8351	-85.4643
N&T-54		AL	Barbour	31.7620	-85.4086
N&T-55		AL	Henry	31.3524	-85.1693
N&T-56		AL	Geneva	31.0891	-85.9455
N&T-6	Pan American Petroleum #1 J.B. Hill	AL	Sumter	32.8218	-88.1994
N&T-9	Johnston #1 Willis	AL	Greene	32.7153	-87.9577
ORG-347	Robert A. Valentine	SC	Orangeburg	33.4019	-81.0128
ORG-393	USGS Clark Middle School, Orangeburg	SC	Orangeburg	33.5081	-80.8650
RIC-305		SC	Richland	34.0083	-80.8275
RIC-348		SC	Richland	33.8189	-80.6383
RIC-432		SC	Richland	33.8936	-80.7222
RIC-543	USGS Webber School Complex, Eastover	SC	Richland	33.8750	-80.7022
RIC-613		SC	Richland	34.1119	-80.8847
SSW6	Round O	SC	Colleton	32.8816	-80.5819
Sum-1920OT	Mabeleanor Well	SC	Dorcestor	33.0366	-80.1803
SUM-104		SC	Sumter	33.9358	-80.3478
SUM-111		SC	Sumter	33.9333	-80.3464
SUM-120		SC	Sumter	33.8631	-80.3814
SUM-140		SC	Sumter	33.9347	-80.3500
SUM-146		SC	Sumter	33.9361	-80.3458
SUM-153		SC	Sumter	33.8650	-80.3767
SUM-161		SC	Sumter	33.9164	-80.3244
SUM-165		SC	Sumter	33.8933	-80.3681
SUM-175		SC	Sumter	33.8625	-80.3817
SUM-340	USGS Sumter Municpal Airport	SC	Sumter	33.9903	-80.3589
SUM-56		SC	Sumter	33.9361	-80.3486
SUM-64		SC	Sumter	33.9353	-80.3500
SUM-65		SC	Sumter	33.9211	-80.3739

Well ID	Well Name	State	County	Latitude (degrees)	Longitude (degrees)
SUM-69		SC	Sumter	33.9353	-80.3464
SUM-7		SC	Sumter	33.9356	-80.3481
SUM-71		SC	Sumter	33.9172	-80.3217
SUM-8		SC	Sumter	33.9344	-80.3464
SUM-84		SC	Sumter	33.9164	-80.3244
TR 1005-1				30.9928	-80.2439
WIL-29		SC	Williamsburg	33.7283	-79.8058

Table A.2. Elevations of base of Coastal Plain (CP) and basement where encountered in wells, and references.

Well ID	Elevation (m)	Elevation Reference	TD (m)	Elevation Base CP (m)	Elevation Basement (m)	Reference
32Y020	76.2		422.1	-342.9		Falls and Prowell (2001)
36Q318	6.1		1038.5			Logs
A-19	9.4	Surface	1411.8	-1389.0	-1389.0	Applin (1951)
A-23	22.6	Surface	1413.4	-1384.1	-1384.1	Applin (1951)
A-25	9.8	Surface	1186.3	-1170.7	-1170.7	Applin (1951)
A-26	13.4	Surface	1653.2	-1633.4	-1633.4	Applin (1951)
A-36	34.1	Surface	960.1	-921.4	-921.4	Applin (1951)
A-37	51.2	Surface	981.5	-915.0	-915.0	Applin (1951)
A-38	40.2	Surface	983.9	-940.3	-940.3	Applin (1951)
A-39	39.6	Surface	1020.8	-979.0	-979.0	Applin (1951)
A-40	43.0	Surface	965.3	-914.1	-914.1	Applin (1951)
A-41	35.1	Surface	1786.7	-1100.3	-1100.3	Applin (1951)
A-42	43.0	Surface	1354.5	-1018.3	-1018.3	Applin (1951)
A-44	26.5	Surface	929.9	-897.9	-897.9	Applin (1951)
A-47	10.1	Surface	2289.0	-1583.4	-1583.4	Applin (1951)
A-48	12.5	Surface	1555.7	-1516.4	-1516.4	Applin (1951)
A-49	10.1	Surface	1118.9	-1100.9	-1100.9	Applin (1951)
A-50	28.3	Surface	1143.9	-1065.3	-1065.3	Applin (1951)
A-51	23.5	Surface	1026.0	-997.0	-997.0	Applin (1951)
A-53	39.0	Surface	2817.9	-2533.5	-2533.5	Applin (1951)
A-54	15.5	Surface	2411.9	-2072.6	-2395.1	Applin (1951)
A-55	13.7	Surface	1068.9	-1047.0	-1047.0	Applin (1951)
A-56	26.5	Surface	1375.3	-1346.6	-1346.6	Applin (1951)
A-57	15.8	Surface	1290.8	-1265.8	-1265.8	Applin (1951)

Well ID	Elevation (m)	Elevation Reference	TD (m)	Elevation Base CP (m)	Elevation Basement (m)	Reference
A-58	21.3	Surface	1259.7	-1207.0	-1207.0	Applin (1951)
A-59	4.3	Surface	1783.1	-1766.6	-1766.6	Applin (1951)
A-60	17.7	Surface	1404.8	-1316.4	-1316.4	Applin (1951)
A-61	10.4	Surface	1218.3	-1196.6	-1196.6	Applin (1951)
A-62	32.6	Surface	1641.3	-1378.0	-1378.0	Applin (1951)
A-63	22.3	Surface	1248.5	-1215.2	-1215.2	Applin (1951)
A-64	59.4	Surface	1321.0	-1056.1	-1056.1	Applin (1951)
A-65	24.4	Surface	1883.7	-1225.3	-1225.3	Applin (1951)
A-66	24.1	Surface	1172.0	-1097.3	-1097.3	Applin (1951)
A-67	33.5	Surface	1470.4	-1380.7	-1380.7	Applin (1951)
A-68	62.8	Surface	1014.4	-949.1	-949.1	Applin (1951)
A-69	22.3	Surface	963.5	-904.3	-904.3	Applin (1951)
A-70	29.3	Surface	956.8	-926.6	-926.6	Applin (1951)
A-71	49.4	Surface	1088.7	-1017.4	-1017.4	Applin (1951)
A-73	57.0	Surface	2231.1	-2061.4	-2061.4	Applin (1951)
A-81	29.3	Surface	1598.1			Applin (1951)
A-82	12.5	Surface	1681.6			Applin (1951)
A-83	11.0	Surface	1906.2			Applin (1951)
AIK-2448	149.4		51.8	112.3	112.3	SCDNR
AIK-2449	150.6		103.6	55.2	55.2	SCDNR
AIK-465	87.2					Cumbest et al. (1992)
AIK-59	140.2		274.3	-70.1	-70.1	SCDNR
AIK-593	82.0					Cumbest et al. (1992)
AIK-595	76.5					Cumbest et al. (1992)
AIK-596	79.9					Cumbest et al. (1992)
AIK-603	90.8					Cumbest et al. (1992)

Well ID	Elevation (m)	Elevation Reference	TD (m)	Elevation Base CP (m)	Elevation Basement (m)	Reference
AIK-614	83.2					Cumbest et al. (1992)
AIK-637	87.5					Cumbest et al. (1992)
AIK-687	77.1					Cumbest et al. (1992)
AIK-688	86.0					Cumbest et al. (1992)
AIK-689	108.8					Cumbest et al. (1992)
AIK-690	97.8					Cumbest et al. (1992)
ALL-324	61.9					Aadland et al. (1995)
ALL-348	85.6		527.9	-440.4	-440.4	SCDNR; Aadland et al. (1995)
ALL-357	75.6		432.8	-356.0	-356.0	SCDNR; Aadland et al. (1995)
B-1	56.7	DF	872.0	-743.1	-743.1	Barnett (1975)
B-10	6.7	KB	1834.9	-1787.3	-1787.3	Barnett (1975)
B-13	58.2	KB	880.9	-809.9	-809.9	Barnett (1975)
B-14	47.9	KB	974.1	-920.2	-920.2	Barnett (1975)
B-17	29.0	DF	1140.9	-1079.6	-1079.6	Barnett (1975)
B-18	28.5	DF	1073.2	-1025.3	-1025.3	Barnett (1975)
B-19	27.6		1295.4	-1237.5	-1237.5	Barnett (1975)
B-2	46.0	KB	1018.0	-964.1	-964.1	Barnett (1975)
B-20	11.3	DF	4353.8	-4210.2		Barnett (1975)
B-21	10.5	KB	4357.7	-4336.2	-4336.2	Barnett (1975)
B-22	7.7	KB	4442.2	-4411.6		Barnett (1975)
B-23	24.8	KB	4049.0	-3906.5	-3906.5	Barnett (1975)
B-28	42.7	DF	3414.1	-3078.5		Barnett (1975)
B-29	16.9	KB	2144.0	-1994.7	-2039.8	Barnett (1975)
B-3	20.4	KB	3753.0	-3715.8	-3715.8	Barnett (1975)
B-30	22.8	KB	1676.7	-1109.8	-1109.8	Barnett (1975)
B-34	10.6	KB	3190.0	-2565.0		Barnett (1975)

Well ID	Elevation (m)	Elevation Reference	TD (m)	Elevation Base CP (m)	Elevation Basement (m)	Reference
B-35	7.6	KB	1443.2	-1392.9	-1392.9	Barnett (1975)
B-36	19.1	KB	3697.5	-3563.3		Barnett (1975)
B-37	23.2	KB	3779.5	-3646.6	-3646.6	Barnett (1975)
B-4	45.7	KB	961.3	-863.8	-863.8	Barnett (1975)
B-40	11.0	KB	1667.0	-1539.2	-1539.2	Barnett (1975)
B-41	56.7	KB	4648.2	-4564.1		Barnett (1975)
B-42	52.1	KB	4423.9	-4244.0		Barnett (1975)
B-54	10.2	DF	1698.3	-1338.7	-1338.7	Barnett (1975)
B-55	12.8	DF	1478.3	-1459.4	-1459.4	Barnett (1975)
B-56	12.2	KB	1396.9	-1378.3	-1378.3	Barnett (1975)
B-58	29.7	KB	1377.7	-1106.0	-1117.0	Barnett (1975)
B-59	32.7		1370.4	-1076.8	-1076.8	Barnett (1975)
B-60	19.2	KB	2144.6	-1750.8	-1750.8	Barnett (1975)
B-63	45.7	KB	933.0	-882.7	-882.7	Barnett (1975)
B-64	42.4		925.1	-880.9	-880.9	Barnett (1975)
B-65	30.5	KB	37313.6	-3527.8	-3688.1	Barnett (1975)
B-66	13.5	KB	4424.2	-4400.0	-4400.0	Barnett (1975)
B-67	65.2	DF	3761.2	-3679.2	-3679.2	Barnett (1975)
B-68	43.0	KB	3515.3	-3438.4		Barnett (1975)
B-69	89.9	KB	3666.1	-3380.5		Barnett (1975)
B-70	26.2		4181.9	-3253.4	-3381.5	Barnett (1975)
B-71	39.0	KB	3563.7	-3482.6	-3482.6	Barnett (1975)
B-72	46.3	KB	3533.5	-3452.8	-3452.8	Barnett (1975)
B-9	7.3	KB	1461.2	-1436.8	-1436.8	Barnett (1975)
BFT-2055	3.0		1168.3	-1165.3	-1165.3	Snipes et al. (1995)
BRK-644	22.9		556.6	-522.4		Core

Well ID	Elevation (m)	Elevation Reference	TD (m)	Elevation Base CP (m)	Elevation Basement (m)	Reference
BRN-239	64.0		350.2	-195.1	-195.1	SCDNR; Costain et al. (1986)
BRN-245	63.1	GL	400.2	-307.8		Marine and Siple (1974); Steele and Colquhoun (1985)
BRN-336	79.9					Cumbest et al. (1992)
BRN-337	90.2		821.1	-215.8	-710.5	Marine and Siple (1974); Steele and Colquhoun (1985)
BRN-338	76.5		1282.0	-280.4		Marine and Siple (1974); Steele and Colquhoun (1985)
BRN-339	83.5					Cumbest et al. (1992)
BRN-340	89.0					Cumbest et al. (1992)
BRN-349	63.7					Aadland et al. (1995)
BRN-357	81.1					Aadland et al. (1995)
BRN-364	92.4			-229.2	-229.2	SCDNR
BRN-379	80.8					Cumbest et al. (1992)
BRN-888	84.1					Cumbest et al. (1992)
BRN-889	81.7					Cumbest et al. (1992)
BRN-890	96.6					Cumbest et al. (1992)
BRN-891	63.4					Cumbest et al. (1992)
BRN-892	73.5					Cumbest et al. (1992)
BRN-893	28.0					Cumbest et al. (1992)
BRN-894	86.9					Cumbest et al. (1992)
BRN-895	89.0					Cumbest et al. (1992)
CAL-132	106.7		148.7	-33.5	-33.5	SCDNR
CAL-224A	-9.1	0	3208.3			Ball et al. (1988)
CC#1	5.5		791.9	-744.6		Gohn et al. (1983)
CC#2	6.1		907.1	-769.9		Gohn et al. (1983)
CC#3	6.1		1152.1	-769.0		Gohn (1983)

Well ID	Elevation (m)	Elevation Reference	TD (m)	Elevation Base CP (m)	Elevation Basement (m)	Reference
COL-241	24.4		4191.0	-582.2		Logs
COST GE-1	30.2	KB	4039.8	-3322.6	-3322.6	Scholle (1979)
CTF-60	161.5		149.4	16.8	16.8	SCDNR
DAR-124	65.5			-71.0	-71.0	SCDNR
DIL-121	29.0		196.9	-162.5	-162.5	SCDNR
DOR-211	23.8		627.9	-575.2		Core
DP-160	102.1	GL	1030.2	-568.5		Logs
DP161	146.3	KB	5430.0	-1091.2	-5154.2	Logs
DP163	123.3	DF	2253.7	-711.9		Logs
DP39	88.4	DF	652.3			Chowns and Williams (1983)
FLO-103				-177.4		Steele and Colquhoun (1985)
FLO-123				-182.6		Steele and Colquhoun (1985)
FLO-124				-185.0		Steele and Colquhoun (1985)
FLO-125				-182.9		Steele and Colquhoun (1985)
FLO-126				-164.6		Steele and Colquhoun (1985)
FLO-127				-176.2		Steele and Colquhoun (1985)
FLO-139				-183.8		Steele and Colquhoun (1985)
FLO-140				-178.3		Steele and Colquhoun (1985)
FLO-146				-175.9		Steele and Colquhoun (1985)
FLO-149				-184.1		Steele and Colquhoun (1985)
FLO-154				-173.7		Steele and Colquhoun (1985)
FLO-262	32.6		1426.5	-263.0		SCDNR
FLO-268	34.4		218.2	-175.3		Core
FLO-274	22.9		332.2	-305.1		SCDNR; Falls (1994)
FLO-293	29.0		230.7	-201.8	-201.8	SCDNR
FLO-33				-176.5		Steele and Colquhoun (1985)

Well ID	Elevation (m)	Elevation Reference	TD (m)	Elevation Base CP (m)	Elevation Basement (m)	Reference
FLO-5				-179.2		Steele and Colquhoun (1985)
FLO-87				-172.8		Steele and Colquhoun (1985)
GEO-24				-560.8		Steele and Colquhoun (1985)
GGS-107	66.1	GL	1309.4	-1220.1	-1220.1	Logs; Herrick (1961)
GGS-108	110.9		1527.0	-1175.3		Chowns and Williams (1983)
GGS-109	100.6	GL	2282.0	-1795.3		Logs
GGS-1145	57.9		2306.4	-1950.1	-1962.9	Chowns and Williams (1983)
GGS-119	22.9		1333.5	-1302.4	-1302.4	Herrick (1961); Chowns and Williams (1983)
GGS-1197	4.0		1350.6	-1314.0	-1314.0	Chowns and Williams (1983)
GGS-1198	4.3		1429.5	-1377.1	-1377.1	Chowns and Williams (1983)
GGS-1199	6.7		1401.2	-1377.7	-1377.7	Chowns and Williams (1983)
GGS-120	21.3	GL	1327.4	-1303.9	-1303.9	Logs
GGS-121	57.0	DF	2231.1	-1703.8	-1954.7	Applin and Applin (1964)
GGS-131	39.3		189.0		-144.2	Herrick (1961)
GGS-144	53.9	DF	1172.9	-1114.7	-1114.7	Applin and Applin (1964)
GGS-148	66.8	GL	1249.1	-1175.3		Herrick (1961); Chowns and Williams (1983)
GGS-150	43.9	DF	1220.1	-1070.8	-1070.8	Applin and Applin (1964)
GGS-153	15.8		1510.3	-1408.8	-1408.8	Chowns and Williams (1983)
GGS-158	47.5	DF	1193.6	-1144.5	-1144.5	Applin and Applin (1964)
GGS-166	45.1		1178.1	-1107.6	-1107.6	Chowns and Williams (1983)
GGS-169	43.3	DF	1238.1	-1093.6	-1093.6	Applin and Applin (1964)
GGS-172	61.0	GL	558.7			Logs
GGS-189	55.2	DF	1275.6	-1200.6	-1200.6	Applin and Applin (1964)
GGS-190	89.3	DF	1043.6	-944.0		Chowns and Williams (1983)

Well ID	Elevation (m)	Elevation Reference	TD (m)	Elevation Base CP (m)	Elevation Basement (m)	Reference
GGS-192	105.2		1604.8	-1068.3		Applin and Applin (1964); Chowns and Williams (1983)
GGS-193	127.7	DF	455.4			Chowns and Williams (1983)
GGS-194	110.9		517.6	-402.6	-402.6	Herrick (1961); Chowns and Williams (1983)
GGS-223	146.3		184.4	26.8	26.8	Chowns and Williams (1983)
GGS-296	155.1					Chowns and Williams (1983)
GGS-3001	29.9		2163.5	-2064.1	-2104.9	Chowns and Williams (1983)
GGS-3080	51.2	KB	1240.5	-1111.3		Logs; Chowns and Williams (1983)
GGS-3099	74.1	GL	1598.4	-1418.2		Chowns and Williams (1983)
GGS-3105	92.0	GL	1380.4	-749.2	-749.2	Logs
GGS-3113	50.9	KB	2606.6	-1432.0		Logs; Chowns and Williams (1983)
GGS-3114	81.1	GL	2033.6	-1916.3		Chowns and Williams (1983)
GGS-3115	61.3	GL	1524.6	-1320.1		Chowns and Williams (1983)
GGS-3120	55.5	KB	1540.2	-1230.8		Logs; Chowns and Williams (1983)
GGS-3122	58.2	GL	1524.9	-1367.0		Chowns and Williams (1983)
GGS-3127	85.3		1322.5	-1227.1	-1227.1	Chowns and Williams (1983)
GGS-3128	82.9	GL	1238.4	-1118.0		Logs; Chowns and Williams (1983)
GGS-3137	98.8		1883.7	-570.9		Chowns and Williams (1983)
GGS-3146	17.7		1367.6	-1335.6	-1335.6	Chowns and Williams (1983)
GGS-3147	134.1	GL	470.9			Chowns and Williams (1983)
GGS-3154	99.1		1696.8	-1554.5		Chowns and Williams (1983)
GGS-3165	146.3		471.5	-229.2		Chowns and Williams (1983)
GGS-3201	22.6		1332.3	-1285.0	-1285.0	Chowns and Williams (1983)
GGS-3353	104.2	GL	1219.2	-254.2		Logs; Chowns and Williams (1983)
GGS-336	56.4	GL	1219.8			Chowns and Williams (1983)

Well ID	Elevation (m)	Elevation Reference	TD (m)	Elevation Base CP (m)	Elevation Basement (m)	Reference
GGS-338	53.6	DF	1398.4	-1117.7	-1117.7	Applin and Applin (1964); Chowns and Williams (1983)
GGS-341	167.6		367.3	-193.5	-193.5	Herrick (1961); Chowns and Williams (1983)
GGS-3439	113.7	GL	785.2	-218.5	-218.5	Logs
GGS-3441	118.9	GL	1719.4	-216.4		Logs
GGS-3447	116.4	GL	2860.9	-221.9	-2422.6	Logs
GGS-3456	106.1		2103.7	-1408.8		Logs; McFadden et al. (1986)
GGS-3457	87.5	GL	3496.1	-1131.7		Logs
GGS-3514	134.1	GL	415.1	-222.5		Logs
GGS-357	110.9		92.4	19.2	19.2	Herrick (1961); Chowns and Williams (1983)
GGS-361	93.0		77.1	17.1	17.1	Herrick (1961); Chowns and Williams (1983)
GGS-363	7.9	DF	1296.6	-1287.5	-1287.5	Logs; Chowns and Williams (1983)
GGS-3632	70.1	GL	916.8	-440.1		Logs
GGS-3633	27.4	KB	1399.6	-1344.2	-1344.2	Logs
GGS-3634	68.9		1266.1	-1118.0		Logs
GGS-375	71.9	GL	1221.6	-1147.3		Logs
GGS-3758	74.7		261.8	-185.0	-185.0	Falls and Prowell (2001)
GGS-3794	73.2		308.0	-230.4	-230.4	Falls and Prowell (2001)
GGS-442	131.4		1597.2	-763.2		Chowns and Williams (1983)
GGS-468	93.9	GL	1258.8	-1158.8	-1158.8	Chowns and Williams (1983)
GGS-476	182.9		539.5	-301.8	-301.8	Herrick (1961)
GGS-481	44.8	DF	1246.0	-1160.1	-1160.1	Applin and Applin (1964)
GGS-491	100.0		1839.5	-616.3		Chowns and Williams (1983)
GGS-496	62.5	GL	1289.9	-1204.0	-1204.0	Logs; Applin and Applin (1964); Chowns and Williams (1983)

Well ID	Elevation (m)	Elevation Reference	TD (m)	Elevation Base CP (m)	Elevation Basement (m)	Reference
GGS-505	182.9		1222.2	-551.7		Chowns and Williams (1983)
GGS-509	91.1	GL	1083.9	-1161.6	-1161.6	Logs
GGS-51	85.3	GL	776.6	-536.4		Logs; Chowns and Williams (1983)
GGS-52	22.3	DF	1410.0	-1370.7		Chowns and Williams (1983)
GGS-619	134.7		1142.4	-935.7	-935.7	Herrick (1961); Chowns and Williams (1983)
GGS-651	14.9		1385.0	-1300.9	-1300.9	Chowns and Williams (1983)
GGS-7	109.1		155.1	-42.1	-42.1	Herrick (1961); Chowns and Williams (1983)
GGS-719	4.6		1443.5	-1428.0	-1428.0	Chowns and Williams (1983)
GGS-730	107.0	GL	987.6	-823.6	-823.6	Chowns and Williams (1983)
GGS-789	74.7	GL	969.3	-890.3	-890.3	Logs
GGS-855	39.0	GL	815.9	-723.0	-776.0	Logs; Milton and Hurst (1965); Chowns and Williams (1983); McFadden et al. (1986)
GGS-876	7.6		1395.7	-1357.9	-1357.9	Chowns and Williams (1983)
GGS-94	141.7		265.9	-123.7	-123.7	Herrick (1961); Chowns and Williams (1983)
GGS-95	60.4		1121.7	-1056.1		Herrick (1961); Chowns and Williams (1983)
GGS-960	93.0	DF	892.8	-669.0		Chowns and Williams (1983)
HOR-547	6.1		479.8	-473.7	-473.7	SCDNR
JAS-426	19.2		883.9			
KER-100	123.4		71.0	52.4	52.4	SCDNR
KER-66	67.7		55.5	12.2	12.2	SCDNR
LEE-75	60.0		168.9	-103.5	-103.5	Core
LEX-844	111.9		167.0	-52.7	-52.7	Core
MLB-112	41.8		105.2	-55.8	-55.8	SCDNR

Well ID	Elevation (m)	Elevation Reference	TD (m)	Elevation Base CP (m)	Elevation Basement (m)	Reference
MLB-137	29.9		112.5	-78.3	-78.3	SCDNR
MRN-78	10.7			-342.3	-342.3	Steele and Colquhoun (1985)
MRN-90	19.8		183.2	-163.1	-163.1	SCDNR
N&T-10	62.5	DF	1397.8	-874.8	-874.8	Neathery and Thomas (1975)
N&T-11	32.0	DF	1144.2	-1056.1	-1056.1	Neathery and Thomas (1975)
N&T-12	76.2	DF	1378.6	-1104.9	-1104.9	Neathery and Thomas (1975)
N&T-13	71.6	DF	1224.7	-876.3	-876.3	Neathery and Thomas (1975)
N&T-14	57.3	DF	1829.4	-1241.1	-1241.1	Neathery and Thomas (1975)
N&T-15	73.8	DF	1383.2	-1166.8	-1166.8	Neathery and Thomas (1975)
N&T-16	67.1	DF	1264.3	-1188.7	-1188.7	Neathery and Thomas (1975)
N&T-17	95.7	DF	2635.9	-2530.1	-2530.1	Neathery and Thomas (1975)
N&T-20	76.5	DF	3810.0	-2703.3	-2703.3	Neathery and Thomas (1975)
N&T-23	46.0	DF	1172.9	-1103.1	-1103.1	Neathery and Thomas (1975)
N&T-24	41.1	DF	2167.1	-2113.8	-2113.8	Neathery and Thomas (1975)
N&T-26	56.7	DF	1761.7	-1613.6	-1613.6	Neathery and Thomas (1975)
N&T-27	55.5	DF	2289.7	-2206.1	-2206.1	Neathery and Thomas (1975)
N&T-28	137.2	DF	3202.2	-3055.6	-3055.6	Neathery and Thomas (1975)
N&T-29	64.9	DF	3159.9	-3056.8	-3059.3	Neathery and Thomas (1975)
N&T-30	76.5	DF	3057.1	-2948.6	-2948.6	Neathery and Thomas (1975)
N&T-31	15.5	DF	4233.7	-3962.1	-3962.1	Neathery and Thomas (1975)
N&T-32	113.4	DF	4403.4	-4287.9	-4287.9	Neathery and Thomas (1975)
N&T-33	112.2	DF	4394.3	-4265.4	-4265.4	Neathery and Thomas (1975)
N&T-34	105.2	DF	4489.7	-4354.1	-4354.1	Neathery and Thomas (1975)
N&T-35	108.8	DF	4604.3	-4480.0	-4480.0	Neathery and Thomas (1975)
N&T-36	89.0	GL	4677.5	-4495.2	-4495.2	Neathery and Thomas (1975)
N&T-37	84.4	DF	3718.6	-3628.0	-3628.0	Neathery and Thomas (1975)

Well ID	Elevation (m)	Elevation Reference	TD (m)	Elevation Base CP (m)	Elevation Basement (m)	Reference
N&T-38	42.7	DF	3704.8	-3631.7	-3631.7	Neathery and Thomas (1975)
N&T-39	130.8	DF	2889.5		-2755.7	Neathery and Thomas (1975)
N&T-40	73.8	DF	634.9	-560.2	-560.2	Neathery and Thomas (1975)
N&T-41	67.7	DF	611.7	-509.9	-509.9	Neathery and Thomas (1975)
N&T-42	82.3	DF	522.4	-433.7	-433.7	Neathery and Thomas (1975)
N&T-43	64.0	DF	513.6	-447.8	-447.8	Neathery and Thomas (1975)
N&T-44	131.1	DF	769.0	-631.5	-631.5	Neathery and Thomas (1975)
N&T-45	104.2	DF	802.4	-698.0	-698.0	Neathery and Thomas (1975)
N&T-46	133.5	DF	820.2	-678.8	-678.8	Neathery and Thomas (1975)
N&T-47	92.0	DF	1948.3	-1843.4	-1843.4	Neathery and Thomas (1975)
N&T-48	42.7	DF	2468.9	-2260.1	-2260.1	Neathery and Thomas (1975)
N&T-49	42.7	DF	3704.8	-3631.7		Neathery and Thomas (1975)
N&T-50	44.2	DF	3922.8	-3848.1		Neathery and Thomas (1975)
N&T-51	77.4	DF	3886.2	-3707.9		Neathery and Thomas (1975)
N&T-52	120.7	DF	3301.0			Neathery and Thomas (1975)
N&T-53	168.9	DF	1589.5	-1033.3		Neathery and Thomas (1975)
N&T-54	153.6	DF	1690.4	-1474.9		Neathery and Thomas (1975)
N&T-55	58.5	DF	2014.7	-1752.0		Neathery and Thomas (1975)
N&T-56	44.5	DF	2679.8	-2595.1		Neathery and Thomas (1975)
N&T-6	38.1	DF	2335.4	-730.0	-730.0	Neathery and Thomas (1975)
N&T-9	39.6	GL	797.4	-679.7	-679.7	Neathery and Thomas (1975)
ORG-347	71.6		342.9	-228.3	-228.3	Steele and Colquhoun (1985)
ORG-393	78.3		346.9	-261.2		Core; Gellici (2007)
RIC-305	91.4			-1.8	-1.8	SCDNR
RIC-348	45.7		207.3	-150.3		Steele and Colquhoun (1985)
RIC-432	61.0		165.8	-103.6	-103.6	SCDNR

Well ID	Elevation (m)	Elevation Reference	TD (m)	Elevation Base CP (m)	Elevation Basement (m)	Reference
RIC-543	56.1		169.8	-103.6	-109.6	Core
RIC-613	126.5		73.2	54.9	54.9	SCDNR
SSW6						
Sum_1920_OT	21.3		780.3	-725.4		Logs; Mansfield (1937)
SUM-104				-157.0		Steele and Colquhoun (1985)
SUM-111				-164.6		Steele and Colquhoun (1985)
SUM-120				-167.6		Steele and Colquhoun (1985)
SUM-140				-164.3		Steele and Colquhoun (1985)
SUM-146				-171.3		Steele and Colquhoun (1985)
SUM-153				-164.3		Steele and Colquhoun (1985)
SUM-161				-144.5		Steele and Colquhoun (1985)
SUM-165				-163.4		Steele and Colquhoun (1985)
SUM-175				-156.4		Steele and Colquhoun (1985)
SUM-340	54.9		210.3	-137.2		Core
SUM-56				-165.5		Steele and Colquhoun (1985)
SUM-64				-183.8		Steele and Colquhoun (1985)
SUM-65				-178.3		Steele and Colquhoun (1985)
SUM-69				-179.2		Steele and Colquhoun (1985)
SUM-7				-160.6		Steele and Colquhoun (1985)
SUM-71				-189.3		Steele and Colquhoun (1985)
SUM-8				-162.8		Steele and Colquhoun (1985)
SUM-84				-178.9		Steele and Colquhoun (1985)
TR 1005-1	30.8	KB	3546.3	-2605.7	-2605.7	Dillon and Popenoe (1988)
WIL-29	18.9		402.0	-342.0		Steele and Colquhoun (1985)

Table A.3. Geology of Jurassic (J) or Triassic (Tr) and basement units encountered in wells.

Well ID	Jurassic or Triassic Lithology	Basement Rock	Maf. Ign.	J/Tr	Pal. Sed.	Met. Bas.	Fel. Ign.
32Y020	Red Beds			*			
36Q318							
A-19		Tuff and volcanic agglomerate of rhyolitic composition					*
A-23		Volcanic agglomerate or tuff of rhyolitic composition					*
A-25		Volcanic ash and tuff					*
A-26		Rhyolitic volcanic rock					*
A-36		Quartzitic sandstone and shale			*		
A-37		Quartzitic sandstone and shale			*		
A-38		Quartzitic sandstone and shale			*		
A-39		Quartzitic sandstone			*		
A-40		Quartzitic sandstone and shale			*		
A-41		Quartzitic sandstone and shale			*		
A-42		Weathered zone? 3482-3492 (ft); Black shale 3492-4444 (ft)	D		*		
A-44		Quartzitic sandstone			*		
A-47		Quartzitic sandstone			*		
A-48		Sandstone and shale			*		
A-49		quartzitic sandstone and shale			*		
A-50		Quartzitic sandstone and shale			*		
A-51		Quartzitic sandstone and shale			*		
A-53		Red and gray sandstone and shale	D		*		
A-54		Quartizitic sandstone		*	*		
A-55		quartzitic sandstone and shale			*		
A-56		Quartzitic sandstone			*		

137

Well ID	Jurassic or Triassic Lithology	Basement Rock	Maf. Ign.	J/Tr	Pal. Sed.	Met. Bas.	Fel. Ign.
A-57		quartzitic sandstone and shale			*		
A-58		Quartzitic sandstone and shale			*		
A-59		Black shale			*		
A-60		Six inches of altered black shale overlying quartzitic sandstone	B		*		
A-61		Quartzitic sandstone			*		
A-62		Black shale	D		*		
A-63		quartizitic sandstone and shale	D		*		
A-64		Quartzitic sandstone			*		
A-65		Quartzitic sandstone			*		
A-66		Quartzitic sandstone			*		
A-67		Black shale	D		*		
A-68		Quartzitic sandstone			*		
A-69		Black shale			*		
A-70		Quartzitic sandstone			*		
A-71		Black shale			*		
A-73		Black shale 6950-7240 (ft), Quartzitic sandstone 7240-7320 (ft)			*		
A-81			D	*			
A-82			D	*			
A-83			D	*			
AIK-2448		"Bedrock"					
AIK-2449		"Bedrock"					
AIK-465						*	
AIK-59		Granite					*
AIK-593						*	
AIK-595						*	

Well ID	Jurassic or Triassic Lithology	Basement Rock	Maf. Ign.	J/Tr	Pal. Sed.	Met. Bas.	Fel. Ign.
AIK-596						*	
AIK-603						*	
AIK-614						*	
AIK-637						*	
AIK-687						*	
AIK-688						*	
AIK-689						*	
AIK-690						*	
ALL-324				*			
ALL-348		Granite					*
ALL-357		Schist				*	
B-1		Quartzite, Ordovician				?	
B-10		Quartzitic sandstone (Devonian)			*		
B-13		Paleozoic			*		
B-14		Paleozoic			*		
B-17		Quartzitic sandstone, Paleozoic			*		
B-18		Quartzitic sandstone, Paleozoic			*		
B-19		Paleozoic			*		
B-2		Quartzite, Ordovician				?	
B-20	Eagle Mills and diabase		D	*			
B-21		Dacite Porphyry					*
B-22	"upper Paleozoic or L. Triassic"			*			
B-23		Granodiorite					*
B-28	Eagle Mills		D	*			
B-29	Eagle Mills	Paleozoic sandstone	D	*	?		
B-3		Granite					*

Well ID	Jurassic or Triassic Lithology	Basement Rock	Maf. Ign.	J/Tr	Pal. Sed.	Met. Bas.	Fel. Ign.
B-30		Paleozoic shale and sandstone			*		
B-34	Eagle Mills and diabase		D	*			
B-35		Devonian			*		
B-36	Eagle Mills and diabase		D	*			
B-37		Altered Granophyre					*
B-4		Quartzitic sandstone, Paleozoic			*		
B-40		Quartzitic sandstone, Paleozoic	D		*		
B-41	Eagle Mills			*			
B-42	Eagle Mills and diabase		D	*			
B-54		Rhyolite					*
B-55		Quartizitic sandstone, white, fine to medium grain, Paleozoic			*		
B-56		Quartizitic sandstone, Paleozoic			*		
B-58		Paleozoic sandstone			*		
B-59		Paleozoic sandstone			*		
B-60		Paleozoic	D		*		
B-63		Paleozoic			*		
B-64		Paleozoic			*		
B-65	Eagle Mills	Paleozoic Shale?	D	*	?		
B-66		Granite					*
B-67		Metamorphosed volcanic sandstone and granule conglomerate			?		?
B-68	Eagle Mills			*			
B-69	Eagle Mills and diabase		D	*			
B-70	Eagle Mills	Ordovician Sediments	D	*	*		
B-71		Cambiran or U. Precambrian meta-arkose and quartzite			?		

Well ID	Jurassic or Triassic Lithology	Basement Rock	Maf. Ign.	J/Tr	Pal. Sed.	Met. Bas.	Fel. Ign.
B-72		Cambiran or U. Precambrian meta-arkose and quartzite			?		
B-9		Quartzitic sandstone, Paleozoic			*		
BFT-2055		Rhyolite					*
BRK-644	Red Beds			*			
BRN-239		"postmetamorphic granitoid"					*
BRN-245	Hard red rock			*			
BRN-336						*	
BRN-337	Red beds	Gneiss		*		*	
BRN-338	Red mudstone, arkosic sandstone			*			
BRN-339				*			
BRN-340				*			
BRN-349						?	
BRN-357						?	
BRN-364		"Bedrock"					
BRN-379				*			
BRN-888						*	
BRN-889				*			
BRN-890						*	
BRN-891						*	
BRN-892				*			
BRN-893				*			
BRN-894				*			
BRN-895				*			
CAL-132		"Bedrock"					
CAL-224A	"Eagle Mills"			*			

Well ID	Jurassic or Triassic Lithology	Basement Rock	Maf. Ign.	J/Tr	Pal. Sed.	Met. Bas.	Fel. Ign.
CC#1	Basalt		B	*			
CC#2	Basalt		B	*			
CC#3	Basalt, Red beds		B	*			
COL-241	Red Beds		D	*			
COST GE-1		Devonian Sed. and Trachyte			*		
CTF-60		Saprolite				?	
DAR-124		"Bedrock"					
DIL-121		"Bedrock"					
DOR-211	Basalt		B	*			
DP-160	Red beds			*			
DP161	Red Beds and diabase	Granitic/Dioritic-orthoquartzite	D	*		?	
DP163	Red Beds and diabase		D	*			
DP39		Schist				*	
FLO-103	Hard Red Clay		D	*			
FLO-123	Hard Red Clay			*			
FLO-124	Hard Red Clay			*			
FLO-125	Hard Red Clay			*			
FLO-126	Hard Red Clay			*			
FLO-127	Hard Red Clay			*			
FLO-139	Hard Red Clay			*			
FLO-140	Hard Red Clay			*			
FLO-146	Hard Red Clay			*			
FLO-149	Hard Red Clay			*			
FLO-154	Hard Red Clay			*			
FLO-262	"Triassic"			*			
FLO-268	Red Beds		D	*			

Well ID	Jurassic or Triassic Lithology	Basement Rock	Maf. Ign.	J/Tr	Pal. Sed.	Met. Bas.	Fel. Ign.
FLO-274	Basalt		B	*			
FLO-293		"Bedrock"					
FLO-33	Hard Red Clay			*			
FLO-5	Hard Red Clay			*			
FLO-87	Hard Red Clay			*			
GEO-24	"Hard Black Shale?"			?			
GGS-107		"Igneous Rock" -- Volcanic Tuff					*
GGS-108	Sandstone			*			
GGS-109	Red Beds		D	*			
GGS-1145	Jurassic? Red beds	Devonian Sed		*	*		
GGS-119		Cryst. Rock -- Granite (according to C&W)					*
GGS-1197		Porphyritic rhyolite					*
GGS-1198		Paleozoic Sed			*		
GGS-1199		Paleozoic Sed			*		
GGS-120		"Weathered Granite"					*
GGS-121	Red Beds	Devonian Sed		*	*		
GGS-131		Saprolite?				*	
GGS-144		Ordovician Sed			*		
GGS-148		Cryst. Rock	B				
GGS-150		Ordovician Sed			*		
GGS-153		Felsic Tuff					*
GGS-158		Ordovician Sed			*		
GGS-166		Ordovician Sed			*		
GGS-169		Ordovician Sed			*		
GGS-172	Red beds?			*			
GGS-189		Silurian Sed	D		*		

Well ID	Jurassic or Triassic Lithology	Basement Rock	Maf. Ign.	J/Tr	Pal. Sed.	Met. Bas.	Fel. Ign.
GGS-190	Diabase in country rock of unknown origin		D	*			
GGS-192	"Diabase overlain by clastic rock"		D	*			
GGS-193		Biotite Gneiss				*	
GGS-194		Cryst. Rock				*	
GGS-223		Biotite Gneiss				*	
GGS-296	Arkosic Sandstone containing diabase		D	*			
GGS-3001	Jurassic? Red beds	Granite		*			*
GGS-3080	"Arkosic sandstone intruded by diabase"		D	*			
GGS-3099	Arkosic sandstone and shale overlain by Jurassic(?) red beds (546 ft)			*			
GGS-3105		Granite					*
GGS-3113	"Arkosic sandstone, shale, and diabase overlain by Jurassic(?) red beds (335 ft)."		D	*			
GGS-3114	Arkosic sandstone, shale and diabase overlain by Jurassic(?) red beds (803 ft)		D	*			
GGS-3115	Red shale overlain by Jurassic(?) red beds (335 ft)			*			
GGS-3120	"Arkosic sandstone, shale, and diabase overlain by Jurassic(?) red beds (546 ft)."		D	*			
GGS-3122	Arkosic sandstone, shale and diabase overlain by Jurassic(?) red beds (290 ft)		D	*			
GGS-3127		Porphyritic rhyolite					*
GGS-3128	Red Beds?		D	*			
GGS-3137	Arkosic sandstone, shale, and diabase		D	*			
GGS-3146		Felsic vitric crystal tuff					*
GGS-3147	Diabase		D	*			
GGS-3154	Arkosic sandstone and red shale			*			
GGS-3165	Red Beds			*			
GGS-3201		Felsic vitric tuff	D				*

144

Well ID	Jurassic or Triassic Lithology	Basement Rock	Maf. Ign.	J/Tr	Pal. Sed.	Met. Bas.	Fel. Ign.
GGS-3353	Red Beds		D	*			
GGS-336	"Ferruginous sandstone"			*			
GGS-338		Igneous Rock					*
GGS-341		Cryst. Rock				*	
GGS-3439		Schist				*	
GGS-3441	Red Beds (Fanglomerate)		D	*			
GGS-3447	Red Beds	Schist		*		*	
GGS-3456	Conglomerate		D	*			
GGS-3457				*			
GGS-3514	Mudstone / Redbeds			*			
GGS-357		Cryst. Rock				*	
GGS-361		Cryst. Rock				*	
GGS-363		"Basement Complex" -- "Porphyritic rhyolite"					*
GGS-3632	Red beds			*			
GGS-3633		Tuff					*
GGS-3634	Red beds			*			
GGS-375	Brick red siltstone			*			
GGS-3758		Biotite Gneiss				*	
GGS-3794		Biotite Gneiss				*	
GGS-442	Arkosic sandstone, red shale, and diabase		D	*			
GGS-468		Granite					*
GGS-476		Cryst. Rock				*	
GGS-481		Ordovician Sed			*		
GGS-491	Arkosic sandstone, red shale, and diabase		D	*			
GGS-496		Igneous Rock	B	*			

Well ID	Jurassic or Triassic Lithology	Basement Rock	Maf. Ign.	J/Tr	Pal. Sed.	Met. Bas.	Fel. Ign.
GGS-505	Arkosic sandstone, red shale, and diabase		D	*			
GGS-509		Granite					*
GGS-51	Red Beds		D	*			
GGS-52	Arkosic Sandstone			*			
GGS-619	Arkosic sandstone	Cryst. Rock		*			
GGS-651		Felsic vitric crystal tuff					*
GGS-7		Cryst. Rock				*	
GGS-719		Granite					*
GGS-730		Quartzofeldspathic gneiss (cataclastic)				*	
GGS-789		Biotite Gneiss				*	
GGS-855	Red Beds?	Granite?		?			?
GGS-876		Paleozoic Sed			*		
GGS-94		Cryst. Rock					*
GGS-95	Conglomeratic arkose	Cryst. Rock		*			
GGS-960	Diabase and "granite wash"		D	*			
HOR-547		"Basement"					
JAS-426	Red Beds			*			
KER-100		"Bedrock"					
KER-66		Granite					*
LEE-75		Saprolite - weathered Schist				*	
LEX-844		Saprolite - weathered Schist				*	
MLB-112		"Bedrock"					
MLB-137		"Bedrock"					
MRN-78		Granite Saprolite					*
MRN-90		"Granite Rock"					*
N&T-10		Dolostone			*		

Well ID	Jurassic or Triassic Lithology	Basement Rock	Maf. Ign.	J/Tr	Pal. Sed.	Met. Bas.	Fel. Ign.
N&T-11		Sandstone and dark-gray shale			*		
N&T-12		Limestone			*		
N&T-13		Slate or phyllite and quartzite				*	
N&T-14		Chlorite sericite phyllite				*	
N&T-15		Black slate, graphite schist, quartzite				*	
N&T-16		Slate				*	
N&T-17		Quartzite				*	
N&T-20		Dolomite marble				*	
N&T-23		Chlorite schist				*	
N&T-24		Chlorite schist				*	
N&T-26		Chlorite and muscovite schist, biotite garnet schist				*	
N&T-27		Tremolite-chlorite phyllite-schist (phyllonite)				*	
N&T-28		Muscovite biotite feldspathic quartz gneiss				*	
N&T-29	"Mesosoic Strata including rhyolite and basalt"	Biotite feldspathic schist and gneiss; microgranular texture, mylonite	B	*		*	
N&T-30		Biotite feldspathic schist and gneiss				*	
N&T-31		Biotite feldspathic gneiss (granite?)				*	
N&T-32		Antigorite (hornfels-ultramafic?)				*	
N&T-33		Volcanic conglomerate					?
N&T-34		Volcanic rubble					?
N&T-35		Granite					*
N&T-36		Basalt	B	?			
N&T-37		Granite					*
N&T-38		Granitic Igneous rock					*
N&T-39	Mesozoic arkosic conglomerate and volcanic rocks including rhyolite porphyry and basalt	Chlorite Schist and phyllite	B	*		*	

Well ID	Jurassic or Triassic Lithology	Basement Rock	Maf. Ign.	J/Tr	Pal. Sed.	Met. Bas.	Fel. Ign.
N&T-40		Metamorphic				*	
N&T-41		Crystallines (granites)					*
N&T-42		Granite gneiss				*	
N&T-43		Hornblende gneiss and amphibolite				*	
N&T-44		Diorite				?	*
N&T-45		Crystalline rock				*	
N&T-46		Graphite-muscovite schist				*	
N&T-47		Quartz diorite or hornblende diorite					*
N&T-48		Sandstone, gray, fine-grained			*		
N&T-49	Igneous Rock			*			
N&T-50	Diabase		D	*			
N&T-51	Igneous Rock			*			
N&T-52	Arkose			*			
N&T-53	Rhyolite and arkosic sandstone		B	*			
N&T-54	Arkose interlayered with diabase		D	*			
N&T-55	Arkose and basalt		B	*			
N&T-56	Rhyolite			?			
N&T-6		Sandstone, coal, quartz-pebble conglomerate			*		
N&T-9		Dolostone			*		
ORG-347		"igneous material"				?	?
ORG-393	Red Beds			*			
RIC-305		"Bedrock"					
RIC-348	"sand with clay, hard and tight drilling"			*			
RIC-432		Granite					*
RIC-543	Red Beds	Saprolite - Biotite Gneiss		*		*	
RIC-613		"Bedrock"					

Well ID	Jurassic or Triassic Lithology	Basement Rock	Maf. Ign.	J/Tr	Pal. Sed.	Met. Bas.	Fel. Ign.
SSW6	Basalt?		B?/D	*			
Sum_1920_OT	Diabase? and Red shale		D	*			
SUM-104	Hard Red Clay			*			
SUM-111	Hard Red Clay			*			
SUM-120	Hard Red Clay			*			
SUM-140	Hard Red Clay			*			
SUM-146	Hard Red Clay			*			
SUM-153	Hard Red Clay			*			
SUM-161	Hard Red Clay			*			
SUM-165	Hard Red Clay			*			
SUM-175	Hard Red Clay			*			
SUM-340	Red Beds			*			
SUM-56	Hard Red Clay			*			
SUM-64	Hard Red Clay			*			
SUM-65	Hard Red Clay			*			
SUM-69	Hard Red Clay			*			
SUM-7	Hard Red Clay			*			
SUM-71	Hard Red Clay			*			
SUM-8	Hard Red Clay			*			
SUM-84	Hard Red Clay			*			
TR 1005-1		Silurian SS			*		
WIL-29	"red sandy clay, hard; rock, very hard"			?			

APPENDIX B – SEISMIC REFRACTION DATA

Seismic refraction data was compiled from several previous studies (Tables B.1, B.2, B.3, B.4, and B.5). Most of these studies reported the data (seismic velocities and depths to refracting layers) as points on a map. When coordinates were not directly given, maps were digitized and geo-referenced, and coordinates extracted from the point locations. For each table, latitude and longitude are reported in decimal degrees. Latitudes are north of the equator, and the negative for longitudes denotes west of Greenwich. Elevations reported in each table are in meters and are relative to mean sea level.

Tables B.1, B.2, and B.5 are similar with the first column ("Point", "Site", or "STN #") indicating the identification designated by each study. The "Velocity" columns for Tables B.1, B.2, and B.5 list the reported sub-Coastal Plain (CP) seismic velocities in km/s. "Elevation Base CP" (just "Elevation" in Table B.5) is the elevation of the bottom of the Coastal Plain. "Elevation Basement" is the elevation of interpreted pre-Triassic basement.

Pooley (1960) used a 6 layer model (when the 6th layer could be detected) for interpreting the shallow crustal seismic velocity structure (Table B.3). Layer 5 (L5) was interpreted to originate from immediately beneath the Coastal Plain. Layer 6 (L6) was a deeper layer, interpreted to originate from pre-Triassic basement.

Smith (1982) used a 3 layer model for interpreting the shallow crustal seismic velocity structure (Table B.4). Layer 0 represents the Coastal Plain, and is not reported in Table B.4. Layer 1 (L1) is interpreted to originate from immediately beneath the Coastal Plain. Layer 2 (L2) is interpreted to originate from pre-Triassic basement. Apparent (app.) velocities are reported at the shot point for each test. True velocities are reported where profiles could be reversed.

Table B.1. Seismic refraction velocities and elevations reported by Ackermann (1983).

Point	Latitude (degrees)	Longitude (degrees)	Velocity (km/s)	Elevation Base CP (m)	Elevation Basement (m)
1a	33.103	-80.457	5.6	-634	
1b	33.134	-80.403	5.6	-606	
1c	33.118	-80.434			-2200
2a	33.176	-80.27	5.7		
2b	33.197	-80.253	5.1		
3a	33.221	-80.174	5.2	-538	-1489
3b	33.205	-80.152	5.2	-557	-1384
4a	33.055	-80.259	5.4	-653	
4b	33.011	-80.24	5.4	-702	
4c	33.029	-80.249			-2490
4d	32.995	-80.234			-2240
4e	32.965	-80.223			-1300
4f	33.018	-80.242		-700	
5a	33.11	-80.21	5	-620	-1671
5b	33.09	-80.199	4.7	-628	-1654
6a	33.063	-80.156	4.4	-640	-2300
6b	33.11	-80.144	4.4	-606	-2400
6c	33.006	-80.17			-1500
7a	33.152	-80.094	5.3	-570	
7b	33.153	-80.082			-1645
8a	33.101	-80.066	5.2		
8b	33.084	-80.064	5.2	-634	
8c	33.094	-80.065			-1350
9a	33.134	-79.961	4.9	-727	
9b	33.161	-79.96	4.9	-721	

Point	Latitude (degrees)	Longitude (degrees)	Velocity (km/s)	Elevation Base CP (m)	Elevation Basement (m)
9c	33.149	-79.96			-1400
10a	32.892	-80.329	5.7	-772	-1258
10b	32.924	-80.289	5.7	-747	
10c	32.901	-80.32			-1219
10d	32.921	-80.295			-1180
10e	32.908	-80.309		-775	
11a	32.91	-80.248	5.4	-749	-1286
11b	32.945	-80.21	5.4	-717	-1285
11c	32.928	-80.229			-1263
11d	32.917	-80.242			-1315
11e	32.922	-80.235		-725	
12a	32.952	-80.16			-1359
12b	32.959	-80.144			-1280
12c	32.962	-80.132			-1264
13	33.022	-80.078			-1160
14a	33.033	-80.004	5.2	-674	-1270
14b	33.041	-80.001			-1290
14c	33.058	-79.992			-1208
15a	33.092	-79.886	6.1		-1030
15b	33.117	-79.882	6.1		-750
15c	33.11	-79.883			-840
15d	33.102	-79.884			-996
16a	33.1	-79.78	6.1	-704	-704
16b	33.056	-79.757	6.1		
16c	33.078	-79.768			-830
16d	33.0665	-79.761			-860
17a	32.85	-80.34	5.5	-765	-1246
17b	32.848	-80.317	5.5	-788	-1242
18a	32.875	-80.187	5.1	-893	
18b	32.885	-80.166	4.8		
18c	32.894	-80.143	4.6	-882	
18d	32.879	-80.18			-1534
18e	32.891	-80.152			-1597
18f	32.882	-80.169		-873	
19a	32.868	-80.156	4.7		-1770
19b	32.872	-80.124	4.7	-907	
19c	32.868	-80.163			-1920
19d	32.869	-80.149			-1840
19e	32.871	-80.13			-1770

Point	Latitude (degrees)	Longitude (degrees)	Velocity (km/s)	Elevation Base CP (m)	Elevation Basement (m)
20a	32.904	-80.098	4.8		
20b	32.919	-80.091	4.8	-815	
21a	32.922	-79.87	4.2	-882	-2236
21b	32.932	-79.846	4.2	-890	-2376
22a	32.838	-80.269	5.4	-881	-1410
22b	32.832	-80.239	5.4	-959	
22c	32.834	-80.248			-1340
22d	32.829	-80.221			-1390
22e	32.823	-80.192			-1503
22f	32.819	-80.169			-1744
23a	32.804	-80.115	4.9	-882	
23b	32.818	-80.09	4.6		-2060
23c	32.831	-80.069	4.4	-880	
23d	32.814	-80.098			-1900
23e	32.821	-80.087			-2120
23f	32.828	-80.075			-2150
24a	32.68	-80.296	4.9	-905	-2060
24b	32.689	-80.27	4.3	-920	-2060
25a	32.687	-80.078	4.4	-1024	
25b	32.673	-80.053	4.4	-1060	
25c	32.682	-80.065			-2000

Table B.2. Seismic refraction velocities and elevations reported by Amick (1978).

Site	Latitude (degrees)	Longitude (degrees)	Velocity (km/s)	Estimated Elevation Base CP (m)	Estimated Elevation Basement (m)
BEQ	33.35083	-80.2305	5.75	-700	-700
GTQ	33.33333	-79.67	6	-600	-600
NHS	33.09867	-80.2062	4.75	-700	-2200
MED	33.058	-80.002	6	-1200	-1200
PMS	32.876	-80.2355	5.75	-800	-1000

Table B.3. Seismic refraction velocities and elevations reported by Pooley (1960).

Point	Latitude (degrees)	Longitude (degrees)	Velocity L5 (km/s)	Elevation L5 (m)	Velocity L6 (km/s)	Elevation L6 (m)
1	31.91667	-81.35	5.36	-1237		
1r	31.825	-81.3	5.36	-1466		
2	32.06667	-81.3583	5.33	-1326		
2r	32.02833	-81.3183	5.33	-1554		
3	32.26667	-81.3667	5.61	-1207	6.46	-1423
3r	32.21667	-81.3167	5.61	-1125	6.46	-1369
4	32.54167	-81.4	5.27	-911	6.40	-2237
4r	32.53333	-81.3917	5.27	-1045	6.40	-2600
5	32.49167	-81.675	4.91	-914		
5r	32.425	-81.6417	4.91	-945		
6	32.2	-81.7667	5.06	-1036		
6r	32.15	-81.7583	5.06	-1146		
7	31.81667	-81.775	5.27	-1439		
7r	31.76667	-81.775	5.27	-1475		
8	31.61667	-81.6667	5.61	-1500		
8r	31.55	-81.625	5.61	-1814		
9	32.30833	-81.1167	4.57	-1256		
9r	32.25	-81.1083	4.57	-966		
10	32.59167	-80.975	4.85	-796	7.04	-3322
10r	32.525	-80.9833	4.85	-823	7.04	-3292
11	32.475	-80.625	5.79	-887		
11r	32.43333	-80.6417	5.79	-927		

Table B.4. Seismic refraction velocities and elevations reported by Smith (1982).

Shot Point	Velocity L1 app. (km/s)	Velocity L1 true (km/s)	Velocity L2 app. (km/s)	Elevation L1 (m)	Elevation L2 (m)	Latitude (degrees)	Longitude (degrees)
LB1	5.95	5.5	6.25	440	2120	33.41217	-80.5933
LB11	5.12		6.61	410	1810	33.2825	-80.7907
RO1	4.87	4.9	6.21	350	780	33.37067	-80.8522
RO10	5.02		6.4	280	1860	33.40833	-80.6772
RB1	3.96	4.5	6.3	330	1460	33.37083	-80.8522
RB11	5.23		--	400	--	33.28233	-80.7905
OB1	5.56	5.2	6.41	260	1970	33.43467	-80.8083
OB10	4.96		6.31	430	3070	33.32317	-80.5823
SB1	4.97	5	--	270	--	33.40883	-80.6772
SB11	5.11		--	490	--	33.32333	-80.5825
DC1	4.53		5.91	360	2490	33.323	-80.5823

Table B.5. Seismic refraction velocities and elevations reported by Woollard (1967).

STN #	State	County	Latitude (degrees)	Longitude (degrees)	Velocity (km/s)	Elevation (m)
19	SC	Chesterfield	34.69833	-79.9283	4.98	22
20	SC	Marlboro	34.61	-79.74	5.79	-62
21	SC	Marlboro	34.51333	-79.6617	5.85	-88
22	SC	Marlboro	34.38333	-79.64	6.28	-142
23	SC	Dillon	34.325	-79.4833	5.18	-169
24	SC	Dillon	34.315	-79.3	5.18	-143
25	SC	Marion	34.19167	-79.4517	4.88	-194
26	SC	Marion	34.03667	-79.3667	5.94	-276
27	SC	Marion	33.89833	-79.3917	5.97	-340
28	SC	Williamsburg	33.75	-79.3433	5.43	-391
29	SC	Georgetown	33.60833	-79.33	5.73	-451
30	SC	Georgetown	33.44667	-79.3333	6.83	-569
31	SC	Georgetown	33.30333	-79.3617	6.77	-592
32	SC	Chesterfield	34.66333	-80.33	5.29	111
33	SC	Chesterfield	34.58833	-80.2267	5.09	68
34	SC	Chesterfield	34.51667	-80.1617	6.04	-5
35	SC	Darlington	34.425	-80.0933	4.97	-64
36	SC	Darlington	34.31333	-79.9217	5.79	-102
37	SC	Florence	34.22667	-79.8117	5.67	-155
38	SC	Florence	34.03333	-79.7717	4.77	-235
39	SC	Kershaw	34.25333	-80.6867	4.72	63
40	SC	Kershaw	34.37833	-80.6133	4.82	98
41	SC	Kershaw	34.27667	-80.515	4.80	26
42	SC	Lee	34.20833	-80.45	6.22	-20
43	SC	Lee	34.09333	-80.265	3.93	-112
44	SC	Sumter	33.985	-80.125	6.80	-235
45	SC	Clarendon	33.83333	-79.9333	6.34	-308
46	SC	Clarendon	33.6	-80.2833	5.43	-339
47	SC	Lexington	33.985	-81.055	5.79	48
48	SC	Lexington	33.89	-81.0467	6.10	-4
49	SC	Calhoun	33.81	-80.9867	5.94	-78
50	SC	Calhoun	33.705	-80.875	6.16	-141
51	SC	Calhoun	33.58667	-80.6917	4.85	-267
52	SC	Orangeburg	33.45833	-80.5967	6.16	-414
53	SC	Dorchester	33.26333	-80.44	5.55	-482
54	SC	Orangeburg	33.36667	-80.8533	6.77	-397

STN #	State	County	Latitude (degrees)	Longitude (degrees)	Velocity (km/s)	Elevation (m)
55	SC	Barnwell	33.26833	-81.22	6.40	-278
56	SC	Aiken	33.45333	-81.84	5.55	-15
57	SC	Barnwell	33.30333	-81.6367	5.94	-173
58	SC	Barnwell	33.145	-81.605	4.83	-304
59	SC	Allendale	33.03	-81.4067	5.18	-446
60	SC	Allendale	32.86333	-81.4217	5.39	-669
100	GA	Atkinson	31.25	-82.8833	5.15	-1246
101	GA	Tift	31.48333	-83.5333	6.28	-1626
Humble#1	GA	Pierce	31.38333	-82.2333	5.79	-1280
8m	SC	offshore	32.96667	-79	5.76	-937
9m	SC	offshore	32.1	-79.5333	5.64	-2035
10m	SC	offshore	32.33333	-79.75	6.13	-1419
11m	SC	Port Royal Sd	32.3	-80.75	6.07	-928
12m	SC	St Helena Sd	32.46667	-80.45	6.04	-1184
14m	GA	Wassau Sd	31.89167	-80.9833	5.88	-1228
15m	GA	St Catherine's Sd	31.7	-81.175	5.88	-1296
16m	GA	Duboy Sd	31.41667	-81.3167	5.30	-1242

APPENDIX C – ISOPACH DATA

Interpretations of stratigraphic thickness for the SGR basins are based on wells, and interpretations of seismic reflection and refraction data (Table C.1). Interpretations of thicknesses from wells are derived from subtracting the elevation of pre-Triassic basement from the base of the Coastal Plain (Table A.2). Several deep wells which bottomed in the basin were used to provide a minimum stratigraphic thickness where other data was sparse. Stratigraphic thicknesses derived from interpretations of seismic reflection data were based on subtracting the two-way travel time of the basin bottom from the base of the Coastal Plain. The resultant isochron value was converted to thickness based on an interval velocity of 4.5 km/s. Interpretations of stratigraphic thickness derived from seismic refraction data was taken straight from the referenced studies. Stratigraphic thickness was assumed to be 0 (i.e. outside the basin) where sub-Coastal Plain velocities were > 6 km/s.

The 7 columns for Table C.1 are: 1) ID – identification number based on the source for the data; 2) Type – describes the type of data; 3) Num. / Stn. – refers to the well number (Num) or station (Stn) from which the thickness is derived; 4) Reference / Line – refers to the reference for the study, or the name of the seismic line from which the thickness is derived; 5) Latitude – latitude of the well in decimal degrees, north of the equator; 6) Longitude – longitude of the well in decimal degrees, negative denotes west of Greenwich.; 7) T – stratigraphic thickness (T) in meters.

Table C.1. Stratigraphic thicknesses derived from well and seismic data.

ID	Type	Num. / Stn.	Reference / Line	Latitude (degrees)	Longitude (degrees)	T (m)
W-B70	Well	B-70		30.752	-85.607	128
W-DP161	Well	DP161		31.754	-83.745	3904
W-BRN337	Well	BRN-337		33.239	-81.616	495
W-GGS3447	Well	GGS-3447		32.919	-82.636	2201
W-NT29	Well	N&T-29		31.728	-87.307	2
W-RIC543	Well	RIC-543		33.875	-80.702	6
W-A54	Well	A-54		30.336	-83.977	322
Ac-3a	Refraction	3a	Ackermann, 1983	33.221	-80.174	951
Ac-3b	Refraction	3b	Ackermann, 1983	33.205	-80.152	827
Ac-5a	Refraction	5a	Ackermann, 1983	33.110	-80.210	1051
Ac-5b	Refraction	5b	Ackermann, 1983	33.090	-80.199	1026
Ac-6a	Refraction	6a	Ackermann, 1983	33.063	-80.156	1660
Ac-6b	Refraction	6b	Ackermann, 1983	33.110	-80.144	1794
Ac-10a	Refraction	10a	Ackermann, 1983	32.892	-80.329	486
Ac-11a	Refraction	11a	Ackermann, 1983	32.910	-80.248	537
Ac-11b	Refraction	11b	Ackermann, 1983	32.945	-80.210	568
Ac-14	Refraction	14	Ackermann, 1983	33.033	-80.004	596
Ac-16a	Refraction	16a	Ackermann, 1983	33.100	-79.780	0
Ac-17a	Refraction	17a	Ackermann, 1983	32.850	-80.340	481
Ac-17b	Refraction	17b	Ackermann, 1983	32.848	-80.317	454
Ac-21a	Refraction	21a	Ackermann, 1983	32.922	-79.870	1354
Ac-21b	Refraction	21b	Ackermann, 1983	32.932	-79.846	1486
Ac-22a	Refraction	22a	Ackermann, 1983	32.838	-80.269	529
Ac-25a	Refraction	24a	Ackermann, 1983	32.680	-80.296	1155
Ac-24b	Refraction	24b	Ackermann, 1983	32.689	-80.270	1140
Po-3	Refraction	3	Pooley, 1960	32.267	-81.367	216
Po-3r	Refraction	3r	Pooley, 1960	32.217	-81.317	244
Po-4	Refraction	4	Pooley, 1960	32.542	-81.400	1326
Po-4r	Refraction	4r	Pooley, 1960	32.533	-81.392	1554
Po-10	Refraction	10	Pooley, 1960	32.592	-80.975	2527
Po-10r	Refraction	10r	Pooley, 1960	32.525	-80.983	2469
Am-NH	Refraction	NHS	Amick, 1979	33.099	-80.206	1500
Am-ME	Refraction	MED	Amick, 1979	33.058	-80.002	0
Am-PM	Refraction	PMS	Amick, 1979	32.876	-80.236	200
S4-1650	Reflection	1650	SeisData-4	33.161	-80.714	1800
S4-1000	Reflection	1000	SeisData-4	32.972	-80.391	2039
S4-1150	Reflection	1150	SeisData-4	33.054	-80.396	1775

ID	Type	Num. / Stn.	Reference / Line	Latitude (degrees)	Longitude (degrees)	T (m)
S4-1470	Reflection	1470	SeisData-4	33.110	-80.604	556
S4-1440	Reflection	1440	SeisData-4	33.102	-80.585	637
S4-1410	Reflection	1410	SeisData-4	33.098	-80.564	673
S8-2050	Reflection	2050	SeisData-8	32.207	-82.361	2945
S8-2150	Reflection	2150	SeisData-8	32.227	-82.426	3620
S8-1840	Reflection	1840	SeisData-8	32.142	-82.247	2102
S8-1400	Reflection	1400	SeisData-8	31.993	-82.003	0
S8-2950	Reflection	2950	SeisData-8	32.614	-82.617	855
S8-3330	Reflection	3330	SeisData-8	32.792	-82.748	1879
G19-160	Reflection	160	COCORP GA-19	32.308	-83.728	365
G19-350	Reflection	350	COCORP GA-19	32.148	-83.713	2412
G19-500	Reflection	500	COCORP GA-19	32.028	-83.697	3528
G19-580	Reflection	580	COCORP GA-19	31.957	-83.699	2725
G19-650	Reflection	650	COCORP GA-19	31.897	-83.715	1688
G19-720	Reflection	720	COCORP GA-19	31.841	-83.722	2570
G11-550	Reflection	550	COCORP GA-11	31.688	-83.927	3854
G11-440	Reflection	440	COCORP GA-11	31.606	-83.874	4802
G11-300	Reflection	300	COCORP GA-11	31.492	-83.879	1618
G11-170	Reflection	170	COCORP GA-11	31.378	-83.885	3177
G11-100	Reflection	100	COCORP GA-11	31.318	-83.870	2102
F1-200	Reflection	200	COCORP FL-1	30.551	-83.224	2543
F1-105	Reflection	105	COCORP FL-1	30.626	-83.257	1546
G10-200	Reflection	200	COCORP GA-10	30.618	-83.562	2842
G10-370	Reflection	370	COCORP GA-10	30.719	-83.663	2273
G10-520	Reflection	520	COCORP GA-10	30.844	-83.666	1402
G5-1450	Reflection	1450	Petersen et al., 1984	32.960	-82.315	0
G5-1670	Reflection	1670	Petersen et al., 1984	32.886	-82.103	2500
G5-900	Reflection	900	Petersen et al., 1984	33.291	-82.678	0
G5-1760	Reflection	1760	Petersen et al., 1984	32.842	-82.028	600
G5-1500	Reflection	1500	Petersen et al., 1984	32.936	-82.271	0
S8A-250	Reflection	250	SeisData-8A	32.845	-82.685	1636
S8A-300	Reflection	300	SeisData-8A	32.864	-82.665	1739
S8A-503	Reflection	503	SeisData-8A	32.970	-82.618	0
G19-100	Reflection	100	COCORP GA-19	32.357	-83.711	0
G19-50	Reflection	50	COCORP GA-19	32.395	-83.733	0
S4-2000	Reflection	2000	SeisData-4	33.291	-80.879	0
S8-3500	Reflection	3500	SeisData-8	32.888	-82.786	0
S8-2600	Reflection	2600	SeisData-8	32.411	-82.608	0
S8-2400	Reflection	2400	SeisData-8	32.304	-82.550	817
S8-2500	Reflection	2500	SeisData-8	32.358	-82.580	0

ID	Type	Num. / Stn.	Reference / Line	Latitude (degrees)	Longitude (degrees)	T (m)
G8-150	Reflection	150	COCORP GA-8	32.705	-81.992	0
S8-4100	Reflection	4100	SeisData-8	33.206	-82.888	0
SRS3-701	Reflection	701	SRS-3 – Domoracki, 1995	33.235	-81.581	1600
SRS3-401	Reflection	401	SRS-3 – Domoracki, 1995	33.214	-81.550	2200
SRS3-101	Reflection	101	SRS-3 – Domoracki, 1995	33.195	-81.518	1200
SRS7x-1800	Reflection	1800	SRS-7ex – Domoracki, 1995	33.151	-81.631	2025
SRS7x-2091	Reflection	2091	SRS-7ex – Domorack, 1995i	33.123	-81.596	900
W-B10	Well	B-10		28.830	-82.807	0
W-B13	Well	B-13		30.207	-82.600	0
W-B14	Well	B-14		30.273	-82.606	0
W-B17	Well	B-17		30.247	-81.954	0
W-B18	Well	B-18		30.231	-82.019	0
W-B19	Well	B-19		30.391	-81.851	0
W-B30	Well	B-30		29.857	-83.021	0
W-B35	Well	B-35		29.092	-82.918	0
W-B4	Well	B-4		30.112	-82.089	0
W-B40	Well	B-40		30.648	-81.600	0
W-B55	Well	B-55		29.955	-81.393	0
W-B56	Well	B-56		29.852	-81.457	0
W-B58	Well	B-58		30.282	-83.117	0
W-B59	Well	B-59		30.233	-83.047	0
W-B60	Well	B-60		30.232	-83.700	0
W-B63	Well	B-63		30.042	-82.522	0
W-B64	Well	B-64		30.097	-82.427	0
W-B9	Well	B-9		28.974	-82.648	0
W-COST GE-1	Well	COST GE-1		30.619	-80.300	0
W-GGS-1198	Well	GGS-1198		30.852	-81.858	0
W-GGS-1199	Well	GGS-1199		30.843	-81.735	0
W-GGS-144	Well	GGS-144		30.929	-82.799	0
W-GGS-150	Well	GGS-150		30.615	-82.782	0
W-GGS-158	Well	GGS-158		30.739	-82.925	0
W-GGS-166	Well	GGS-166		30.683	-82.878	0
W-GGS-169	Well	GGS-169		30.693	-82.686	0
W-GGS-189	Well	GGS-189		30.758	-82.911	0
W-GGS-481	Well	GGS-481		30.856	-82.722	0
W-GGS-876	Well	GGS-876		30.792	-81.992	0

ID	Type	Num. / Stn.	Reference / Line	Latitude (degrees)	Longitude (degrees)	T (m)
W-N&T-10	Well	N&T-10		32.722	-88.205	0
W-N&T-11	Well	N&T-11		32.507	-87.998	0
W-N&T-12	Well	N&T-12		32.390	-87.867	0
W-N&T-48	Well	N&T-48		31.004	-85.339	0
W-N&T-6	Well	N&T-6		32.822	-88.199	0
W-N&T-9	Well	N&T-9		32.715	-87.958	0
W-TR 1005-1	Well	TR 1005-1		30.993	-80.244	0
W-B-67	Well	B-67		30.783	-86.351	0
W-B-71	Well	B-71		30.469	-85.769	0
W-B-72	Well	B-72		30.543	-85.790	0
W-A-53	Well	A-53		30.844	-85.360	0
W-A-73	Well	A-73		31.167	-85.067	0
W-A-62	Well	A-62		30.439	-83.348	0
W-A-63	Well	A-63		30.354	-83.232	0
W-A-57	Well	A-57		30.125	-83.237	0
W-A-56	Well	A-56		30.010	-83.276	0
W-A-58	Well	A-58		29.938	-83.077	0
W-A-55	Well	A-55		29.952	-82.946	0
W-A-49	Well	A-49		29.804	-82.943	0
W-A-48	Well	A-48		29.742	-83.280	0
W-A-47	Well	A-47		29.553	-83.235	0
W-A-59	Well	A-59		29.180	-83.000	0
W-A-60	Well	A-60		29.083	-82.621	0
W-A-61	Well	A-61		29.224	-82.637	0
W-A-50	Well	A-50		29.710	-82.786	0
W-A-51	Well	A-51		29.813	-82.754	0
W-A-69	Well	A-69		30.020	-82.844	0
W-A-70	Well	A-70		30.074	-82.828	0
W-A-71	Well	A-71		30.297	-82.807	0
W-A-44	Well	A-44		30.112	-82.700	0
W-A-42	Well	A-42		30.490	-82.588	0
W-A-39	Well	A-39		30.490	-82.310	0
W-A-67	Well	A-67		30.764	-81.934	0
W-A-41	Well	A-41		30.021	-81.796	0
W-A-40	Well	A-40		29.978	-82.279	0
W-A-37	Well	A-37		29.847	-82.399	0
W-A-36	Well	A-36		29.780	-82.474	0
W-A-38	Well	A-38		29.696	-82.152	0
W-A-68	Well	A-68		29.702	-81.828	0

ID	Type	Num. / Stn.	Reference / Line	Latitude (degrees)	Longitude (degrees)	T (m)
W-A-64	Well	A-64		29.334	-82.251	0
W-A-65	Well	A-65		29.114	-82.282	0
W-A-66	Well	A-66		29.263	-82.054	0
W-GGS-1145	Well	GGS-1145		31.171	-85.074	0
W-GGS-121	Well	GGS-121		31.172	-85.078	0
W-ALL-357	Well	ALL-357		33.113	-81.506	0
W-DP39	Well	DP39		32.200	-84.033	0
W-GGS-131	Well	GGS-131		33.238	-81.923	0
W-GGS-193	Well	GGS-193		32.440	-83.817	0
W-GGS-194	Well	GGS-194		32.401	-83.733	0
W-GGS-223	Well	GGS-223		32.990	-83.004	0
W-GGS-341	Well	GGS-341		32.245	-84.799	0
W-GGS-3439	Well	GGS-3439		32.955	-82.638	0
W-GGS-357	Well	GGS-357		32.780	-83.637	0
W-GGS-361	Well	GGS-361		32.780	-83.637	0
W-GGS-3758	Well	GGS-3758		33.230	-81.879	0
W-GGS-3794	Well	GGS-3794		33.178	-81.786	0
W-GGS-476	Well	GGS-476		32.286	-84.463	0
W-GGS-7	Well	GGS-7		32.716	-83.699	0
W-GGS-730	Well	GGS-730		32.389	-82.540	0
W-GGS-789	Well	GGS-789		32.361	-82.474	0
W-LEE-75	Well	LEE-75		34.203	-80.174	0
W-LEX-844	Well	LEX-844		33.746	-81.108	0
W-N&T-13	Well	N&T-13		32.424	-87.548	0
W-N&T-14	Well	N&T-14		32.217	-87.635	0
W-N&T-15	Well	N&T-15		32.212	-87.481	0
W-N&T-16	Well	N&T-16		32.186	-87.443	0
W-N&T-17	Well	N&T-17		31.957	-87.804	0
W-N&T-20	Well	N&T-20		32.020	-88.420	0
W-N&T-23	Well	N&T-23		32.117	-87.128	0
W-N&T-24	Well	N&T-24		32.106	-87.292	0
W-N&T-26	Well	N&T-26		31.970	-87.091	0
W-N&T-27	Well	N&T-27		31.925	-87.321	0
W-N&T-28	Well	N&T-28		31.862	-87.751	0
W-N&T-30	Well	N&T-30		31.618	-87.352	0
W-N&T-31	Well	N&T-31		31.539	-87.582	0
W-N&T-32	Well	N&T-32		31.328	-87.524	0
W-N&T-40	Well	N&T-40		32.253	-86.400	0

ID	Type	Num. / Stn.	Reference / Line	Latitude (degrees)	Longitude (degrees)	T (m)
W-N&T-42	Well	N&T-42		32.201	-85.887	0
W-N&T-43	Well	N&T-43		32.188	-85.895	0
W-N&T-45	Well	N&T-45		31.845	-85.984	0
W-N&T-46	Well	N&T-46		31.624	-86.122	0
W-BRN-888	Well	BRN-888		33.293	-81.530	0
W-BRN-890	Well	BRN-890		33.252	-81.620	0
W-BRN-891	Well	BRN-891		33.203	-81.701	0
W-BRN-336	Well	BRN-336		33.281	-81.648	0
W-AIK-688	Well	AIK-688		33.279	-81.658	0
W-AIK-603	Well	AIK-603		33.285	-81.650	0
W-AIK-595	Well	AIK-595		33.276	-81.670	0
W-AIK-593	Well	AIK-593		33.287	-81.652	0
W-AIK-596	Well	AIK-596		33.296	-81.671	0
W-AIK-637	Well	AIK-637		33.290	-81.657	0
W-AIK-690	Well	AIK-690		33.320	-81.731	0
W-AIK-614	Well	AIK-614		33.333	-81.598	0
W-AIK-687	Well	AIK-687		33.277	-81.737	0
W-AIK-689	Well	AIK-689		33.327	-81.743	0
W-AIK-465	Well	AIK-465		33.286	-81.664	0
W-AIK-59	Well	AIK-59		33.642	-81.321	0
W-ALL-348	Well	ALL-348		33.025	-81.385	0
W-B-21	Well	B-21		29.754	-85.255	0
W-B-23	Well	B-23		30.171	-85.373	0
W-B-3	Well	B-3		30.376	-85.940	0
W-B-37	Well	B-37		30.133	-84.863	0
W-B-54	Well	B-54		29.513	-81.569	0
W-B-66	Well	B-66		30.399	-86.292	0
W-BRN-239	Well	BRN-239		33.437	-81.237	0
W-GGS-107	Well	GGS-107		31.267	-82.950	0
W-GGS-119	Well	GGS-119		31.396	-82.071	0
W-GGS-1197	Well	GGS-1197		31.374	-81.567	0
W-GGS-153	Well	GGS-153		31.042	-81.880	0
W-GGS-3105	Well	GGS-3105		32.258	-83.289	0
W-GGS-3146	Well	GGS-3146		31.518	-81.873	0
W-GGS-3201	Well	GGS-3201		31.548	-81.726	0
W-GGS-338	Well	GGS-338		30.783	-82.439	0
W-GGS-363	Well	GGS-363		31.689	-81.347	0

ID	Type	Num. / Stn.	Reference / Line	Latitude (degrees)	Longitude (degrees)	T (m)
W-GGS-3633	Well	GGS-3633		31.500	-81.747	0
W-GGS-468	Well	GGS-468		31.713	-82.894	0
W-GGS-509	Well	GGS-509		31.717	-82.896	0
W-GGS-651	Well	GGS-651		31.520	-81.684	0
W-GGS-719	Well	GGS-719		31.246	-81.633	0
W-GGS-94	Well	GGS-94		32.957	-82.808	0
W-KER-66	Well	KER-66		34.416	-80.329	0
W-MRN-78	Well	MRN-78		33.862	-79.331	0
W-N&T-35	Well	N&T-35		31.208	-87.525	0
W-N&T-37	Well	N&T-37		31.311	-87.213	0
W-N&T-38	Well	N&T-38		31.192	-86.950	0
W-N&T-41	Well	N&T-41		32.256	-86.298	0
W-N&T-47	Well	N&T-47		31.309	-85.178	0
W-RIC-432	Well	RIC-432		33.894	-80.722	0
W-N&T-33	Well	N&T-33		31.271	-87.406	0
W-N&T-34	Well	N&T-34		31.245	-87.472	0
W-MRN-90	Well	MRN-90		34.247	-79.520	0
W-A-25	Well	A-25		29.531	-81.706	0
W-A-19	Well	A-19		29.565	-81.485	0
W-A-23	Well	A-23		29.104	-82.008	0
W-A-26	Well	A-26		29.246	-81.247	0
W-GGS-3001	Well	GGS-3001		30.861	-84.886	0
Ac-15a	Refraction >6km/s	15a	Ackermann, 1983	33.092	-79.886	0
Ac-15b	Refraction >6km/s	15b	Ackermann, 1983	33.117	-79.882	0
Ac-16b	Refraction >6km/s	16b	Ackermann, 1983	33.056	-79.757	0
Wo-22	Refraction >6km/s	22	Woollard, 1957	34.383	-79.640	0
Wo-30	Refraction >6km/s	30	Woollard, 1957	33.447	-79.333	0
Wo-31	Refraction >6km/s	31	Woollard, 1957	33.303	-79.362	0
Wo-34	Refraction >6km/s	34	Woollard, 1957	34.517	-80.162	0
Wo-42	Refraction >6km/s	42	Woollard, 1957	34.208	-80.450	0
Wo-44	Refraction >6km/s	44	Woollard, 1957	33.985	-80.125	0
Wo-45	Refraction >6km/s	45	Woollard, 1957	33.833	-79.933	0
Wo-48	Refraction >6km/s	48	Woollard, 1957	33.890	-81.047	0

ID	Type	Num. / Stn.	Reference / Line	Latitude (degrees)	Longitude (degrees)	T (m)
Wo-50	Refraction >6km/s	50	Woollard, 1957	33.705	-80.875	0
Wo-52	Refraction >6km/s	52	Woollard, 1957	33.458	-80.597	0
Wo-54	Refraction >6km/s	54	Woollard, 1957	33.367	-80.853	0
Wo-55	Refraction >6km/s	55	Woollard, 1957	33.268	-81.220	0
Wo-101	Refraction >6km/s	101	Woollard, 1957	31.483	-83.533	0
Wo-10m	Refraction >6km/s	10m	Woollard, 1957	32.333	-79.750	0
Wo-11m	Refraction >6km/s	11m	Woollard, 1957	32.300	-80.750	0
Wo-12m	Refraction >6km/s	12m	Woollard, 1957	32.467	-80.450	0
Am-GTQ	Refraction >6km/s	GTQ	Amick, 1979	33.333	-79.670	0
W-BRN-338	Well - bot Tr	BRN-338		33.204	-81.580	925
W-COL-241	Well - bot Tr	COL-241		33.015	-80.929	3584
W-FLO-262	Well - bot Tr	FLO-262		33.962	-79.872	1131
W-GGS-3113	Well - bot Tr	GGS-3113		30.990	-83.252	1124
W-GGS-3137	Well - bot Tr	GGS-3137		32.326	-83.541	1214
W-GGS-3353	Well - bot Tr	GGS-3353		32.931	-82.610	861
W-GGS-3441	Well - bot Tr	GGS-3441		32.936	-82.621	1384
W-GGS-3457	Well - bot Tr	GGS-3457		31.759	-82.757	2277
W-GGS-442	Well - bot Tr	GGS-442		32.018	-84.308	703
W-GGS-491	Well - bot Tr	GGS-491		32.301	-83.480	1123
W-GGS-505	Well - bot Tr	GGS-505		32.149	-84.436	488
W-N&T-53	Well - bot Tr	N&T-53		31.835	-85.464	387